Doctoral Thesis

B Cell Antigen Receptor-intrinsic Costimulation of IgG and IgE Isotypes

In partial fulfillment of the requirements for the degree

"Doctor rerum naturalium (Dr. rer. nat.)"

in the Molecular Medicine Study Program at the

Georg-August University Göttingen

Submitted by

Lars Morten König

Born in Göttingen

March 2012

This thesis was conducted in the Institute of Cellular & Molecular Immunology at the Georg-August-University in Göttingen from March 2008 until March 2012 under the supervision of Dr. Niklas Engels in the group of Prof. Dr. Jürgen Wienands.

Members of the thesis committee

Supervisor:	**Prof. Dr. Jürgen Wienands**
Institute:	Cell. & Mol. Immunology
2nd Member:	**Prof. Uwe-Karsten Hanisch**
Institute:	Neuropathology
3rd Member:	**Prof. Dr. Steven Johnsen**
Institute:	Molecular Oncology
4th Member:	**Dr. Niklas Engels**
Institute:	Cell. & Mol. Immunology

Date of Disputation: _____

Parts of this thesis were published in:

Niklas Engels, Lars Morten König, Christina Heemann, Johannes Lutz, Takeshi Tsubata, Sebastian Griep, Verena Schrader, and Jürgen Wienands.

Recruitment of the cytoplasmic adaptor Grb2 to surface IgG and IgE provides antigen receptor-intrinsic costimulation to class-switched B cells.

Nature Immunology **10**, 1018–1025 (2009).

AFFIDAVIT

I herewith declare that my doctoral thesis entitled

"**B Cell Antigen Receptor-intrinsic Costimulation of IgG and IgE Isotypes**"

has been written independently with no other sources and aids than those indicated.

Date	Signature

Table of Contents

List of Figures

1 Abstract

B cells express different isotypes of the B cell antigen receptor (BCR) on their surface and secrete soluble forms of their antigen binding immunoglobulins (Ig) upon differentiation to plasma cells. Naïve mature B cells use Ig heavy chains of the μ and δ isotypes while antigen-experienced cells change the isotype to either α, γ and ε during an ongoing immune response, a process called Ig class-switch recombination. The change of isotype alters the effector function of the respective secreted immunoglobulin while preserving its antigen specificity. The humoral immune response upon first encounter of an antigen is therefore characterized by the secretion of immunoglobulin M (IgM), while antibodies of class-switched isotypes are secreted upon secondary encounter of the same antigen, with IgG being the predominant isoform. Moreover, the secondary immune response is much more rapid and vigorous, which is based on the fast reactivation, proliferation and differentiation of memory B cells into plasma cells.

B cell activation during primary and secondary immune responses relies on signals through the BCR. Both, naïve and Ig class-switched B cells use the canonical BCR pathway initiated by the Ig-associated Igα/β heterodimer. Signaling through mIgM- and mIgD-BCRs is completely dependent on the Igα/β heterodimer as both Igs only contain cytoplasmic parts of three amino acids. However, mIgG and mIgE heavy chains both contain cytoplasmic tails of 28 amino acids that has been shown to be essential for mounting robust secondary immune responses (Achatz et al., 1997; Kaisho et al., 1997). The molecular mechanisms of this enhanced signaling remained completely elusive. Previous work of Niklas Engels showed that a conserved tyrosine residue within these cytoplasmic tails, entitled the immunoglobulin tail tyrosine (ITT), is phosphorylated upon BCR stimulation and amplifies BCR-induced Ca^{2+} mobilization by the recruitment of Grb2 (Engels et al., 2009). In the work presented here I could show that the enhanced signaling through IgG- and IgE-BCRs in fact culminate in a proliferative burst that is one hallmark of the memory B cell response. Recruitment of Grb2 engaged additional or stabilized existing protein complexes of the BCR signalosome. I could demonstrate that the N-terminal SH3 domain of Grb2 is necessary and sufficient to increase Ca^{2+} mobilization and PKC activity, while the C-terminal SH3 leads to an increased phosphorylation of SLP-65 and Vav1. Thus, by Ig class-switching B cells not only alter the effector function of the respective secreted antibody but also add another signaling motif to the BCR providing receptor-intrinsic “costimulation”.

2 Introduction

The immune system is an enormously powerful cellular system to protect a host organism from a variety of different pathogens. While the innate immunity recognizes common molecular patterns of certain pathogens, cells of the adaptive immune system express antigen receptors with unbelievably diverse binding specificities enabling recognition of any pathogen. There are two branches of the adaptive immune system. The cellular immune system fights infections by intracellular pathogens and is mediated by T lymphocytes, while the humoral immunity reacts to extracellular pathogens and their toxic products with the secretion of highly specific antibodies that neutralize toxins or mark pathogens for destruction by different effector mechanisms of the innate immune system. The effectors of the humoral immune response are cells of the B cell lineage.

Each B cell expresses a B cell antigen receptor (BCR) of unique specificity on its surface. Upon binding of an antigen to the BCR, the B cell is activated and gives rise to plasma cells that are specialized antibody secreting cells. In addition, long-lived B cells, called memory B cells, are formed that preserve the antigen receptor specificity facilitating a rapid immune response upon secondary encounter with the same antigen. In most cases, such a secondary immune response is so rapid and vigorous that the pathogen is eliminated before it can establish an infection. Both, the primary and secondary (or memory) immune reaction, rely on signaling through the B cell antigen receptor. However, signals upon secondary encounter of antigen translate into a much stronger immune response. Part of this divergence is based on differences in the isotype of the B cell receptor and its signaling capacity, which will be investigated in this study.

2.1 A Cellular View on B Cell Activation – Germinal Centers and B Cell Memory

Once a B cells has survived positive and negative selection processes during its development in the bone marrow it migrates to the spleen where it further differentiates into a mature naïve B cell. The BCR isotypes expressed on naïve mature B cells are IgM and IgD that constitute the only isotypes that are exposed simultaneously on the surface of a B cell. In this state it is ready to join the many

immune cells that may lead to an effective eradication of pathogens. B cells specific for a foreign antigen contribute to this process by establishing the humoral immune response, which is based on the formation of memory B cells and plasma cells secreting high-affinity, mostly isotype-switched antibodies (Tarlinton, 2006; Cyster, 2010; Victora and Nussenzweig, 2011).

B cells can recognize antigens in different forms and may be activated by soluble antigens as well as particulate antigens that are mostly found in form of immune complexes bound to complement receptors or Fc-receptors on the surface of antigen presenting cells such as macrophages or dendritic cells (Carrasco and Batista, 2006). Upon binding of the antigen, the BCR triggers many signaling cascades. Furthermore, the antigen is captured and processed to be displayed on MHC II molecules enabling the presentation of antigen peptides to cognate T helper cells in order to receive further activation stimuli. The activated B cells can then differentiate along two different pathways. They may differentiate to extrafollicular plasmablasts that produce a transient wave of antibodies of relatively low affinity, which are important for an early antigen-specific response; or they migrate to the center of B cell follicle in secondary lymphoid organs (SLOs) to establish a germinal center (GC) (McHeyzer-Williams et al., 2011). A GC is a specialized secondary follicular structure in which B cells undergo clonal expansion, affinity maturation and Ig class-switch recombination (CSR). It is structurally and functionally divided into two parts, named the dark zone (DZ) and the light zone (LZ). The DZ is the site of clonal expansion and concomitant receptor diversification by somatic hypermutation. The LZ is dispersed by follicular dendritic cells (FDCs) that harbor an antigen reservoir on the surface. B cells with high-affinity BCRs get a stronger signal through the BCR and capture more antigens from FDCs for subsequent presentation to T follicular helper (Tfh) cells as their low-affinity counterparts (reviewed in (Batista and Harwood, 2009; Cyster, 2010; McHeyzer-Williams et al., 2011; Nutt and Tarlinton, 2011; Victora and Nussenzweig, 2011). As B cells compete for a limited number of Tfh cells the ones with more peptide-MHC II molecules are more likely to interact with the Tfh cells and are provided with proliferation and survival cues (Victora et al., 2010). Cells with lower affinity or mutations that abrogate BCR expression will die by apoptosis, which is the default cellular outcome of GC B cells. Only those cells that are provided with anti-apoptotic signals through the BCR and through T cell help may re-enter the cycle of proliferation, mutation and selection. Affinity

maturation of the BCR is therefore an iterative Darwinian-like selection process of higher affinity variants (Victora and Nussenzweig, 2011). Dependent on the type of Tfh cells and their cytokine footprint, B cells switch their Ig isotype to IgG, IgE or IgA to adapt the effector function of the respective secreted antibody to the nature of the antigen (McHeyzer-Williams et al., 2011). Also, as described in detail in the next chapter and throughout this thesis, the isotype of the surface BCR has influence on proliferation and survival of the B cells. Once B cells are selected to exit the GC they give rise to high-affinity plasma cells and memory B cells, both of which contribute to the immunological memory of the B cell lineage. Long-lived plasma cells (LLPC) reside in survival niches in the bone marrow and provide long-term protective immunity by constantly secreting antigen-specific antibodies (Ahmed and Gray, 1996). Class-switched memory B cells proliferate robustly upon antigen re-exposure and differentiate rapidly into high-affinity plasma cells (Gray, 1993; Ahmed and Gray, 1996). The more rapid response may be attributed to several differences of memory versus naïve B cells. First, the frequency of antigen-specific B cells is naturally higher with a pool of memory B cells residing within the body after antigen elimination. Second, memory B cells have been in a germinal center reaction and selected for high affinity BCRs, which could explain the lower activation threshold described for memory B cells. Third, alteration of surface receptor expression or modification of the genetic program, that may be coherent with differentiation into memory B cells, could account for greater reactivation. And last, as already hinted at, the isotype of the BCR might play a role in modifying the signaling capacity of the BCR leading to an enhanced survival, proliferation and/or differentiation of class-switched B cells. Indeed, several studies demonstrated that the extended cytoplasmic tails of surface IgG- or IgE-BCRs are essential to mount a robust secondary immune response. Before the differences of isotype-specific BCR signals are discussed in detail, I will introduce the signal mechanisms that are shared by all isotypes of the BCR.

2.2 A Molecular View on B Cell Activation

Binding of an antigen to the B cell antigen receptor initiates a complex signal transduction cascade. This signal initiation is characterized by an orchestra of concomitant events during which cytoskeletal rearrangements, BCR clustering and translocation into lipid rafts, post-translational modification of proteins and lipid modifications lead to the assembly of the BCR signalosome. This assembly of signaling proteins including kinases, phosphatases, adaptor proteins and lipid modifying enzymes allow the coordinated and spatio-temporal-restricted regulation of downstream signaling events. Different co-receptors may be in- or excluded from this BCR signalosome further modifying and fine-tuning the transmitted signal in order to respond properly to the surrounding microenvironment. These highly regulated and complex processes enable the BCR to establish a wide range of signals in terms of magnitude, duration and diversification of signaling pathways. This fact is reflected by the variety of different cellular responses, which may be induced by the BCR such as apoptosis, induction of tolerance, proliferation and differentiation depending on the developmental stage of the B cell and properties of the antigen.

2.2.1 The B Cell Antigen Receptor

The B cell antigen receptor (BCR) is a multimeric protein complex consisting of membrane-bound immunoglobulins (mIgs) that make up the antigen recognition part of the receptor and a signal-transducing heterodimer of Ig associated α (Igα) and β (Igβ) (Reth, 1992) transmembrane proteins. This disulfide-linked heterodimer is non-covalently associated to mIg at a 1:1 stoichiometry (Reth et al., 2000; Schamel and Reth, 2000). Five different isotypes of mIgs are distinguished based upon expression of the different heavy chain, namely μm, δm, γm, εm and αm (Venkitaraman et al., 1991; Reth, 1992). Naïve mature B cells simultaneously express BCRs of the IgM and IgD isotypes. During an ongoing immune response many B cells change their BCR isotype by an irreversible genetic rearrangement in which the Cμ and Cδ genes are deleted and replaced by the further downstream positioned Cγ, Cε or Cα, a process called Ig class-switch recombination (CSR) (Honjo and Kataoka, 1978; Honjo et al., 2002). The change of isotype alters the effector function of the respective secreted immunoglobulin while preserving its specificity. As will be discussed throughout this thesis, some isotypes differ in their cytoplasmic domain of

the surface Ig that contributes to the signaling capacity of the BCR. However, despite these differences, all BCR isotypes use the associated Igα/β heterodimer as a signaling unit initiating the canonical BCR signaling pathway (Venkitaraman et al., 1991).

2.2.2 The Canonical BCR Signaling Pathway

Early Events in BCR Activation

The exact mechanism of the early events of BCR engagement is still not clear (Models reviewed in (Harwood and Batista, 2010; Pierce and Liu, 2010), but the predominant model proposes that crosslinking of several BCR monomers upon antigen binding induces clustering and translocation of the BCRs into lipid microdomains, called lipid rafts ((Cheng et al., 1999), reviewed in (Pierce, 2002)). These lipid rafts contain high concentrations of protein tyrosine kinases (PTKs) of the Src-family (Casey, 1995), such as Lyn. Thus, translocation of the BCR results in an association with Src PTKs that in turn phosphorylate the signal transducing heterodimer Igα/β (Yamanashi et al., 1991; Campbell and Sefton, 1992) initiating signaling cascades. Recently, cytoskeletal rearrangements have been demonstrated to play an important role in the early events leading to signal initiation (Treanor et al., 2010; 2011).

Protein Tyrosine Kinases in Signal Initiation

Igα and β both contain an immunoreceptor tyrosine-based activation motif (ITAM) in their cytoplasmic tail that is characterized by conserved tandem tyrosine motif with the consensus sequence D/E x^7 D/E xx **Y**xxI/L x_7 **Y**xxI/L (x is any amino acid) (Reth, 1989). This activation motif is found in many lymphocyte receptors and constitute a common signaling entity for lymphocyte activation. Phosphorylation of the ITAMs by Src PTKs establish a docking site for the tandem SH2-domains of another PTK, spleen tyrosine kinase (Syk) (Kurosaki et al., 1995; Wienands et al., 1995; Fütterer et al., 1998). Recruitment and binding to the phospho-ITAMs results in a conformational change releasing autoinhibition of Syk. Further transphosphorylation of Syk by Src PTKs and autophosphorylation lead to its full activation. Consecutively, Syk phosphorylates the SH2-domain-containing leukocyte adaptor protein of 65kD (SLP-65) (also named BLNK or BASH) (Fu et al., 1998; Goitsuka et al., 1998; Wienands et al., 1998) and other signaling proteins. SLP-65 is

directly recruited to the BCR by a non-ITAM phospho-tyrosine (pY_{204}) residue in Igα (Engels et al., 2001). There, it acts as a central adaptor controlling various downstream signaling cascades (Oellerich et al., 2009) that drive Ca^{2+} mobilization, activation of protein kinase C (PKC), small GTPases of Ras and Rho-family members and mitogen-activated kinases (MAPKs) eventually resulting in nuclear translocation of transcription factors and activation of target gene expression. Figure 1 depicts an overview of signaling cascades of the canonical BCR pathway.

Ca^{2+} Initiation Complex

SLP-65 plays a very central role in the assembly of the Ca^{2+} initiation complex, which is composed of Bruton's tyrosine kinase (Btk), SLP-65 and phospholipase C-γ2 (PLC-γ2) (Engelke et al., 2007; Scharenberg et al., 2007). Phosphorylated tyrosines on SLP-65 allow binding of the SH2 domains of Btk and PLC-γ2 facilitating subsequent Btk-dependent phosphorylation and activation of PLC-γ2 (Hashimoto et al., 1999). PLC-γ2 itself is a main effector protein downstream of the BCR that feeds several signaling pathways by hydrolysis of PIP_2 creating the second messengers diacylglycerol (DAG) and inositol-1,4,5-tris phosphate (IP3) (Reth and Wienands, 1997).

DAG remains in the plasma membrane and recruits PKC-β and RasGRP leading to the activation of the transcription factor complex NFκB (Saijo, 2002) and the Ras/Erk MAP Kinase pathway (Oh-hora, 2003), respectively, that in turn activate the transcription of important target genes for B cell activation, proliferation and differentiation.

Upon hydrolysis of PIP_2, IP3 is released from the plasma membrane into the cytosol and is sensed by IP3-receptors 1-3 (IP3R1-3) in the ER-membrane. These ligand-operated Ca^{2+} channels open upon IP3 binding and lead to the passive flux of the key second messenger Ca^{2+} along its concentration gradient from the ER into the cytoplasm (Engelke et al., 2007; Scharenberg et al., 2007). The depletion of Ca^{2+} ions in the ER leads to the opening of so called store-operated Ca^{2+} channels (SOCs) in the plasma membrane. The mechanism by which signals from the ER opens ion channels in the plasma membrane has been extensively studied. It is now well established that the stromal interaction protein 1 (STIM1) senses depletion of Ca^{2+} ions in the ER through a luminal EF-hand Ca^{2+} binding motif near the N-terminus of STIM1 (Zhang et al., 2005). In the inactive state dimerized STIM1 resides evenly distributed in the

ER membrane with the EF-hand bound to Ca^{2+}. Store depletion causes Ca^{2+} to be released from the low-affinity EF-hand of STIM. In its Ca^{2+} unbound form STIM1 oligomerizes and translocates along microtubules into distinct punctae at ER-plasma membrane junctions (Baba et al., 2006). It could be shown that the C-terminus of STIM1-cluster directly interacts with the Ca^{2+} release-activated Ca^{2+} (CRAC) channel Orai and mediates its assembly and activation (Park et al., 2009), reviewed in (Cahalan, 2009). Opening of the CRAC channels leads to a characteristic sustained Ca^{2+} influx across the plasma membrane into the cytosol, which is termed store-operating Ca^{2+} entry (SOCE). In addition to Orai, other SOCs like the transient receptor potential (TRP) family seem to be activated by the same mechanism.
The described processes result in a major increase in cytosolic Ca^{2+} concentration rising from 10-100 nM in resting cells up to 10 μM in activated cells within tens of seconds. The cytosolic Ca^{2+} ions trigger the translocation of the transcription factor nuclear factor of activated T cells (NFAT) into the nucleus to activate target gene expression. In addition, Ca^{2+} binding to the conserved region 2 (C2-domain) of PKC-β is necessary for its full activation, thereby feeding into the PKC/NFκB pathway (Engelke et al., 2007).

Phosphoinositide 3′-Kinase

Engagement of the BCR also leads to the recruitment of phosphoinositide 3′-kinase (PI3K) to the plasma membrane by the co-receptor CD19 and the B-cell adaptor for PI3K (BCAP). PI3K is composed of a regulatory p85 subunit and a catalytic p110 subunit. Different isoforms of both subunits may interact and recruit the intact PI3K to their respective target sites, with p85α and p110∂ being the predominant isoforms acting downstream of the BCR (Okkenhaug and Vanhaesebroeck, 2003). PI3K uses the same substrate as PLC-γ2, phosphatidyl-inositol-4,5-bisphosphate (PtdIns(4,5)P_2 or PIP_2) and phosphorylates the 3′ position of the inositol ring. The resulting phosphatidyl-inositol-3,4,5-trisphosphate (PtdIns(3,4,5)P_3 or PIP_3) is recognized by pleckstrin-homology (PH)-domains of several effector and adaptor proteins. One of the major downstream effectors is Akt (also named protein kinase B, PKB), which is often used as a readout for PI3K activity (Kurosaki and Hikida, 2009). The PI3K/Akt pathway triggers important survival signals in B cells (Okkenhaug and Vanhaesebroeck, 2003; Srinivasan et al., 2009; Conley et al., 2012).

PI3K activity also contributes to the assembly of the Ca^{2+} initiation complex in that its product PIP_3 establishes a binding site for the PH-domains of Btk and PLC-γ2. Btk in turn constitutively binds phosphatidylinositol-4-phosphate 5-kinase (PIP5K) increasing the production of the PLC-γ2 and PI3K substrate PIP_2 at sites of active signaling. This feed-forward loop amplifies the assembly of signaling molecules after BCR engagement and is only one example of many positive and negative feedback loops that allow signaling pathway crosstalk, signal integration and fine-tuning of the cellular response to various extracellular cues.

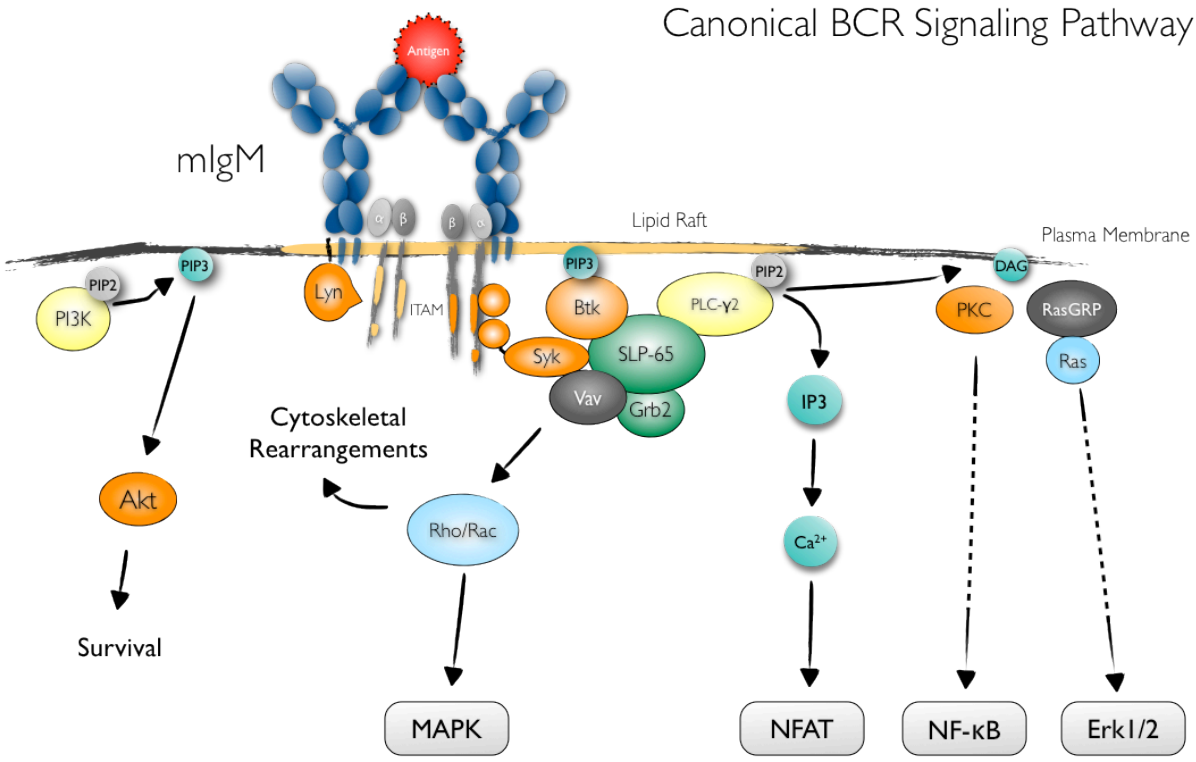

Figure 1 Schematic drawing of ITAM-mediated activating signaling events initiated by the B cell antigen receptor upon antigen binding. Crosslinking of the BCR by antigen causes translocation into lipid rafts (yellow line), where the ITAMs in Igα/β are phosphorylated by Src PTKs, such as Lyn. Subsequently, assembly of the BCR signalosome comprised of Syk, Btk, SLP-65, PLC-γ2, Vav, Grb2 and PI3K triggers many downstream signaling cascades. Further details are described in the text. Arrows indicate positive direct or indirect effector functions. Color-code: IgM-BCR is depicted in blue, kinases in orange, adaptor proteins in green, second-messengers in turquoise, small GTPases in light blue and GRPs/GEFs in dark grey.

Signal Integration Determines the Cellular Outcome – Negative Regulation

For the tight regulation of B cell activation negative regulatory functions are as important as positive signaling pathways. Besides others, two phosphatases play a major role in confining B cell activation. One is the SH2 domain containing 5′-inositol phosphatase (SHIP) that removes the 5′ phosphate from PIP_3 thereby targeting the recruitment of signaling proteins that are activated upon relocalization to the plasma membrane by virtue of their PH-domains such as Btk and Akt. This leads to the abrogation of all downstream signaling pathways. The other phosphatase is the SH2 domain-containing protein tyrosine phosphatase (SHP-1) that dephosphorylates tyrosine residues of SLP-65 and of the ITAMs in Igα/β (Nitschke and Tsubata, 2004). These negative regulators are activated in feedback-inhibition loop downstream of the BCR and are recruited to immunoreceptor tyrosine-base inhibitory motifs (ITIMs) in the cytoplasmic tails of inhibitory coreceptors, such as CD22, CD72 and FcγRIIb.
These negative regulatory pathways play a crucial role in tuning BCR signaling in response to different extracellular environments and setting activation thresholds for B cells needed for an appropriate development and immune response.

2.2.3 The Cytosolic Adaptor Grb2

Adaptor proteins are very important in establishing positive signaling complexes, but also for integrating negative regulatory circuits into the BCR signalosome. One adaptor that is associated with both functions is the growth factor receptor-bound protein 2 (Grb2). Due to the central role in the course of this thesis, I would like to describe it in more detail.
Grb2 is a cytosolic adaptor protein with a very simple architecture comprising of a central Src homology 2 (SH2) domain that is flanked by two SH3 domains. The SH3 domains establish constitutive binding to proline-rich motifs of binding partners. The N-terminal SH3 domain has been shown to bind typical polyproline motif with the consensus binding sequence PxxPxR (Feng et al., 1994; Sparks et al., 1996), while the C-SH3 domain interacts with an atypical PXXXR/KXXKP motif (Lewitzky et al., 2001). The SH2 domain in turn binds only to phosphorylated tyrosine-motifs with the consensus sequence pYxN (Songyang et al., 1994; Kessels et al., 2002; Machida and Mayer, 2005). Hence, Grb2 can be recruited along with its SH3-bound partners to sites of active signaling.

Grb2 was first described as an adaptor downstream of receptor tyrosine kinases linking the receptors to the Ras signaling cascade (Lowenstein et al., 1992). The SH2 domain of Grb2 binds to pYxN motifs of the epidermal and platelet-derived growth factor receptor (EGFR and PDGFR) and recruits the guanine nucleotide exchange factor called (GEF) Son of sevenless (Sos) that in turn activates Ras. This Grb2/Sos complex was originally thought to act downstream of the BCR as well. However, gene targeted knock out of Sos in the chicken DT40 B cell line showed no effect on BCR-induced Ras activation (Oh-hora, 2003). Rather it was demonstrated that Ras is predominantly activated by RasGRP downstream of PLC-γ2 activity, as described above. Still, Grb2-deficient DT40 cells showed a slightly reduced Erk activity indicating that there is more than one pathway resulting in Erk activation (Hashimoto et al., 1998).

Little is known about the exact function of Grb2 in B lymphocytes, though it appears to have ambivalent roles with involvement in both negative and positive signaling pathways (Jang et al., 2009). Overall, the negative function seems to dominate as Grb2-deficient DT40 cells show an enhanced Ca^{2+} mobilization after BCR stimulation (Stork et al., 2004). It was shown that recruitment of Grb2 with the adaptor downstream of kinase 3 (Dok-3) is pivotal for the negative regulation of Ca^{2+} flux. Dok-3 is recruited to the plasma membrane after BCR stimulation by its PH-domain and phosphorylated by Lyn on a YxN motif, enabling binding of the Grb2-SH2 domain. Although the exact mechanism is still to be investigated, the Grb2/Dok-3 complex attenuates Btk-dependent phosphorylation of PLC-γ2 leading to a decreased Ca^{2+} mobilization (Stork et al., 2007).

Grb2 is also involved in integrating negative regulatory coreceptors into the BCR signalosome. The Fc-receptor for IgG FcγRIIb for example recruits SHIP in association with Shc via its immunoreceptor tyrosine-based inhibition motif (ITIM). Grb2 itself binds to a pYxN motif in FcγRIIb and facilitates complex formation of FcγRIIb and SHIP (Isnardi et al., 2004). In addition inhibitory coreceptors CD22 and CD72 are phosphorylated by Lyn after BCR ligation and recruit SHP-1 (Nitschke and Tsubata, 2004). Analogous to the above-mentioned mechanism, Grb2 was shown to be important for SHP-1 recruitment to CD22 and CD72 coreceptors to exert its negative regulatory function (Fusaki et al., 2000; Otipoby, 2001).

Grb2 also exerts positive signaling function within the BCR signalosome. For example, Grb2 and SLP-65 cooperate in recruiting Vav into membrane rafts (Johmura

et al., 2003) by forming a ternary complex (Wienands et al., 1998). Vav is recruited to a phospho-tyrosine motif in SLP-65 after BCR engagement and Grb2 binds SLP-65 via its SH2 or C-SH3 domain. Grb2 also binds Vav through an atypical dimerization of SH3 domains (Ye and Baltimore, 1994; Nishida et al., 2001). Ablation of either Grb2 or SLP-65 leads to a reduction of Rac1 activation by 50% (Johmura et al., 2003), that is caused by the loss of Vav's GEF activity.

The multitude of Grb2 functions downstream of the BCR is mirrored by the plethora of positive and negative regulatory binding partners that were identified in an Grb2 interactome study by (Neumann et al., 2009) from our group (figure 2). The characteristics of the binding partners also suggest functions of Grb2 in PI3K signaling, cytoskeleton rearrangements and adaptor functions for ubiquitin ligases.

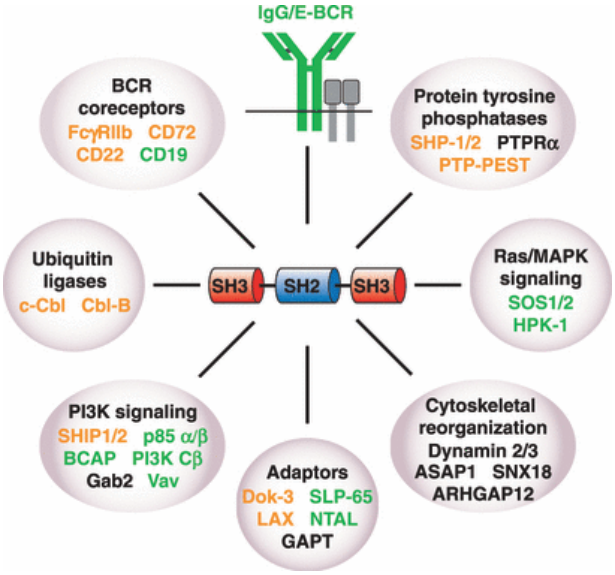

Figure 2 The Grb2 interactome in B cells. Schematic drawing of the domain structure of Grb2 in the center with its positive and negative regulatory binding partners around it (green and orange, respectively) from Neumann et al. 2009.

Recently, two groups have independently analyzed the function of Grb2 in B cells *in vivo* by genetically engineering a B cell specific $Grb2^{-/-}$ mouse. The studies also recapitulate the ambivalent role of Grb2. While the negative role is demonstrated by an increased Ca^{2+} mobilization and higher proliferation and activation of naïve mature B cells leading to increased production of serum IgM (Ackermann et al., 2011; Jang et al., 2011), the B cells also show an impaired development, defect in germinal

center establishment (Jang et al., 2011) and strongly reduced secondary immune response (Ackermann et al., 2011).
Taken together, Grb2 contributes to proper B cell development and productive immune responses by integrating several positive and negative signaling pathways fine-tuning the cellular response on the extracellular environment.

2.3 Isotype-Specific BCR Signaling - The Tail-Story

Naïve mature B cells express BCRs with Ig heavy chains of the isotypes μ and δ on their surface. However, upon antigen encounter B cells can undergo irreversible genetic rearrangements of the heavy chain locus during germinal center reactions resulting in a switch of isotype to either γ, ε, or α (Honjo and Kataoka, 1978; Honjo et al., 2002). With this move B cells modulate the effector function of the respective secreted antibody adapting it to the nature of the antigen. Furthermore, also the mIg heavy chains differ in that they posses cytoplasmic tails of 28 (γm, εm) and 14 amino acids (αm), respectively, compared to only three amino acids (KVK) in μm and ∂m (Reth, 1992). The γm- and εm-tails are very conserved between different species and subtypes. Alone the fact that these receptor isotypes are only expressed after class-switch of activated B cells has suggested a specialized function of their cytoplasmic domains in these class-switched and/or memory B cells (Reth, 1992).
Evidence that the tails play an important role in the B cell memory response came from genetic approaches, in which gene-targeted mice lacking the cytoplasmic tail of mIgG1 (Kaisho et al., 1997) or mIgE (Achatz et al., 1997), generate poor antigen-specific primary and strongly reduced secondary immune responses of the respective Ig-isotype. The drawback of these experimental setups was that in these Ig-tail-truncated mice other differences like receptor-affinity and altered surface expression may have influenced the phenotype. To investigate the role of the cytoplasmic tails independently of the above-mentioned differences, Martin and Goodnow used transgenic mice expressing hen-egg lysozyme-specific chimeric BCRs with equal affinity. These BCRs contained the extracellular part of IgM fused to the cytoplasmic tail of either μm, δm or γm. With these model they could show that the cytoplasmic tail of mIgG is sufficient to enhance antibody production, clonal expansion and reduce cell loss after activation, all of which are key-determinants of the immunological memory response Furthermore, they demonstrate that the

enhanced antibody response correlated to an increased number of plasma cells (Martin and Goodnow, 2002).

One potential mechanistic explanation was the exclusion of the inhibitory co-receptor CD22 from IgG and IgE BCRs. According to the studies, activation of CD22 and its downstream negative effector SHP-1 was diminished after mIgG and mIgE, but not after mIgM/D/A-BCR ligation (Wakabayashi et al., 2002; Sato et al., 2007).

However, in a back-to-back publication, the groups of Klaus Rajewsky and Chris Goodnow showed independently that IgG1-BCR signaling is indeed inhibited by CD22 and that enhancement of antibody responses by the cytoplasmic tails is independent of any inhibitory function of CD22 (Horikawa et al., 2007; Waisman et al., 2007). Both studies further investigated the signaling capabilities of the cytoplasmic tails using transgenic mouse models demonstrating an enhancement of Ca^{2+} mobilization after IgG1-BCR crosslinking. Surprisingly, the suggested signal amplification was not translated into stronger phosphorylation of major BCR downstream kinases, such as Erk, JNK and Akt. In fact, a detailed microarray analysis by Horikawa et al. explores BCR induced gene expression profiles after IgM- versus IgMG- (IgM with cytoplasmic tail of IgG1 attached) BCR engagement showing a reduced induction of many of the IgM-induced genes. This interesting finding lead the authors to conclude with a "less-is-more" hypothesis, in which a decreased signaling to a subset of BCR response genes enhances plasma cell differentiation and antibody response (Horikawa et al., 2007).

The above-described studies elucidate the great significance of the cytoplasmic tails of mIgG and mIgE in that their presence is absolutely essential to mount effective secondary immune responses. It is still to investigate if the tails are important for memory cell formation and/or maintenance or if they lead to a more rapid differentiation into antibody-secreting plasma cells upon stimulation of class-switched B cells. Also, the molecular mechanisms by which these tails communicate with intracellular signaling components to mediate the enhanced reactivation capacity of Ig class-switched BCRs remained totally elusive and will be the subject of this thesis.

Previous work of the group

The topic of this PhD thesis was based on findings by Niklas Engels and co-workers that the motif around a conserved tyrosine residue in the cytoplasmic tail of surface IgG and IgE resembles a consensus target site for protein tyrosine kinases. Indeed, using B cell line transfectants expressing either wild-type mIgG2a or a tyrosine-phenylalanine (YF) mutant, it was shown that the wild-type but not YF mutant cytoplasmic tail is phosphorylated in a stimulation-dependent manner. This tyrosine residue was subsequently entitled the "immunoglobulin tail tyrosine" (ITT).

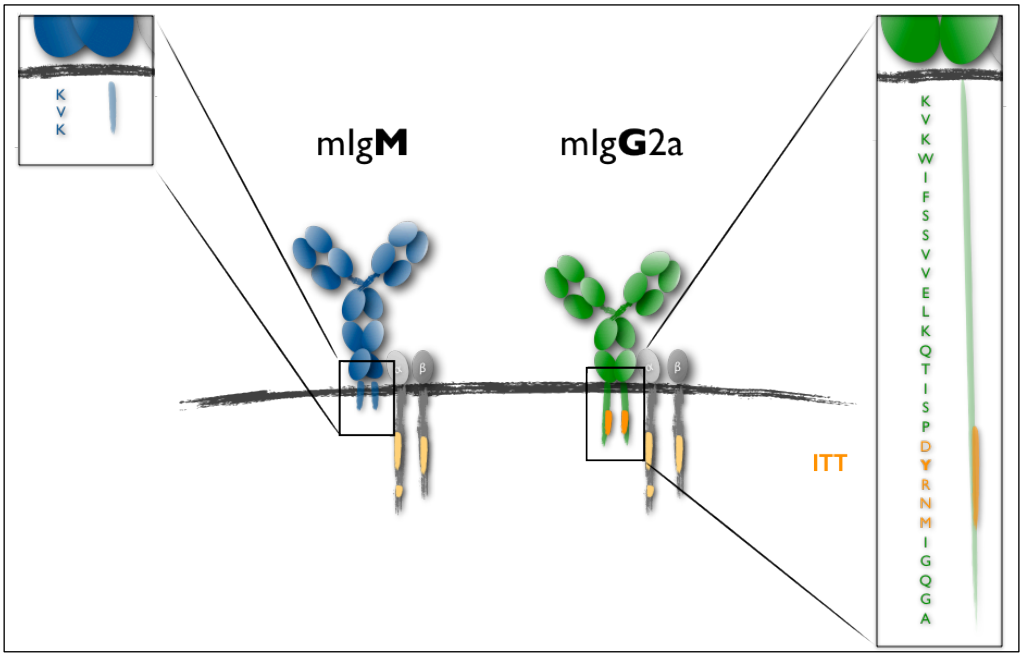

Figure 3 Schematic illustration depicting the differences of the cytoplasmic tails of IgM-BCR and IgG2a-BCR. mIgM contain only 3 amino acids (aa) in the cytoplasm, whereas mIgG have an elongated cytoplasmic tail of 28 aa. The conserved tyrosine motif, entitled immunoglobulin tail tyrosine (ITT) motif, is highlighted in orange.

The phosphorylated ITT motif of mIgG2a with the conserved amino acid sequence "DYRNM" also constitutes a consensus-binding site for the SH2 domains the p85 subunits of the PI3K and Grb2 suggesting an active role in signal transduction.
Moreover, it was shown that engagement of the wild-type ITT containing IgG2a-BCR, but not the YF mutant IgG2a-BCR, lead to a stronger phosphorylation of SLP-65 and PLC-γ2, much stronger IP3 production followed by an enhanced and sustained Ca^{2+} mobilization. Grb2 was identified as the main proximal binding partner using

phosphorylated and non-phosphorylated mIgG tail-peptides for affinity purification followed by silver staining of SDS-PAGE and mass spectrometry. This binding ability was further verified by affinity-purification of only phosphorylated IgG2a-BCR from Ramos cell lysates using recombinant GST-Grb2SH2 fusion proteins.
Upon this foundation I began my PhD thesis verifying the above mentioned results in primary B cells and exploring the molecular mechanism of ITT-signaling in more detail as described in the following chapter: Aims of This Work.

3 Aims of this Work

The cytoplasmic tails of mIgG and mIgE BCRs have been shown to be absolutely essential for the induction of a vigorous immune response (Achatz et al., 1997; Kaisho et al., 1997). How these tails exert this function was long completely elusive. The recent findings of our group that a conserved tyrosine residue within these tails is phosphorylated upon BCR ligation and amplifies Ca^{2+} mobilization possibly through recruitment of Grb2 constitutes a major advance in the mechanistic understanding of their function. The goal of my studies was to decipher the mechanism by which the cytoplasmic tails of mIgG and mIgE enhance BCR signaling of class-switched and memory B cells.

Following questions and issues were addressed:

1. The first goal was the validation of the previous results of our group using primary mouse B cells. To this end, methods to culture and transfect primary mouse B cells had to be optimized in order to allow monitoring of Ca^{2+} flux after stimulation of exogenously expressed BCRs.

2. What is the mode of action of ITT-based signal amplification? Is it an independent signaling unit or does it need to be integrated into the BCR signalosome?

3. Is Grb2 the exclusive downstream mediator of ITT signaling? As the ITT motif contains putative binding sites for the SH2 domains of Grb2 and p85 of PI3K, it was important to analyze which of these proteins mediates the enhanced signaling capacity.

4. How does Grb2 amplify BCR signaling? Which domains are important and what are downstream effectors of Grb2?

5. Which signaling pathways are modified by the ITT function other than Ca^{2+} mobilization and what impact does this have on the cellular response?

4 Materials & Methods

4.1 Materials

4.1.1 Chemicals & Proteins

All chemicals and reagents were purchased at Carl Roth or Sigma if not otherwise specified below.

Bromphenol Blue (Na^+-salt)	Merck
BSA	PAA
CIP	NEB
dNTPs	NEB
Ethanol (analytical grade)	UMG Apotheke
Indo-1 AM	Invitrogen
FCS	PAA
LPS (L2880-100MG)	Sigma
Pfu Polymerase	Fermentas
Phusion Polymerase	Finnzymes/NEB
Hexadimethrine Bromide (Polybrene)	Sigma
Protease Inhibitor Cocktail (P2714)	Sigma
Pyruvat	Biochrome
Restriction enzymes	NEB
T4-DNA-Ligase	NEB
Taq Polymerase	NEB
Trypsin/EDTA (0,05%)	Gibco

4.1.2 Technical Devices

Agarose gel trays and chambers		Peglab
Aqua bidest. Supply		Sartorius
Blot Detection Imager		Intas
Centrifuges	Multifuge 3 S-R RC 3B Plus Centrifuge 5415D Centrifuge 5417R (4°C)	Heraeus Sorvall Eppendorf Eppendorf
Cell Culture Microscope	Axiovert 35	Zeiss
FACS	Calibur LSRII	BD
Transfection	GenePulser & Cap. Extender Nucleofector II	BioRad Amaxa/Lonza
Incubators	HERACell 150	Heraeus
MACS	MultiStand & MidiMACS separator AutoMACS	Miltenyi Biotech
PCR machine	MasterCycler **ep**gradient	Eppendorf
Photospectrometer	BioPhotometer	Eppendorf
pH-Meter	inoLab® pH Level 1	WTW
Power supply	EPS-301/-3501 XL	GE Heathcare
Scales	BP61 H95	Sartorius
SDS gel chambers	Hoefer SE600 Ruby	GE Heathcare
Sonifier	Sinopuls UW/HD 2070	Bandelin
Thermoblock	comfort	Eppendorf
UV workbench	GelImager	Intas
Western blot device (semi-dry)	Semiphor Transpher Unit	GE Heathcare

4.1.3 Additional Materials

GeneRulerTM 1 kb DNA ladder (#SM0311)	MBI Fermentas
Glutathione-sepharose	GE Heathcare
LS Columns (130-042-401)	Miltenyi Biotech
Prestained Protein Marker, Broad Range (6.5-175 kDa) (#P7708)	NEB
Protease Inhibitor Cocktail (P 2714)	Sigma-Aldrich
Cell Culture Material	Greiner, Sarstedt, Nunc
Electroporation cuvettes (4 mm gap) (71-2030)	Peqlab
Nitrocellulose filter Hybond ECL™	GE Heathcare
Pre-seperation filters, 30 μm (130-041-407**)**	Miltenyi Biotech
Streptavidin-sepharose	GE HealthCare
Whattman Paper GB005	Schuett

4.1.4 Kits

- **Promega** Wizard® SV Gel and PCR Clean-Up System (A2982)
- **Promega** Wizard® Plus SV Minipreps DNA Purification System (A1460)
- **Promega** PureYield™ Plasmid Midiprep System (A2492)
- **Invitrogen** TA Cloning® Kit (with pCR®2.1 vector) (K2020-20)
- TransIT®-293 Transfection Reagent (**Mirus:** MIR 2700)
- **Sigma** CellVue® Claret Far Red Fluorescent Cell Linker Kit (MIDCLARET-1KT)
- Human B Cell Nucleofector® Kit (**Lonza**: VPA-1001)

4.1.5 Antibodies

Antibodies for Western Blotting

The following primary antibodies were diluted in TBST containing 3% BSA and 0,01% NaN_3.

Antigen	Source/Isoptype	Cat. #	Supplier
α-Grb2 (3F2)	mouse IgG1	610111	BD Transduction Laboratories™
α-Grap	goat	PAB6031	Abnova
α-Btk	mouse IgG2a	B80520	BD Transduction Laboratories™
α-pBLNK (pTyr96)	rabbit	3601	Cell Signaling Technology
α-BLNK (2C9)	mouse IgG_1	MMS-223R	Covance
α-pErk1/2	mouse IgG_1	9106	Cell Signaling Technology
α-Vav1	rabbit	2502	Cell Signaling Technology
α-pVav1	rabbit	2133-1	Epitomics
α-c-Cbl	mouse IgG_1	C40320	BD Transduction Laboratories™
α-Cblb	rabbit	sc-1704	SantaCruz Biotech
α-pTyr 100	mouse IgG_1	9411	Cell Signaling Technology
α-pTyr (4G10)	mouse IgG_{2b}	05-321	upstate
α-Sos1/2 (D-21)	rabbit	sc-259	SantaCruz Biotech
α-CD8-Biot.	mouse IgG_{2a}	1B-207-C100	EXBIO
α-IgG-Biot.	goat	2040-08	Southern Biotech
α-GST	rabbit	A-5800	Molecular Probes

Secondary antibodies were diluted 1:10 000 in TBST.

Antigen	Source	Cat. #	Supplier
α-mouse IgG_1-HRPO	goat	1070-05	Southern Biotech
α-mouse IgG_{2a}-HRPO	goat	1080-05	Southern Biotech
α-mouse IgG_{2b}-HRPO	goat	1090-05	Southern Biotech
α-mouse IgG-HRPO	goat	1030-05	Southern Biotech
α-rabbit IgG-HRPO	goat	4030-05	Southern Biotech

Antibodies for FACS

Antigen	Source	Cat. #	Supplier
α-hCD8-FITC (Mem-31)	mouse IgG2a	21270083	Immunotools
α-hCD8-PE (Mem-31)	mouse IgG2a	H12132P	EuroBioScience
α-mouse-IgG2a-FITC (γ chain specific)	goat	1080-02	Southern Biotech
α-mouse-IgG-Cy5 (γ chain specific)	goat	1030-15	Southern Biotech

Antibodies for BCR stimulation

Antigen	Type	Cat. #	Supplier
goat-α-mouse-IgG (Fc_γ fragment specific)	$F(ab')_2$	115-006-071	Jackson ImmunoResearch
goat-α-human-IgM ($Fc_{5\mu}$ fragment specific)	$F(ab')_2$	109-006-129	Jackson ImmunoResearch
goat-α-mouse-IgM (μ chain specific)	$F(ab')_2$	115-006-075	Jackson ImmunoResearch

4.1.6 Plasmids

Table : Plasmids used in this study.

Backbone/Name	Insert		Source
Vectors for Cloning/cDNA Resource			
pCR2.1			Invitrogen
pCRII-Topo			Invitrogen
pBlueScript SK+			Stratagene
pmaxKS			N. Engels
pTagRFP-C			Evrogen
pGEX-4T1			GE Healthcare
pMSCVpuro			Clontech
pMSCVblast			M. Engelke
MigRII			E. Vigorito
MiRFP			This work
pcDNA3puro			Invitrogen/G. Yigit
pcDNA3puro	CD8-Dap10t	wt	M. Engelke
		YF	
pCRII-Topo	lmp2a (EBV B95-8) cDNA		N. Engels
pGEX	Mouse Grb2		J. Wienands
pCMV-SPORT6	Human Grap		OpenBiosystems
pQCXIN	Ecotropic Receptor		T. Brummer, Freiburg
pcDNA3.1	CKAR		K. Svoboda (via Addgene)
pRK5	cytEKAR		A. Newton (via Addgene)
Expression Vectors			
pSVγ2am neo			P. Weiser, Freiburg
pSVγ2amΔtail neo			N. Engels
pSVγ2am YF neo			
pSVγ2am YF neo	mGrb2C-SH3		This work
pcDNA3puro	CD8mε	wt	N. Engels
		YF	

Retroviral Expression Vectors			
pMSCVpuro	γ2am	wt	N. Engels
		YA	This work
		NA	
		MV	
	γ2am YF-Grb2N-SH3	wt	
		W36K	
	γ2am YF-Grb2C-SH3	wt	
		W193K	
		F165A	
MigRII	γ2am	wt	
		YF	
		NA	
	γ2am YF-Grb2N-SH3	wt	
		W36K	
	γ2am YF-GrapN-SH3	wt	
		W36K	
	γ2am-Dap10t	wt	
		YF	
	γ2am-CD28Δ25t	wt	
		YF	
	γ2am-lmp2aCtail	wt	
		YF	
MiRFP	mGrb2	wt	
		W36K	
		F165A	
pMSCVblast	Ecotropic Receptor		
GST-Fusions			
pGEX-4T1	Grb2N-SH3	wt	This work
		W36K	
	GrapN-SH3	wt	
		W36K	
Transient Expression of Biosensors			
pmaxKS	EKAR		This work
	CKAR		

4.1.7 Oligonucleotides

Table 2: Oligonucleotides used in this study.

#	Name	Sequence (5'-3' direction)
Primer for Cloning		
1	EKAR fwd	gcctcgagagatctgtaccggtcgccaccatg
2	EKAR rev	gcctcgaggcaggtcgactctagatc
3	tagRFPncoifwd	gccccatggtgtctaagggcgaag
4	tagRFPstopsalrev	gccgtcgacttaaagtttgtgccccagtttgc
5	DAP10tNhei_fwd	ggccatgctagcgtgcgcacgcccacgccg
6	DAP10tNheiStop_rev	ggccatgctagctcagcccctgcctggcatg
7	CD28fwd	ggccatgctagcctggacaaatagtagaaggaac
8	CD28d25rev	ggccatgctagctcaagtcatgttcatgtagtcac
9	CD28d25YFrev	ggccatgctagctcaagtcatgttcatgaagtcac
10	lmp2anheifwd	ggccatgctagctagatgctgccgctactgc
11	lmp2anheistoprev	ggccatgctagcttatacagtgttgcgatatgg
12	lmp2aCtYFNherev	ggccatgctagcttatacagtgttgcgaaatgg
13	Grb2NheiGlyfwd	gccgctagcggtatggaagccatcgccaaatatg
14	Grb2NSH3StopNheirev	gccgctagcttaatgtggtttcatttctatg
15	Grb2CSH3Nheifwd	gccgctagcccacagcagccaacctacgtccag
16	Grb2StopNheirev	gccgctagcttagacgttccggttcactgg
17	Grb2fwdbglnco	gcagatctaccatggaagccatcgccaaatatgacttc
18	Grap fwd	gcgaattcgctagcggtatggagtccgtggccctg
19	Grap NSH3 rev	gcctcgaggctagcttaatggggcttgacgcggatg
20	Grap CSH3 fwd	gcgaattcgctagccctggggcctgctttgc
21	Grap rev NheXho	gcctcgaggctagctcacaggtgcacgggctgcacgtaac
Primer for site-directed mutagenesis		
22	g2amutBfwd	gattgggcagggagccgctagctaggccacttcctctg
23	g2amutBrev	cagaggaagtggcctagctagcggctccctgcccaatc
24	pCRIIg2amutBfwd	gggcagggagccgctagctagaagggcgaattc
25	pCRIIg2amutBrev	gaattcgcccttctagctagcggctccctgccc
26	N-SH3 W36K fwd	gaatgtgaccagaacaagtataaggcagaactcaatg
27	N-SH3 W36K rev	cattgagttctgccttatacttgttctggtcacattc
28	R86Kmutfwd	ccttcctgatcaaagagagcgagagcgctc
29	R86Kmutrev	gagcgctctcgctctctttgatcaggaagg
30	grb2W193Kfwd	gataactcagatcccaataagtggaaaggggc
31	grb2W193Krev	gccccttccacttattgggatctgagttatc

32	C-SH3 F165A fwd	ctacgtccaggcgctcgctgactttgacccccag
33	C-SH3 F165A rev	ctgggggtcaaagtcagcgagcgcctggacgtag
34	Grap W36K fwd	gaggatgaccagaacaagtacaaggccgagctc
35	Grap W36K rev	gagctcggccttgtacttgttctggtcatcctc
36	Grap W195K fwd	gcccagacccccacaagtggcggggccggtcctg
37	Grap W195K rev	caggaccggccccgccacttgtgggggtctgggc

Sequencing Primer

40	M13 fwd	tgtaaaacgacggccagt
41	M13 rev	caggaaacagctatgacc
42	g2aCH3fwd	ctctggacgaccatcaccatc

4.1.8 Bacterial Strains

Name	Genotype
Top10F′	F'[lacIq Tn10(tetR)] mcrA Δ(mrr-hsdRMS-mcrBC) ϕ80lacZΔM15 ΔlacX74 deoR nupG recA1 araD139 Δ(ara- leu)7697 galU galK rpsL(StrR) endA1 λ-
BL21 (DE3)	F^- ompT gal dcm lon $hsdS_B(r_B^- m_B^-)$ λ(DE3 [lacI lacUV5-T7 gene 1 ind1 sam7 nin5])

4.1.9 Software

CloneManager	SECentral
FlowJow 8.8.6	TreeStar
CellQuest Pro	BD
Papers 2	Mekentosj
Office for Mac 2011	Microsoft
iWorks ‘09	Apple
ImageJ	National Institute of Health, USA

4.2 Methods

4.2.1 Molecular Biology/Cloning

4.2.1.1 Cultivation of *E. coli* Strains

E. coli cells were grown in LB or 2YT medium supplemented with appropriate selective antibiotics under aeration. For short time storage cells were streaked out on LB-agar plates with selective antibiotics, grown overnight at 37°C and stored at 4°C. A glycerol-stock was made by adding 500-1000 µl overnight culture to an autoclaved microcentrifuge tube with screwable top containing 500 µl glycerol for long-term storage at - 80°C.

Media & Antibiotics

LB-medium	Ingredient	2YT medium
10 g/l	tryptone	16 g/l
5 g/l	Yeast extract	10 g/l
5 g/l	NaCl	10 g/l

- for medium add H_2O, mix until solved → bottle in appropriate volume, autoclave, add antibiotics if needed
- for agar plates, add 15 g/l agar, autoclave, let solution cool down a little while stirring, add antibiotics if needed, pour plates
- Following antibiotics were used:

Antibiotic	**Concentration**
Ampicillin	100 $^{\mu g}/_{ml}$
Kanamycin	50 $^{\mu g}/_{ml}$

4.2.1.2 Preparation of Plasmid DNA

For the purification of plasmid DNA from *E. coli,* an overnight culture was inoculated in selective 2YT medium. Plasmid preparation was performed the next day from 2 ml culture using the Promega Wizard® Plus SV Minipreps DNA

Purification System or from 50 ml culture using the Promega PureYield™ Plasmid Midiprep System as depicted in the manufacturer's protocol. To elute DNA from the column, 50 µl and 600 µl $H_2O_{bidest.}$ was used for MiniPreps and MidiPreps, respectively.
The isolated plasmids were validated by restriction enzyme control digest and new cDNAs were sent to SeqLab (Göttingen) for sequencing.

4.2.1.3 Restriction Endonuclease Digest

Preparative Digest
Plasmid and insert were cut by restriction enzymes as a preparation step for ligation. To this end, 2-3 µg DNA were incubated in a 40 µl reaction volume containing the respective 10x NEB reaction buffer and restriction enzyme(s) for 2-3h. The enzymes, buffers and conditions were applied as described by the manufacturer New England Biolabs. Vector backbones with compatible cohesive ends, e.g. cut with only one enzyme, the 5' phosphate group was removed by the addition of 1 µl CIP for 15-30 min in order to decrease religation tendency. Purification was done by agarose gel electrophoresis followed by gel extraction.

Analytical Restriction Enzyme Digest
For analysis of plasmid DNA the plasmid was cut with appropriate restriction enzymes using a 30 µl restriction enzyme mix (3 µl DNA, 3 µl 10x buffer, 1 µl enzyme and 23 µl H_2O). The reaction mix was then incubated for 1 h at 37°C followed by agarose gel electrophoresis.

4.2.1.4 Polymerase Chain Reaction (PCR)

Inserts of interest were amplified from a template via polymerase chain reaction. To this end, the following reaction mix was prepared and amplification program was used:

PCR sample preparation (50μl)

Volume [μl]	Reagent
1	Template (50-250 ng/μl)
10	5x Phusion HF-buffer
1	dNTP mix (25 mM each)
1	Forward primer (10 μM)
1	Reverse primer (10 μM)
35,5	$H_2O_{dest.}$
0,5	Phusion polymerase

PCR amplification program

1. Initial Denaturing	1 min, 98°C	
2. Denaturing	15 sec, 98°C	32 cycles
3. Annealing	30 sec, 58-62°C	
4. Elongation	15-30s/1000bp, 72°C	
5. Final elongation	5 min, 72°C	

The PCR products were analyzed and purified by agarose gel electrophoresis followed by gel extraction using the Promega Wizard® SV Gel and PCR Clean-Up System.

4.2.1.5 Site-Directed Mutagenesis PCR

PCR allows site-directed mutagenesis of double-stranded plasmid DNA. To this end, primer with the desired mutations are used to amplify plasmid DNA by proofreading polymerases resulting in nicked circular strands that have incorporated the mutations. The parental DNA template strand without the mutation is afterwards digested by DpnI, which only cuts methylated DNA. The residual DNA comprises only the single-stranded mutated plasmid DNA, which transformed into Top10F', where the nicked mutated strands are repaired resulting in double-stranded plasmid DNA that contains the desired mutation.
The reaction was set up as described in 4.2.1.4. The amplification program was modified reducing the annealing temperature to 55°C and elongation temperature

was decreased to 68°C applying an appropriate elongation time. The reaction was repeated 20 cycles. Afterwards, 1 µl DpnI was added to the reaction mix and incubated for 1 hour at 37°C. 2 µl of this solution was then transformed into competent Top10F' and plated on selective media.

4.2.1.6 TA-Cloning

PCR products were cloned into pCR2.1 vector using the TA Cloning® Kit (Invitrogen) as described in the manufacturer's instructions. PCR products without 3' adenosine overhang were treated with Taq polymerase and additional dATPs for 20 min at 72°C. After purification with the Promega Wizard® SV Gel and PCR Clean-Up System the product was used for TA cloning.

4.2.1.7 Agarose Gel Electrophoresis

Agarose flatbed gel electrophoresis with appropriate concentrations (0.7-2%) of agarose was used to separate DNA fragments according to their size. To this end, agarose was dissolved in TAE buffer by heating it in a microwave. The solution was filled into a tray with combs and ethidium bromide was added in concentrations of 0.1 % (v/v) to allow visualization of DNA fragments. After the agarose had solidified, the gel was put into the gel chamber, samples were loaded after the addition of 6x DNA loading buffer and the gel electrophoresis was performed in TAE buffer at 1,2 V/cm^2.

TAE-buffer	40 mM	Tris-acetate (pH 8.0)
	10 mM	NaOAc
	1 mM	EDTA
	in	ddH_2O

6x loading buffer	50% (v/v)	glycerol
	0,25% (w/v)	bromophenol blue
	in	ddH_2O

4.2.1.8 DNA Extraction from Agarose

To isolate DNA fragments of interest from an agarose gel, the corresponding bands of a preparative agarose gel were cut out and extracted using the Promega Wizard® SV Gel and PCR Clean-Up System. DNA was eluted from the column with 20µl $H_2O_{bidest.}$.

4.2.1.9 Ligation of DNA Fragments

To ligate an insert of interest into a compatible vector T4-DNA-ligase was used in a 10 µl reaction mix. Plasmid DNA and insert were added in an estimated molar ratio of 1:3. After the addition of 1 µl 10x T4-Ligase buffer (NEB), ddH_2O and 0,5 µl of T4-DNA-Ligase the reaction mix was incubated at room temperature for 30-60 min. A control was made in parallel determining the religation propensity of the plasmid. To this end, no insert was included in the reaction mix. Both, the actual ligation mix and the control were transformed into Top10F' cells and plated on corresponding selective media.

4.2.1.10 Preparation of Chemically Competent *E. coli* Cells

Bacterial strains were made competent using the $CaCl_2$ method described in (Inoue et al., 1990).

4.2.1.11 Heat Shock Transformation of Competent *E. coli* Cells

An aliquot of competent cells was thawed on ice and 2 µl of ligation mix (or 0,5 µl for retransformation of a plasmid) was added. After incubating 10 min on ice the cells were heat-shocked at 42°C for 45 sec. in a thermo mixer. Afterwards, the cells were put on ice again for 5 min and plated on selective LB-agar plates. If bacteria were to be selected with kanamycin 900 µl LB medium without antibiotics was added to the heat-shocked bacteria followed by incubation on a shaker at 37°C for 1 hour. Subsequently, cells were harvested by centrifugation for 3 min at 8.000 rpm and 900 µl supernatant was discarded. The pellet was re-suspended in remaining medium and plated on kanamycin containing LB-agar plates.

4.2.2 Biochemistry

4.2.2.1 Expression and Purification of GST-Fusion Proteins

GST-fusion proteins were made by cloning the respective cDNA into the pGEX-4T1 (GE Healthcare). The resulting vector encoding the GST-fusion protein was transformed into BL21, an overnight culture thereof was diluted 1:1000 in 50 ml 2YT medium and expression of the GST-fusion protein was induced at OD 0,5 with 100 μM IPTG at 37°C for 4 ½ hours. Subsequently, bacteria were harvested by centrifugation, the pellet was resuspended in 50 ml PBS and lysed by ultrasonification on ice (3x 30 sec, 1 cycle, 50%). 500 μl 10% Triton X-100 was added to the lysates and incubated for 10 min on ice. Insoluble material was pelleted at 3000g for 6 min and the supernatant was divided into 10 ml aliquots for storage at -20°C. GST-fusion proteins were purified from 10 ml aliquots by adding 250 μl glutathione-sepharose beads and incubating on a rotator at 4 °C for 2h. Afterwards, beads were washed three times with 10 ml and resuspended in 250 μl PBS.

4.2.2.2 Stimulation of B cells via their BCR

Cells were harvested and washed once with PBS. The cell pellet was resuspended in pre-warmed RPMI 1640 without FCS (R0) and cells were incubated for 30 min at 37°C to reduce stimulatory effects from FCS. Cell number was adjusted to 3-5x10^7 cells/ml in R0, transferred into a 1,5 ml microcentrifuge tube and stimulated with 10 μg/ml anti-IgG F(ab')$_2$ or 10 μg/ml of biotinylated anti-IgG at 37°C for 3 min. Then, cells were quickly spun down in a microcentrifuge, the medium was aspirated and the cells were lysed in 200 μl NP40-lysis buffer/10^7 cells on ice for 10 min. Insoluble cell debris were sedimented at 16 000 x g at 4°C for 10 min. 25 μl of the cleared lysates were mixed 1:1 with 2x Laemmli buffer (see 4.2.2.4) and incubated at 95°C for 5 min for complete denaturation of the proteins. The remaining cleared lysate was used for affinity purification.

4.2.2.3 Affinity Purification

For affinity purification of the BCR the precipitating antibody had already been used for stimulating the BCR (see above). 30 μl streptavidin-sepharose beads (GE HealthCare) were added to the cleared lysates and rotated for at least one hour at 4°C. For affinity purification with N-terminally biotinylated γ2a-peptides 2 μM were

added to the cleared lysates and 20 µl Streptavidin-sepharose was added before incubation for an hour at 4°C. Beads were washed three times with NP40-lysis buffer, resuspended in 30 µl Laemmli buffer, heated at 95°C for 5 min and samples were analyzed by SDS-PAGE and immunoblotting.

4.2.2.4 SDS-PAGE

Solutions for preparing a 10% resolving gel and 5% stacking gel for SDS-PAGE

Resolving Gel	Reagent	Stacking Gel
8-12%	AA/BAA (17.5:1)	5%
375 mM	Tris, pH 8.8	-
-	Tris, pH 6.6	125 mM
0,1%	SDS	0,1%
0,00065 %	APS	0,001%
0,001%	TEMED	0,001%
	H_2O	

APS and TEMED were added just before the gel was poured since they start the polymerization reaction.

SDS-Running Buffer

25 mM	Tris
192 mM	Glycine
0,1 % (w/v)	SDS

2x Reducing Sample Buffer (Laemmli)

62,5 mM	Tris/HCl pH 6,8
2% (w/v)	SDS
0,025% (w/v)	Bromphenol blue
20% (v/v)	Glycerol
in	$H_2O_{bidest.}$
5%	β-mercaptoethanol

4.2.2.5 Western Blotting

Western Blot is a technique that allows the immobilization of proteins on a membrane for further analysis and visualizing by immunostaining. The proteins are transferred horizontally out of the gel onto a membrane by electrophoresis. In this work, the semi-dry blotting technique was used. To this end, two Whattman paper and a nitrocellulose membrane were cut into proper size and soaked in blotting buffer (see below). Afterwards, a stack of Whattman paper, membrane, gel and Whattman paper was formed. Air-bubbles were removed from each layer with a pizza roller or a glass pipette. The blot was then run at I const. = 1 mA/cm^2 for 60 min.

Blotting buffer	48 mM	Tris
	39 mM	Glycine
	0,0375% (v/v)	SDS
	20 %	MeOH
	in	$H_2O_{dest.}$

4.2.2.6 Immunostaining

Immunostaining allows the visualization of proteins or peptides on a membrane in a two-step process using specific antibodies (first antibody) and secondary HRPO-coupled antibodies that recognize the Fc-region of first antibody and allows the visualization via the ECL® detection system (GE Healthcare).
First, the membrane was blocked in 5% BSA in TBST for 45 min at RT on a shaker. Afterwards, it was washed 3x in an excess of TBST for 5 min each time and incubated in the 1st antibody for one to three hours at RT or overnight at 4°C on a shaker. After washing the 3x with TBST the 2nd antibody was applied for one hour. Again, the membrane was washed with TBST (5x 5min) and then bathed in 4 ml ECL® solution. Detection was done digitally with the Chemilux Camera System (Intas).

TBST	25 mM	Tris/HCl, pH 8.0	
	125 mM	NaCl	
	0.1%	Tween 20	
	in	$H_2O_{dest.}$	→ adjust to pH 7.4

4.2.3 Cell Biology

4.2.3.1 Cell Lines

Ramos (DSMZ-No: ACC 603)
The Ramos human B cell line was derived from the ascitic fluid of a 3-year-old boy with American-type Burkitt lymphoma in 1972. The cells harbor the (8;14) IgH/MYC translocation and p53 mutations. Ramos cells express BCRs with μ heavy chains and λ light chains (Klein et al., 1975).

DG-75 (DSMZ-No: ACC 83)
This cell line derived from a pleural effusion of 10-year old child with Burkitt lymphoma in 1975. In contrast to other Burkitt lymphoma derived cell lines, DG-75's μ heavy chains are paired with κ light chains (Ben-Bassat et al., 1977).

DG-75 EcoBlast (EB) (this work)
DG-75 cells were modified to express the ecotropic receptor in order to enable retroviral infection using ecotropic viruses. With this derivative infection efficiencies of 10-20% are reached compared to below 0,5% for cells without ecotropic receptor.

Plat-E (Platinum-E)
Plat-E is a retroviral packaging cell line based on HEK293T cells. Compared to other packaging cell lines Plat-E are superior regarding efficiency, stability and safety. The viral structural genes are expressed under the control of the EF1α promotor, which is 100-fold more potent than the MuLV-LTR used in other cell lines. To maintain stable high expression of the viral genes under drug selection, an internal ribosomal entry site (IRES) was inserted between the *gag-pol* and *env* genes and the selectable markers Blasticidin and Puromycin, respectively (Morita et al., 2000).(Engels et al., 2009)(Engels et al., 2009)

4.2.3.2 Cell Culture, Handling & Storage

Cell Culture & Handling
All cells were cultured in a 5 % CO_2 humidified atmosphere at 37 °C. Ramos, DG-75 and primary splenic B cells were grown in R10 (see below). Plat-E cells were cultured in D10 (see below) and selected every two weeks in the presence of puromycin and

blasticidin. The adherent Plat-E cells were grown to maximum confluence of 80% and split using 0,05% Trypsin/EDTA (GIBCO 25300). For harvesting or washing cell lines were centrifuged at 300 g for 4 min, prim B cells at 500 g for 6 min at room temperature if not otherwise indicated. Cell numbers were counted using a Neubauer chamber slide.

Long-Term Storage

For long term storage cells were harvested and resuspended at a density of around $1x10^7$ cells/ml in freezing medium (see below), transferred to a cryo-tube and immediately put at -80 °C in a polystyrene box, thereby guaranteeing a freezing rate of approximately -1 °C/min. Afterwards, cryo-tubes were transferred to -140°C for long term storage.

Cells were thawed rapidly at 37 °C and immediately put into 10 mL culture medium to dilute the DMSO. Then the cells were centrifuged, resuspended in fresh culture medium and transferred to an appropriate Petri dish.

Media

D10 Medium DMEM 4196 + Glutamax (4,5 g/l Glucose)
+ 10% heat-inactivated FCS
+ 3 ml L-glutamine (200 mM)
+ 5 ml pyruvate (stock 100 mM)
+ 50 U/mL penicillin and 50 µg/mL streptomycin

R10 Medium RPMI 1640 + Glutamax
+ 10% heat-inactivated FCS
+ 3 ml L-glutamine (200 mM)
+ 5 ml pyruvate (stock 100 mM)
+ 50 U/mL penicillin and 50 µg/mL streptomycin
+ 50 μM 2-mercaptoethanol

Freezing Medium 90% heat-inactivated FCS
10% DMSO

PlatE Freezing Medium 50% heat-inactivated FCS
40% D10
10% DMSO

Selection Marker were used at the following concentrations:

Selection Marker	Concentration
Puromycin	1 μg/ml
Blasticidin	10 μg/ml
G418	1 mg/ml

4.2.3.3 Isolation of Primary Splenic Mouse B cells

The spleen of an at least 8-week old C57BL/6 mouse was prepared and homogenized through a 70 μm cell filter into a Petri dish. Cells were washed off the culture dish with 10 ml R10, transferred into a 15 ml Falcon tube and centrifuged at 500 g for 6 minutes at 4°C. After discarding the supernatant, cells were resuspended in 1 ml per spleen in erythrocyte lysis buffer (see below) and incubated 2 min on ice in order to get rid of erythrocytes from the preparation. To stop the lysis reaction 14 ml R10 was added, cells were centrifuged and washed once with 10 ml R10. At this point, cells are counted and afterwards subjected to the CD43 depletion magnetic activated cell sorting (MACS) as described by the manufacturer's protocol (Miltenyi) using the CD43 (Ly-48) MicroBeads (Order-No 130-049-801) and LS MACS separation columns (Order-No 130-042-401). The negative fraction of cells were then plated at a density of 1 x 10^6 cells per ml in R10 supplemented with 10 μg/ml LPS (Sigma L2880-100MG). B cell purity was analyzed by FACS and was usually around 92-95% IgM+ CD19+ cells.

Erythrocyte Lysis Buffer
A) 0,16 M NH_4Cl
B) 0,17 mM Tris/HCl pH 7,6
→ mix 9 parts A with 1 part B just before usage, sterile filtrate (0,2 μm filter)

4.2.3.4 Transfection Methods

Electroporation

In order to stably transfect human B cell lines by electroporation $1x10^7$ cells were harvested and resuspended in 700 µl GenePulser buffer (Ramos cells) or RPMI 1640 without supplements (DG-75), transferred into a 4 mm electroporation cuvette (Peqlab) and incubated on ice for 10 min. Electroporation was performed using a Bio-Rad Gene Pulser™ at 250 mV and 960 µFD. Afterwards, cells were shortly put on ice and then seeded on a 24-well plate in pre-warmed R10 and incubated at 37°C. 48 hours later, cells were put under selection pressure. After clonal growth of transfected cells, clones were picked, transferred into a new culture dish and later checked for expression of the transfected cDNA.

Amaxa (Lonza)-Nucleofection

$2x10^6$ cells were harvested and centrifuged at 90 g for 10 min at room temperature. The supernatant was completely removed and nucleofection was performed using the Lonza Human B Cell Nucleofector® Kit (VPA-1001) as described by the manufacturer. In short, 82 µl of Human B Cell Nucleofector® Solution were mixed with 18 µl of Supplement 1. Cells were resuspended in the resulting 100 µl nucleofection solution and transferred into the nucleofection cuvette. After adding 2 µg of plasmid DNA cells were transfected using program T-015 on the Amaxa Nucleofector™ II device and seeded in an appropriate culture dish in pre-warmed R10.

Transfection of PlatE with TransIT® and Virus Production

All volumes and cell numbers indicated are adjusted for a 10 cm Petri dish standard. For other sizes volumes and cell numbers were changed accordingly. 18-24h prior to transfection $3x10^6$ cells of the virus-packaging cell-line PlatE were plated on a 10 cm Petri dish in pre-warmed D10 medium in order to grow to 60-70% confluence until the next. For best transfection efficiency a homogenous distribution of the cells on the plate and the indicated confluence is very important. Higher confluence will reduce transfection efficiency and viral titer. Transfection of PlatE were performed using *Trans*IT®-293 transfection reagent (Mirus). To this end a transfection solution was prepared by mixing 16 µl *Trans*IT solution in 500 µl of FCS-free DMEM medium.

After 15 min incubation at room temperature 6-8 µg of plasmid DNA was added, mixed and incubated for another 15-30 min. Meanwhile the medium of the PlatE cells was aspirated and 5 ml of pre-warmed D10 was carefully pipetted onto the edge of the petri dish to avoid detachment of the cells. Subsequently, the transfection solution was added drop wise and well distributed over the dish. After 24 hours incubation at 37°C 3 ml fresh pre-warmed D10 was added carefully. 48 hours after transfection the virus containing cell medium (virus-supe) was harvested and filtrated through 0,4 µm filter to remove detached cells. For a higher virus-titer cells were moved to 32°C for 6 hours to increase the half-life of the virus before the virus-supe was harvested.

Concentration of the Virus-Supe

For the infection of primary mouse B cell blasts (LPS stimulated) the virus-supe was concentrated by centrifugation at 20.000g at 4°C for 90 min in 2 ml microcentrifuge cups. 1,25 ml supernatant was carefully removed and the invisible pellet was resuspended in the remaining 750 µl. The concentrated virus-supe was directly used for infection.

Retroviral Infection of Cell Culture Cells

For retroviral infection of cell lines 4 ml unconcentrated virus-supe was added to 1-2x10^6 cells in 1 ml R10 and supplemented with 4 µg/ml polybrene. The cells were incubated over night at 37°C, centrifuged and resuspended in fresh medium. 48 hours after infection medium cell were selected by the addition of the respective antibiotic.

Retroviral (Sp)infection of Primary Mouse Splenic B cells

In order to be infectable by retroviruses the primary splenic mouse B cells have to proliferate. To this end they were stimulated with 10 µg/ml lipopolysaccharide (LPS) for 24 or 48 hours. After 48h hours more cells will be proliferating enhancing the amount of cells amenable to infection and it is possible to increase total number of infected cells. Stimulation for 48h is suppose to result in more proliferating follicular B cells while MZ B cells seem to proliferate already after 24h of LPS stimulation. However, if experiments are performed that require the cells to stay alive for a few days the infection should be done as soon as possible (LPS o/n - 24h). Cells can be

kept in LPS containing medium for about a week, but after days 4-5 the number of live cells will decrease rapidly.
For the infection 1-5x10^6 LPS-stimulated cells were transferred to a 50 ml Falcon (the higher surface area at the bottom compared to 15 ml Falcons increases infection efficiency) and the medium was replaced by 500 µl fresh pre-warmed R10. After adding 1,5 ml concentrated virus-supe, 4 µg/ml polybrene and 10 µg/ml LPS cells were centrifuged at 1,500g for 3h 30min at 33°C. This so called "spinfection" leads to a much higher infection rate than just incubating the cells at 37°C. The supernatant was discarded after the spinfection and the cells were resuspended in R10 plus 10 µg/ml LPS and plated at a density of 1-2x10^6 cells/ml. Infection efficiency was checked 24 or 48 hours after infection by FACS analysis.

4.2.3.5 Flow Cytometry

Fluorescent Protein Expression
To analyze expression of a fluorescent protein marker 300 µl cell suspension was transferred to a FACS tube and checked for fluorescence by flow cytometry.

Protein Surface Expression
Protein surface expression was detected by staining with fluorescently labeled antibodies followed by flow cytometry. 0,5x10^6 cells were transferred to a FACS tube and washed once with cold PBS. The supernatant was poured away leaving about 200 µl of PBS remaining in the tube. 0,5 µl of fluorescently labeled antibody raised against the protein of interest was added. After vortexing the cell suspension, cells were incubated on ice for 20 min in the dark and washed once with cold PBS that again was discarded after centrifugation. Cells were resuspended in 200-500 µl PBS and subjected to FACS analysis.

4.2.3.6 Analysis of Ca^{2+} Mobilization

One major signaling event after BCR crosslinking is the release of Ca^{2+} ions as a second messenger from the ER and from extracellular sources into the cytosol. These concentration changes can be observed by a flow cytometric analysis using the Ca^{2+} sensitive dye Indo-1-AM that shifts its fluorescence emission wavelength upon Ca^{2+} binding.

1-2x10^6 Cells were harvested and loaded with 1 μM Indo-1-AM in 700μl R10 containing 0.015% (vol/vol) Pluronic®-F127 at 30°C for 30 min under mild agitation. The cells were washed once with and resuspended in Krebs Ringer solution. The volume was adjusted so that at least 300 cells/sec could be measured for the desired time frame. The fluorescence ratio change of $Ca2^+$-bound Indo-1 (405 nm) to Ca^{2+}-unbound Indo-1 (530 nm) was monitored before and after cells were stimulated with 10 μg/ml anti-IgG F(ab')$_2$ or 20 μg/ml anti-IgM F(ab')$_2$ on an LSR II cytometer (Becton Dickinson). Ca^{2+} mobilization from intracellular and extracellular sources were differentiated by measuring cells in Krebs Ringer solution with 0,5 mM EGTA instead of $CaCl_2$ first to analyze Ca^{2+} release from the ER before adding 1 mM $CaCl_2$ to monitor influx from extracellular sources.

Krebs Ringer
10 mM HEPES, pH 7.0
140 mM NaCl, 4 mM KCl
1 mM $MgCl_2$
1 mM $CaCl_2$
10 mM glucose
ad $H_2O_{bidest.}$

4.2.3.7 Flow Cytometric FRET (FCET) Analysis

For the analysis of FRET-based genetically encoded biosensors, plasmid DNA encoding the respective biosensor was transfected by Amaxa nucleofection (see 4.2.3.4) for transient expression of the biosensor. 48h later cells were harvested and put on starvation in pre-warmed RPMI without FCS at 37°C for 30 min. Afterwards cells were washed with and resuspended in Krebs Ringer solution. The special setup of the LSR II flow cytometer allows measuring FRET between cyan and yellow fluorescent proteins (FPs). To this end, mCFP was excited at 405 nm and detected at 450/50 filter while the FRET signal was detected using a 550BP32 filter set. The change of FRET over mCFP fluorescence was monitored in mCFP/mCitrine (or derivatives of these FPs) double positive cells over time before and after stimulation of the BCR with 10 μg/ml anti-IgG F(ab)$_2$ or 20 μg/ml anti-IgM F(ab)$_2$.

4.2.3.8 Proliferation Assay

At 24 h after retroviral infection, cells were stained with the plasma membrane–intercalating dye CellVue Claret (Sigma) according to the manufacturer's protocol. Stained cells were seeded in 96-well plates at a density of 2 x 10^5 cells per 200 ml R10 medium supplemented with 10 μg/ml LPS. After stimulation for 96 h with goat anti–mouse IgG F(ab)$_2$ fragments (10 μg/ml), the CellVue Claret median fluorescence intensity of eGFP$^+$ cells was normalized to that of eGFP$^-$ cells from the same wells acting as an internal control. The decrease in fluorescence intensity served as measure of proliferation.

5 Results

5.1 The Immunoglobulin Tail Tyrosine (ITT) Delivers Costimulation to the BCR

5.1.1 The ITT Amplifies Ca^{2+} Influx after BCR Stimulation in Primary Splenic Mouse B Cells

To investigate the role of the ITT in mIgG-BCR signaling, wild-type (wt) or tyrosine-phenylalanine (YF) mutant γ2am cDNA was expressed in primary mouse B cells. To this end, splenic B cells from C57BL/6 mice were isolated and pre-stimulated with LPS as a prerequisite for retroviral infection. The LPS stimulated B cell blasts were infected with a retrovirus expressing wt or YF γ2am cDNA together with an internal ribosomal entry site (IRES)-driven translation of eGFP (figure 4a) allowing detection and quantification of infected B cells by flow cytometry (figure 4b). Surface expression of transfected BCRs correlate with eGFP expression (figure 4c). Infection efficiency was very low at the beginning (~5%). Through continuous optimization of the infection protocol and concentration of the virus supernatant I was able to reproducibly infect primary mouse B cells with 50-80% infection efficiency.

Ca^{2+} mobilization after anti-IgG stimulation of the transfected wt or YF mIgG2a was measured by flow cytometric analysis of the ratiometric Ca^{2+}-sensitive dye Indo 1-AM. As shown in figure 4d, only eGFP-positive cells responded to stimulation with anti-IgG $F(ab)_2$ fragments while eGFP-negative cells did not respond at all showing that the IRES-driven co-expression of eGFP is a reliable means to distinguish transfected, γ2am expressing cells from untransfected cells. In addition, LPS-induced Ig class-switching to surface IgG isotypes could be excluded to influence the measurement. In accordance with previous results obtained from tumor B cell lines, Ca^{2+} flux after stimulation of wt mIgG2a BCR compared to YF mutant mIgG2a was strongly increased in primary mouse B cells (figure 4d, eGFP positive fraction).

To distinguish the Ca^{2+} flux from intracellular and extracellular sources, the measurements were repeated first in presence of 0,5 mM EGTA to monitor Ca^{2+} release from the ER before the addition of 1 mM $CaCl_2$. This approach allowed subsequent observation of Ca^{2+} influx from extracellular sources. As the Ca^{2+} mobilization profile in figure 4e shows, the difference in Ca^{2+} mobilization after wt or

YF mIgG2a stimulation is mainly driven by a stronger influx of Ca^{2+} ions across the plasma membrane. Taken together, the results clearly show that the ITT-containing BCR effectively amplifies BCR-driven Ca^{2+} mobilization in primary mouse B cells.

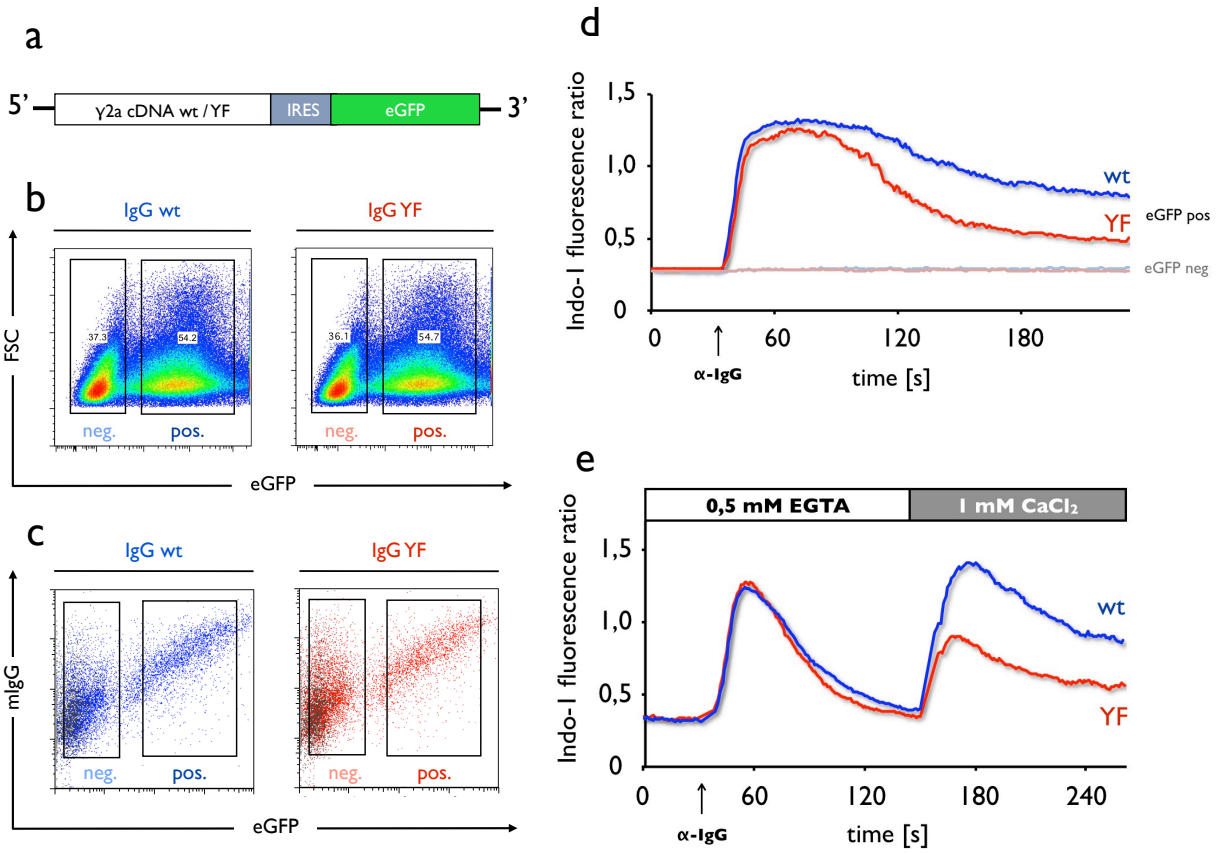

Figure 4 The ITT amplifies BCR-induced Ca^{2+}mobilization in primary mouse B cells. (**a**) Schematic drawing of the retrovirally packaged cDNA. Wild-type or YF mutant γ2am cDNA was cloned into the MCS of MigRII vector (pMSCV backbone). The internal ribosomal entry site (IRES) enables simultaneous expression of eGFP with the mIgG2a permitting transfected and untransfected cells to be distinguished by flow cytometry (**b**). (**c**) Surface expression of transfected mIgG2a-BCRs stained with Cy5-labeled anti-IgG antibodies. (**d**) Flow cytometric analysis of the Ca^{2+} mobilization of primary mouse B cells transfected with either wt or YF mutant mIgG2a. Cells were loaded with the Ca^{2+} sensitive dye Indo1-AM, basal levels were monitored for 30 seconds after which cells were stimulated with 10 µg/ml goat anti-mouse IgG $F(ab`)_2$ fragments (time point indicated by black arrow) and Ca^{2+} flux was measured for an additional 3 ½ minutes. Cells expressing wt or YF mIgG2a (blue and red curve, respectively) were gated on eGFP-negative and eGFP-positive cells (faint or saturated colored, respectively) as indicated in **b, c**. Data are representative of at least 5 independent experiments using different C57BL/6 mice. (**e**) Intra- and extracellular Ca^{2+} flux was measured in the same cells as in **d**, but in Krebs-Ringer solution with 0,5 mM EGTA without $CaCl_2$. After anti-IgG stimulation Ca^{2+} flux from intracellular stores were monitored for 2 min, then extracellular Ca^{2+} concentration was adjusted to 1 mM $CaCl_2$ in order to monitor Ca^{2+} influx across the plasma membrane. Data are representative of two independent experiments.

5.1.2 ITT Signal Amplification Relies on BCR Integration and the Number of ITT Motifs Have a Cumulative Effect on Signaling Strength

To analyze if the ITT signal augmentation was dependent on integration into the ITAM-based signaling machinery of the BCR or if it represented an autonomous signaling unit, the ITT was "outsourced" from the mIgG2a-BCR. For this, the ITT-containing cytoplasmic tail of mouse εm was genetically fused to the extracellular and transmembrane domains of the T cell co-receptor CD8, which was subsequently co-expressed with or without wt or YF mutant mIgG2a on the surface of the Ramos B cell line. This setup enabled the stimulation of CD8-εm and mIgG-BCR individually or in combination by co-crosslinking the anti-CD8 antibody (mouse IgG isotype) and mIgG2-BCR with anti-mouse IgG $F(ab)_2$ fragments (figure 5a).
First, CD8-εm was crosslinked with anti-CD8 (MEM-31) alone for 1 min during which no Ca^{2+} release was observed. Then, CD8-εm and mIgG2a-BCR were co-crosslinked by the addition of goat anti-mouse IgG $F(ab)_2$ antibody fragments integrating CD8-εm into the BCR signaling unit. Co-crosslinking of wt CD8-εm and mIgG2a YF lead to an enhanced and longer lasting Ca^{2+} mobilization (figure 5b, dark blue curve) compared to co-crosslinking of YF mutant CD8-εm and YF mutant mIgG2a, thereby mimicking the Ca^{2+} mobilization pattern of the wt mIgG2a-BCR (figure 5b, red curve). Interestingly, the Ca^{2+} release was even higher when wt CD8-εm was co-crosslinked with wt mIgG2a revealing a cumulative effect depending on the number of ITTs within the BCR signalosome (figure 5b, light blue curve). Co-crosslinking of CD8-εm in the absence of mIgG (grey curve) resulted only in a minor and delayed Ca^{2+} mobilization indicating that the integration into the BCR signaling unit is a prerequisite for ITT signal amplification. In line with these results, phosphorylation of the CD8-εm chimeric protein and subsequent recruitment of Grb2 was only observed after co-crosslinking with the mIgG2a-BCR (figure 5c).
In conclusion, the results show that the ITT needs to be physically incorporated into the BCR signalosome in order to administrate its role in Ca^{2+} signal amplification. As this integration is a fundamental characteristic of costimulation by certain co-receptors it supports the idea of a 'BCR-intrinsic' costimulation of mIgG and mIgE expressing B cells. These cells may thus be less dependent on additional costimulation than mIgM expressing B cells.

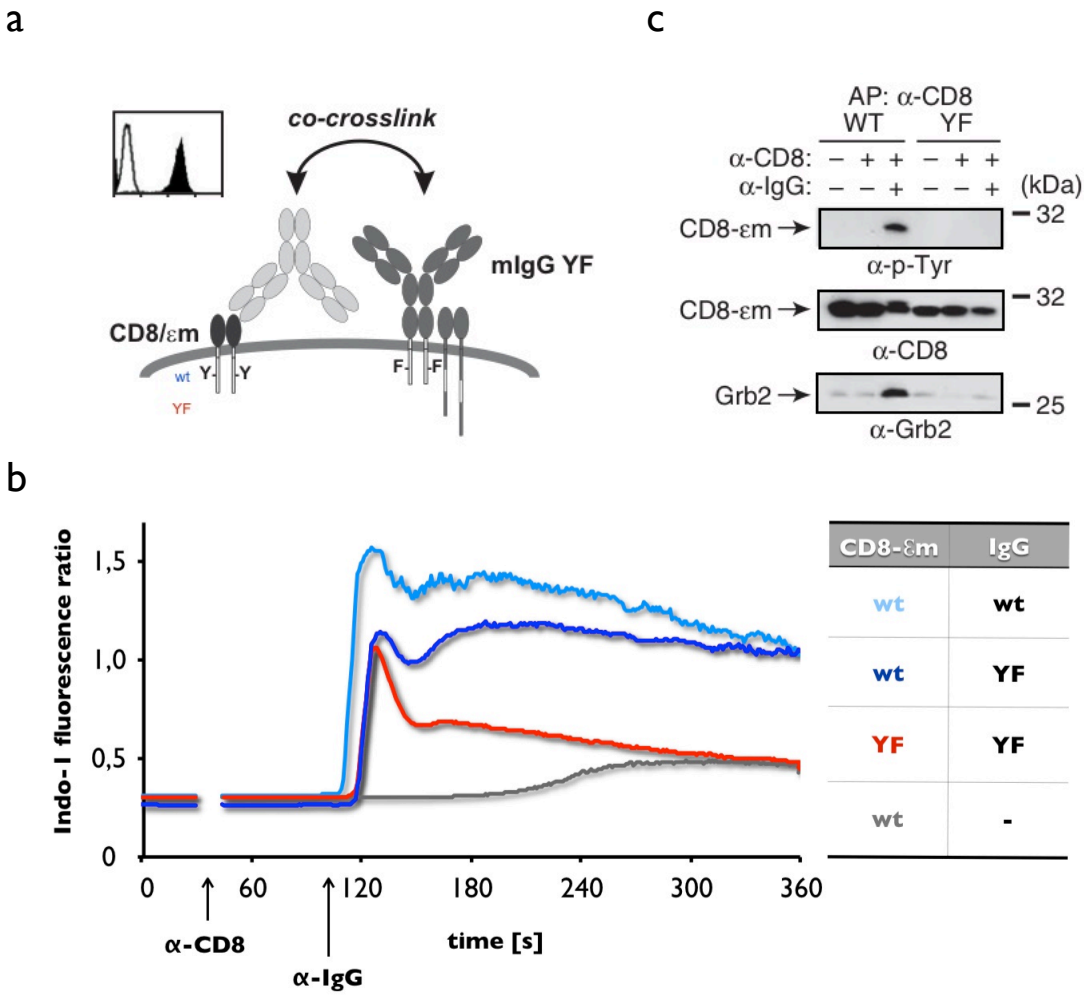

Figure 5 ITT signal amplification is dependent on integration into the BCR signalosome. (**a**) Schematic illustration of the experimental set-up. Ramos B cells co-expressing wt or YF mIgG2a and a chimeric construct composed of the extracellular and transmembrane domains of CD8 and the cytoplasmic tail of wt or YF mutant mouse εm. Cells were stimulated with anti-CD8 antibodies to crosslink CD8-εm and then with anti-IgG F(ab`)$_2$ fragments that co-crosslink the anti-CD8 antibody and the IgG2a-BCR. (**b**) Ca^{2+} mobilization of Ramos transfectants expressing the indicated receptors (see table). Indo1-AM-loaded cells were left untreated for 30 seconds, stimulated with 1,25 µg/ml anti-CD8 (Mem-31) for 1 min and then the transfected receptors were co-crosslinked with 10 µg/ml anti-IgG F(ab`)$_2$ fragments. Data are representative of four experiments using at least four independent clones for each construct (two clones for wt mIgG2a/wt CD8-εm co-expressing cells) with similar surface expression. (**c**) Immunoblot analysis of affinity-purified wt or YF mutant CD8-εm from cells co-expressing YF mIgG2a (dark blue and red line in **b**). Cells were either left untreated, stimulated with biotinylated anti-CD8 alone for 3 min or additionally stimulated with anti-IgG for 5 min. Cells were subsequently lysed, CD8-εm constructs were affinity-purified using streptavidin-sepharose beads and analyzed by western blot probed for phospho-tyrosine, CD8 and Grb2 (as indicated). On the right margin are relative molecular masses of marker proteins. Data are representative of two independent experiments.

5.2 The Cytosolic Adaptor Grb2 is Essential for ITT-based Ca^{2+} Signal Amplification

The amino acid sequence „DYRNM“ (single letter code) of the mIgG2a-ITT motif comprises potential binding sites for the SH2 domains of either Grb2 (p**Y**x**N**) or the regulatory p85 subunits of PI3-Kinase (p**Y**xx**M**). Previous work of our group suggested that the ITT transduced its costimulatory function by the recruitment of Grb2, however, the involvement of other proteins like PI3K or members of the Grb2/Sem-5 family was not ruled out. Therefore, in the following chapters I describe different approaches addressing these issues.

5.2.1 Inactivation of the Grb2 Binding Motif within mIgG Abrogates Ca^{2+} Signal Amplification

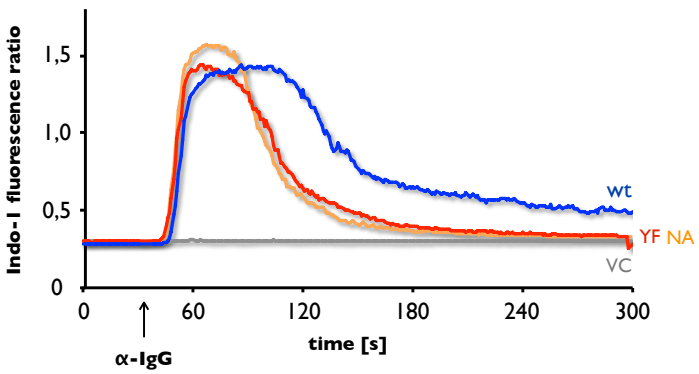

Figure 6 The Grb2 binding site is essential for ITT-based signal amplification. Primary B cells from 8-week-old C57BL/6 mice were retrovirally transfected with wt, YF and NA mutant γ2am cDNA and an IRES-driven co-expression of eGFP or eGFP alone (vector control, VC). Cells were loaded with Indo1-AM and Ca^{2+} mobilization was measured before and after stimulation with 10 µg/ml α-IgG $F(ab)_2$ fragments. Data are representative of three independent experiments.

To test the requirement of the Grb2 SH2 domain consensus binding sequence “pYxN” for the signal amplification of the ITT, an Asn-to-Ala (NA) mutation was introduced into γ2am cDNA. This mutation abrogates binding of Grb2 but retains tyrosine phosphorylation of the ITT as shown earlier by Niklas Engels in cell culture experiments (Engels et al., 2009). The NA mutant mIgG2a-BCR was expressed in primary B cells and compared to wt and YF IgG-BCR for its Ca^{2+} mobilization capacity after stimulation with anti-IgG antibodies. As depicted in figure 6 the NA mIgG-BCR lost its ability to amplify Ca^{2+} mobilization as compared to wt mIgG-BCR and equals the more transient Ca^{2+} response after stimulation of the YF mIgG-BCR. The results show that tyrosine phosphorylation of

the ITT per se is not sufficient for Ca^{2+} signal amplification but only leads to enhanced signaling in the context of the Grb2 consensus binding site.

5.2.2 The Putative p85 Binding Site is Dispensable for Enhanced Ca^{2+} Signaling

To test whether the p85 binding site is also required for the Ca^{2+} flux enhancing role of the ITT, a Met-to-Val (MV) mutant was introduced destroying the p85 binding site while conserving the Grb2 binding motif. Wild-type and mutant mIgG2a-BCRs (YA, NA and MV) were retrovirally expressed in the DG75 EB cell line. Infected cells were selected and surface expression was ascertained by FACS analysis using a Cy5-labeled anti-IgG antibody for staining (figure 7a). The MV mutant did not confine the ITT's function as the Ca^{2+} mobilization after stimulation with anti-IgG antibodies was comparable to wt mIgG2a (figure 7b, blue and green curve) showing a much stronger and sustained Ca^{2+} release compared to the YA and NA mutant mIgG2a-BCRs. The

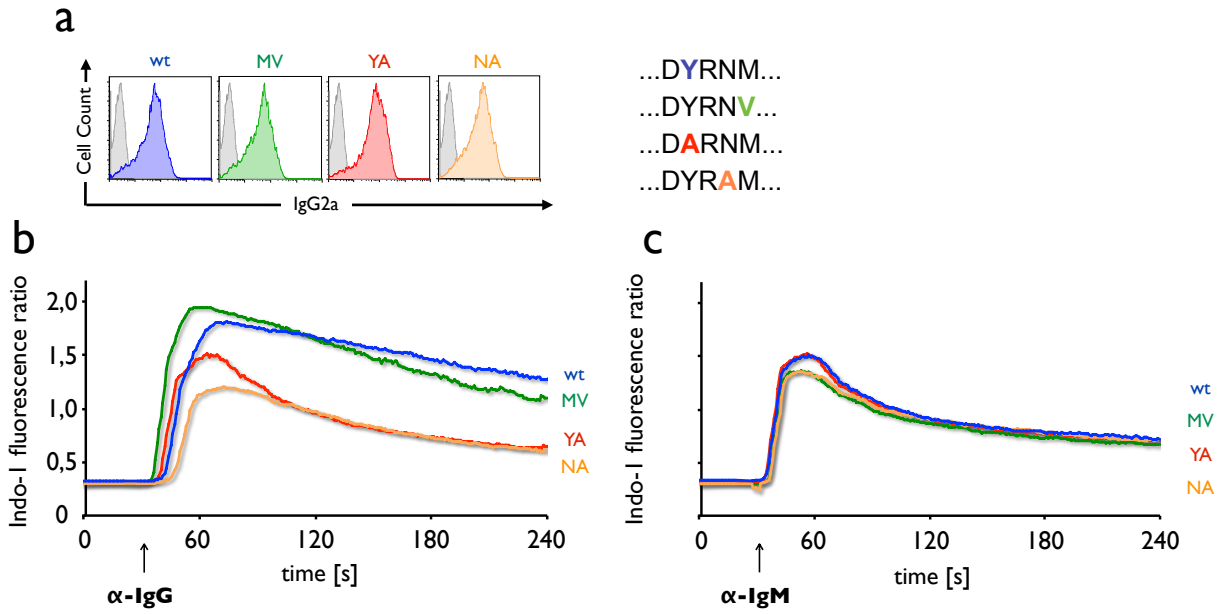

Figure 7 Signal amplification of the ITT is independent of the putative p85 binding sequence. (**a**) DG75 EB were retrovirally transfected with wild-type, YA, NA or MV mutant ɣ2a cDNA (mutation within the ITT motif described on the right side). Infected cells were selected and surface expression was analyzed by flow cytometry using an anti-IgG-Cy5 staining. (**b**) Cells from **a** were loaded with Indo1-AM and Ca^{2+} mobilization was monitored before and after stimulation with 10 µg/ml goat anti-mouse IgG $F(ab)_2$ antibody fragments by flow cytometry. (**c**) Ca^{2+} flux analysis with the same cells as **a, b**, stimulated with 20 µg/ml goat anti-human IgM $F(ab)_2$ fragments. All Data are representatives of three independent experiments.

transfected cells were all tested for equal Ca^{2+} mobilization capacity by stimulation of the endogenous mIgM-BCR (figure 7c). This experiment confirmed that the Grb2 binding consensus sequence but not the p85 binding is essential for the co-stimulatory effect of the ITT.

5.2.3 The Grb2/Sem-5 Family Member Grap Can Bind to the Phospho-ITT Motif

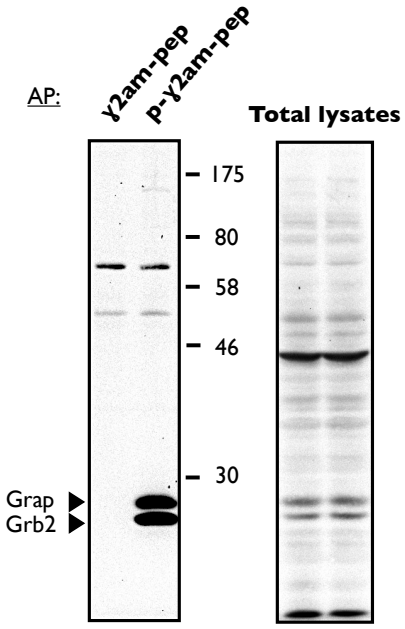

Figure 8 Grap binds to the pITT motif. Proteins were affinity purified from DG75 lysates with N-terminal biotinylated peptides comprising the ITT motif and surrounding amino acids with (p-γ2am-pep) or without (γ2am-pep) a phosphorylated ITT and immobilized with streptavidin-sepharose. Immunoblot of the purified proteins (left) and total lysates (right) were assessed with anti-Grap and anti-Grb2 antibodies. Numbers indicate relative molecular mass of marker proteins in kDa. Blots are

After the necessity of the Grb2 binding motif for Ca^{2+} signal amplification was established, the question arose whether there are other members of the Grb2/Sem-5 family sharing this binding consensus sequence that instead of Grb2 might account for the signaling capacity of the ITT. To pursue this question I affinity-purified proteins with streptavidin-sepharose-bound N-terminally biotinylated peptides resembling the phosphorylated ITT and surrounding amino acids of the cytoplasmic tail of mIgG2a. To distinguish between background and phosphorylation induced binding, non-phosphorylated peptides were used as controls for affinity purification. Immunoblots were probed for co-purification of Grb2 and Grap as an example of another Grb2/Sem-5 family member. Analysis of the purified proteins by western blot clearly demonstrates that, in addition to Grb2, Grap is also enriched by affinity purification in a phosphorylation-dependent manner (figure 8). This raised the possibility that other proteins than Grb2 are recruited to the ITT in order to exert its function.

5.2.4 Grb2 Deficiency Abrogates ITT-based Ca^{2+} Signal Amplification

To analyze whether Grb2 is the only functional binding partner of the ITT or if other family members like Grap are responsible for Ca^{2+} signal amplification I compared the Ca^{2+} release after wt and YF mIgG-BCR stimulation in B cells deficient for Grb2. To this end, I isolated B cells from B cell specific conditional $Grb2^{-/-}$ mice from the group of Lars Nitschke (Department of Biology, Friedrich-Alexander-University, Erlangen) and B cells from wild-type mice and retrovirally transfected them with wt and YF γ2am cDNA. To distinguish between transfected and untransfected cells the

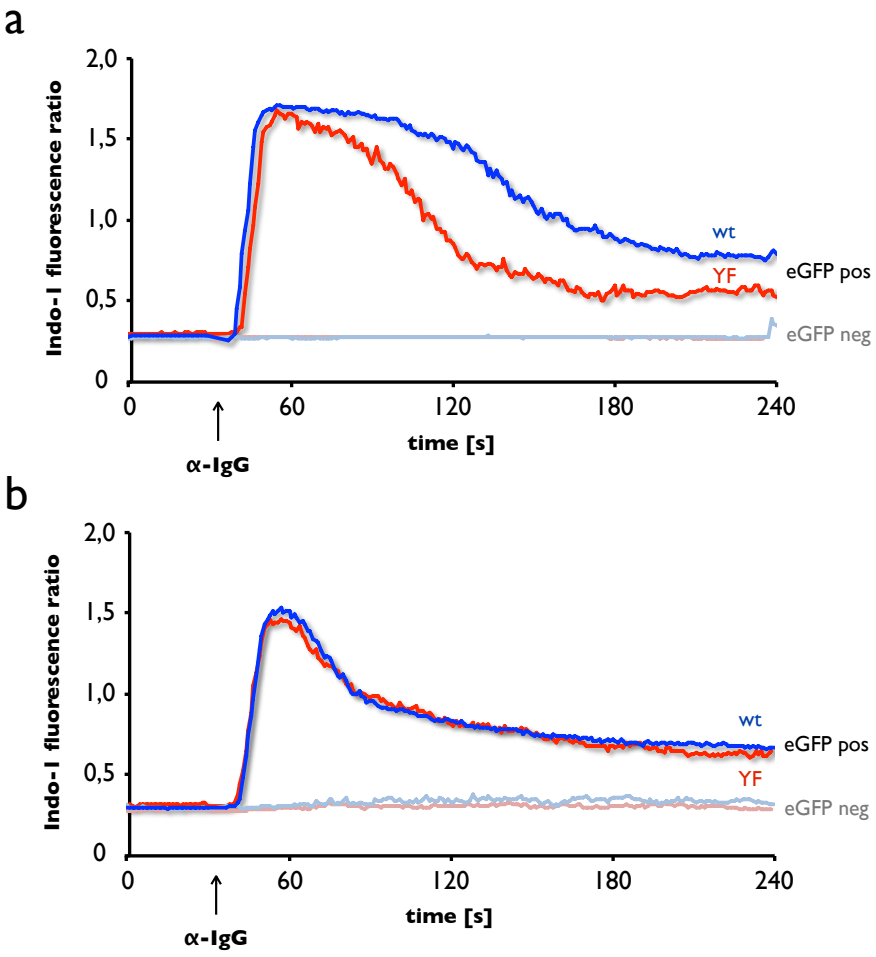

Figure 9 Grb2 is essential for Ca^{2+} signal amplification. Splenic B cells of $Grb2^{fl/fl}$ $mb1^{cre/+}$ and control mice were pre-stimulated with LPS for retroviral infection with viruses harboring either wt or YF mutant γ2am cDNA followed by an IRES-eGFP cassette. Cells were loaded with Indo1-AM and Ca^{2+} flux was analyzed by flow cytometry gating on GFP positive or GFP negative cells as described in figure 1. Cells were stimulated with 10 µg/ml anti-IgG $F(ab)_2$ antibody fragments after 30 seconds and Ca^{2+} mobilization was monitored for additional 3 ½ minutes in B cells from control mice (**a**) and B cell-specific $Grb2^{-/-}$ knockout mice (**b**). Data represent one of three independent experiments.

retrovirus contained an IRES-driven eGFP marker. As shown earlier (figure 4) Ca^{2+} mobilization was much enhanced when stimulating wt mIgG-BCR compared to YF mutant mIgG-BCR in primary B cells from wild-type control mice (figure 9a). However, this signal enhancement of wt mIgG was completely abrogated in B cells deficient for Grb2 with Ca^{2+} release being identical after stimulation of wt and YF mIgG (figure 9b). As internal controls, eGFP-negative cells did not show any Ca^{2+} release due to the absence of exogenous mIgG2a (figure 9, faint red and blue lines).
These data demonstrate that Grb2 is essential for the ITT-based costimulation of mIgG-BCR signaling and that any other proteins with binding ability to the ITT like Grap cannot compensate for its function in boosting Ca^{2+} mobilization.

5.2.5 Reconstitution of Grb2 Restores Costimulation Via the ITT

B cell-specific Grb2-deficient mice show an impaired maturation of B cells leading to a reduced number of transitional and mature follicular B cells in the spleen (Ackermann et al., 2011). Despite the reduced number of mature B cells, those that differentiate into mature B cells appear phenotypically normal. To preclude nevertheless any indirect effect of Grb2-deficiency, like differences in the differentiation state of the B cells, to be the cause for the absence of signal amplification after wt mIgG-BCR compared to YF mIgG-BCR stimulation, I reconstituted the Grb2-deficient B cells with mouse Grb2 (mGrb2) cDNA. To this end, I double-infected LPS-stimulated primary Grb2-deficient B cells with one retrovirus comprising γ2am cDNA and an IRES-eGFP cassette and the other harboring mGrb2 cDNA and an IRES-tagRFP cassette. Hence, during flow cytometric Ca^{2+} measurement it was possible to gate on non-infected (G1, figure 10a), mGrb2 expressing cells (G2), mIgG positive cells (G3) or double positive cells expressing both surface IgG and mGrb2 (G4). As expected, both eGFP (and therefore mIgG) negative populations G1 and G2 did not respond to anti-IgG $F(ab)_2$ treatment with Ca^{2+} release. EGFP only positive cells showed the same transient Ca^{2+} release pattern shown above for Grb2-deficient cells (G3, compare to figure 10b). The reintroduction of mGrb2 resulted in a strong increase in Ca^{2+} mobilization after wt mIgG-BCR stimulation (Fig 10b, G4). As the difference in expression levels of eGFP and, connected to it, of mIgG between G3 and G4 may account for the stronger Ca^{2+} release, I analyzed double-infected cells with either wt or YF γ2am cDNA and

mGrb2 cDNA, respectively. The same gate was used for both double-infected cells (figure 10c, blue and red gate) to ensure equal expression levels. As depicted in figure 10d and in line with earlier results, stimulation of wt mIgG-BCR resulted in an amplified and sustained Ca^{2+} release compared to YF mIgG-BCR in the presence of reconstituted mGrb2.

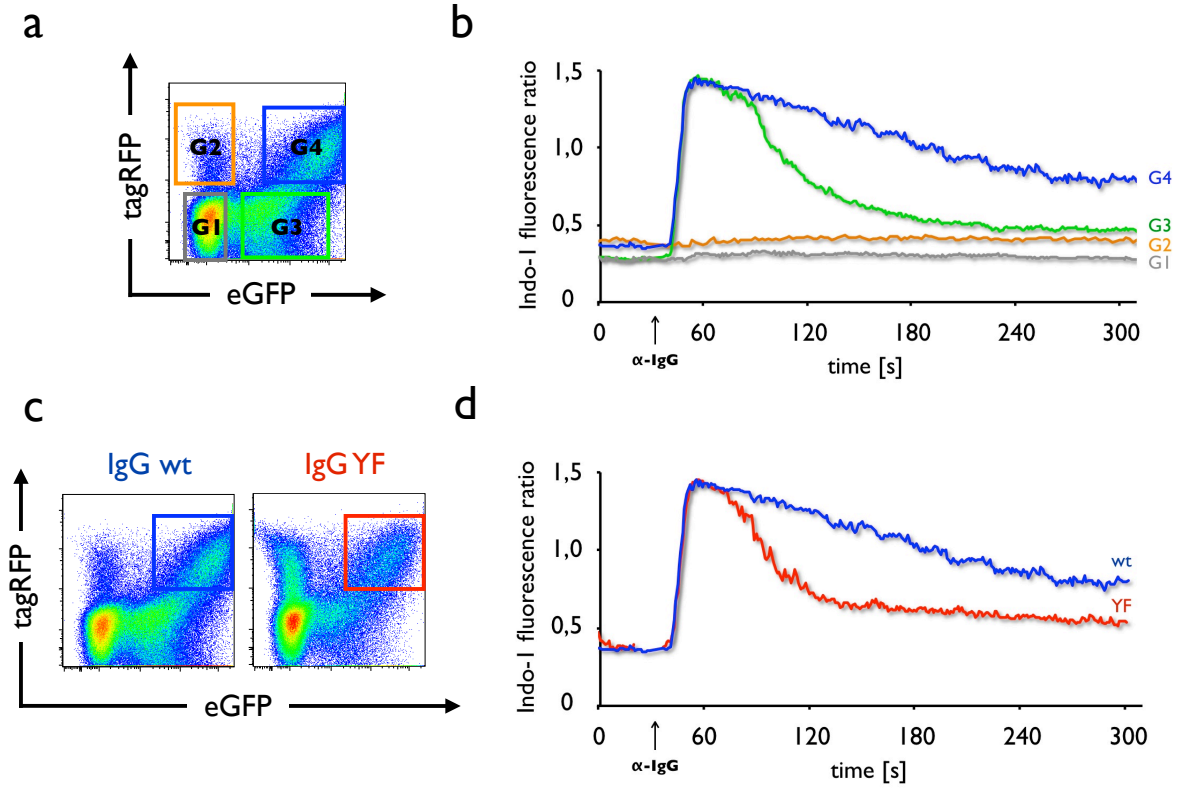

Figure 10 Reconstitution of Grb2 in $Grb2^{-/-}$ primary B cells revives ITT-based amplification of BCR Ca^{2+} signaling. Splenic B cells of $Grb2^{fl/fl}$ $mb1^{cre/+}$ mice were double infected with retroviruses harboring γ2am-IRES-eGFP and mGrb2-IRES-tagRFP cDNA. (**a**) FACS analysis of double infected cells. Cells were gated on double negative (G1), mGrb2/tagRFP positive (G2) IgG wt/eGFP positive (G3) and double positive cells expressing both IgG wt/eGFP and mGrb2/tagRFP (G4). (**b**) Cells from **a** were loaded with Indo1-AM for monitoring intracellular Ca^{2+} mobilization before and after stimulation with anti-mouse IgG $F(ab)_2$ fragments. Gates correspond to G1-4 from **a**. (**c**) Left plot depicts double infected cells expressing mIgG wt and mGrb2 known from **a, b**. Alternatively, YF mutant γ2am cDNA was used instead of wt γ2am cDNA (right plot). Blue and red quadrant correspond to G4 in **a**. (**d**) Flow cytometric Ca^{2+} flux analysis in cells from **c** expressing either wt (blue curve) or YF mIgG2a (red curve) in the presence of reconstituted mGrb2. Cells were gated as indicated in **c** and stimulated with anti-mouse IgG $F(ab)_2$ fragments after 30 seconds. All experiments were performed independently twice. Cells from two different $Grb2^{fl/fl}$ $mb1^{cre/+}$ mice were pooled for each experiment.

In conclusion, the above results demonstrate that the ITT leads to a Ca^{2+} signal amplification by the direct recruitment of Grb2 and rule out the involvement of p85 or any other proteins as direct binding partners of the ITT for enhancing the mIgG-BCR Ca^{2+} signal.

5.3 The ITT Boosts B Cell Proliferation Via Grb2

A fundamental principle of the secondary humoral immune response is the rapid reactivation of Ig class-switched memory B cells. This reactivation is characterized by a proliferative burst and subsequent differentiation into antibody producing plasma cells. The cytoplasmic tails have been shown to encompass an important role during this process as its absence clearly diminishes antibody titers during secondary immune responses (Achatz et al., 1997; Martin and Goodnow, 2002). To test whether this burst-enhancing role of the cytoplasmic tails of mIgG is dependent on ITT phosphorylation and the accompany recruitment of Grb2, the proliferative response after stimulation of wt or mutant mIgG2a in transfected primary B cells was monitored. Primary B cells from C57BL/6 mice were stimulated with LPS for 24 hours, retrovirally infected with wt, YF, NA mutant γ2am cDNA or an empty vector control and stained with the far-red emitting membrane-intercalating dye CellVue Claret 24 hours after infection (figure 11a). Then proliferation was analyzed with or without mIgG-BCR stimulation for 96 hours by the dilution of CellVue Claret as the cells divide. LPS stimulation is required for efficient retroviral infection; thus, the cells already show a robust proliferation without BCR ligation. On top of this basal proliferation, stimulation of wt mIgG2a caused a robust proliferation boost compared to the mIgG-negative population of the same well (figure 11b, G2 and G1, respectively). Unstimulated cells did not show any difference in proliferation between transfected and untransfected cells (figure 11d). Stimulation with anti-IgG antibodies led to a slightly stronger proliferation of YF and NA mutant mIgG2a expressing cells (figure 11e, red and yellow line, respectively), but to a much lesser extent as compared to wt mIgG2a stimulation (figure 11e, blue curve). eGFP only expressing cells (vector control, grey line in figure 11d, e) did not exhibit stronger proliferation than eGFP negative control cells proving that additional proliferation was dependent on mIgG-BCR expression and stimulation (figure 11e). Figure 11f shows the quantified results of CellVue Claret fluorescence decrease of eGFP-positive cells normalized to the eGFP-negative cells from the same well.

The results show that indeed the ITT boost proliferation of primary B cells even on top of the strong mitogen LPS and that this burst-enhancing role is depend on the phosphorylation of the ITT and concomitant binding of Grb2 to the ITT.

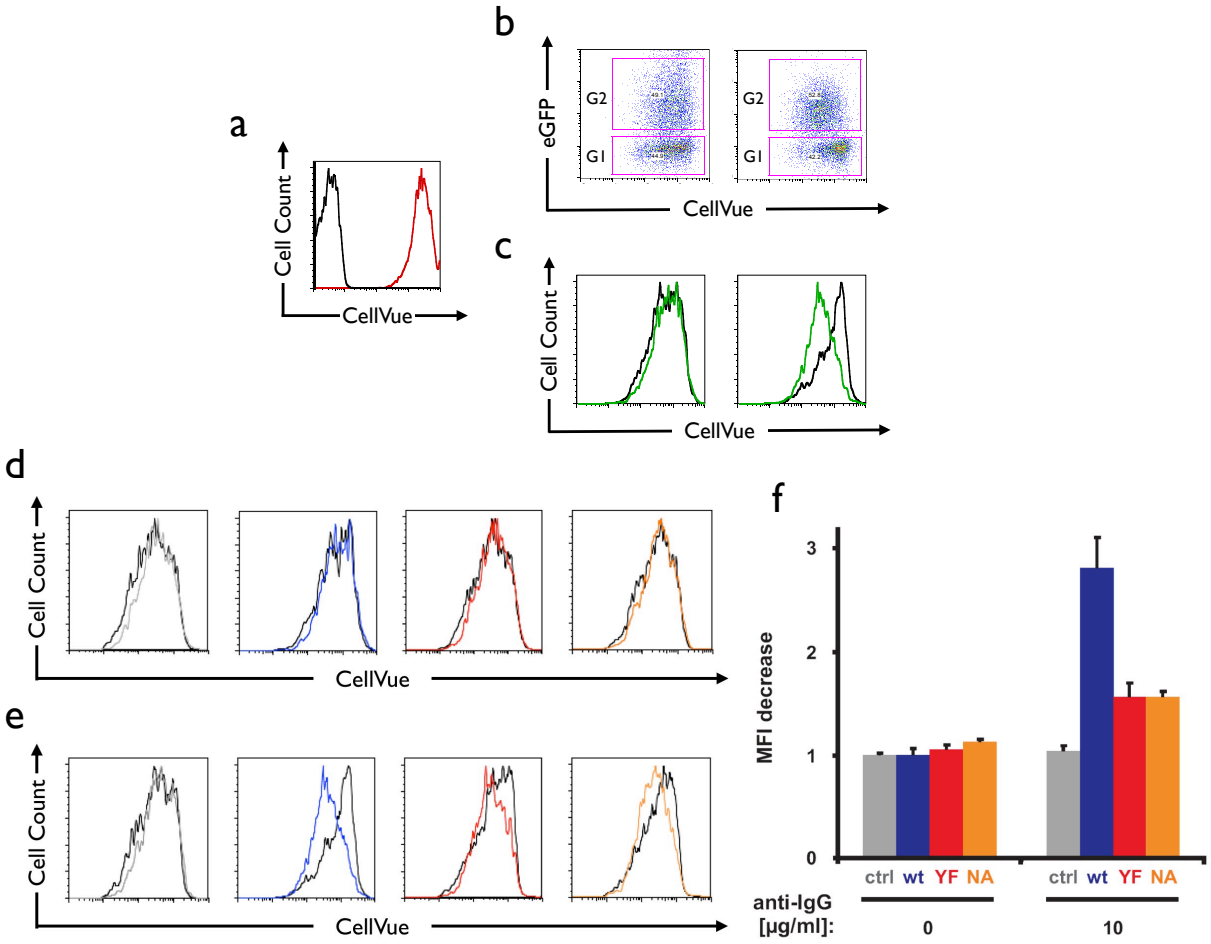

Figure 11 mIgG-BCR induced proliferative burst is dependent on Grb2 recruitment. Splenic B cells from C57BL/6 mice were prestimulated with LPS for 24 hours and retrovirally infected with wild-type, YF or NA mutant γ2am cDNA along with an IRES-driven eGFP cassette or eGFP alone (MigRII empty vector control (ctrl). 24 hours after infection cells were stained with the proliferation marker dye CellVue Claret and cells were incubated without (0 µg/ml) or with anti-IgG F(ab)$_2$ antibody fragments (10 µg/ml) for 96 hours in the presence of 10 µg/ml LPS. (**a**) FACS analysis of unstained primary B cells or after CellVue Claret staining (black and red line, respectively). (**b**) Dot plots of wt mIgG expressing cells left unstimulated (left) or stimulated for 96 hours withanti-IgG (right). eGFP-positive cells (G2) were analyzed for decrease of CellVue Claret fluorescence intensity as a marker of proliferation. Non-infected, eGFP-negative cells (G1) of the same wells served as an internal control. (**c**) Histograms of the CellVue Claret fluorescence intensity of the respective dot plots in **b** depicting either eGFP/mIgG-positive or -negative cells (green and black line, corresponding to G2 and G1 in fig. 8b, respectively). (**d**) Histogram of CellVue Claret intensity of primary B cells expressing eGFP (vector control) (grey line), wt, YF or NA mutant mIgG (blue, red and yellow line, respectively) after 96 hours proliferation without anti-IgG stimulation. Black lines represent the eGFP negative control gate from the respective well. (**e**) Same cells as in **d**, but stimulated with anti-IgG F(ab)$_2$ fragments for 96 hours before FACS analysis. Cells were analyzed in quadruplicates with histograms in **a-e** representing cells from one well. (**f**) Quantification of median fluorescence intensity (MFI) decrease of eGFP$^+$ cells from **d** and **e**. Results were normalized to eGFP-negative control cells from the same well. The experiment was performed five times. Error bars represent s.d. of quadruplicate samples.

5.4 Functional Analysis of the Grb2 SH3 domains in Ca^{2+} Signal Amplification

After the requirement of Grb2 recruitment for the ITT-based costimulation of the BCR has been established, the main issue was how Grb2 accomplishes this. In other words, which SH3 domain of Grb2 is necessary and what are the binding partners in charge for signal amplification?

To examine which SH3 domain mediates the stimulatory effect on Ca^{2+} mobilization I reconstituted Grb2-deficient primary B cells with mutant Grb2 cDNA lacking either function of the N- or C-terminal SH3 domain. As earlier described (chapter 5.2.5), double-infection of mGrb2 cDNA and γ2am cDNA with different fluorescence marker proteins allowed the discrimination of non-infected, single and double positive cells. Blue and red curve in figure 12 are the same as shown in figure 10 demonstrating that reconstitution of wt Grb2 restores signal amplification of wt mIgG-BCR in Grb2 $^{-/-}$ primary B cells. Introduction of W36K and F165A mutant Grb2 cDNA that are functional inactive variants of the N- and C-terminal SH3 domains (green and grey curve), respectively, show an intermediary Ca^{2+} flux phenotype compared to wt and YF mIgG stimulated cells, reconstituted with wt mGrb2.

These data suggest that both SH3 domains contribute to the amplified Ca^{2+} flux after mIgG stimulation. However, in this experimental setup one has to keep in mind that reconstitution of mutant Grb2 will not only modify the ITT pathway but also any other contribution Grb2 has during BCR stimulation including the potential loss of an Ca^{2+} flux inhibitory pathway.

Grb2 binds via its SH2 domain to the ITT motif leaving its flanking SH3 domains available for binding to other proteins. In order to examine the individual contributions of the N-terminal and C-terminal SH3 domains individually I genetically created chimeric proteins consisting of the complete mIgG YF portion fused to either the N- or the C-SH3 domain of Grb2. This simplifies the signaling pathway by skipping the initial recruitment of Grb2 to the ITT. The goal was to elucidate, which of the SH3 domains can functionally reconstitute the inactivated (YF) ITT motif.

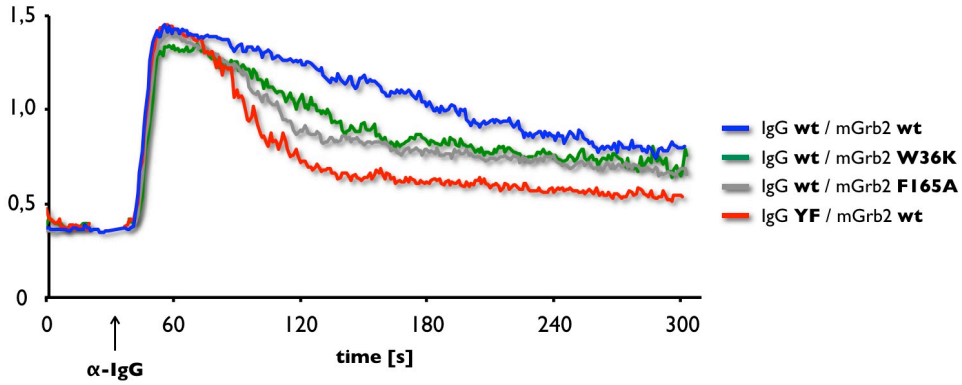

Figure 12 Reconstitution of Grb2-deficient primary B cells with mutant Grb2 partly restores mIgG-BCR signal amplification. Splenic B cells of $Grb2^{fl/fl}$ $mb1^{cre/+}$ mice were double infected with retroviruses harboring wt or YF γ2am-IRES-eGFP and wt or mutant mGrb2-IRES-tagRFP cDNA as described in figure 10, cells were loaded with Indo1-AM and conducted to flow cytometric Ca^{2+} measurement. The blue and red curves are the same as in figure 10d. Instead of wt mGrb2, the N-SH3 inactive W36K mutant or C-SH3 inactive F165A was used to reconstitute the Grb2-deficient primary B cells (green and grey curve, respectively) as indicated in the figure legend at the right margin. Data are representative of two independent experiments using pooled cells of two different mice for each experiment.

5.4.1 The Grb2 N-SH3 Mediates Ca^{2+} Signal Amplification of the ITT

mIgG YF-Grb2N-SH3 and mIgG YF-Grb2C-SH3 fusion proteins and their functional inactive mutants W36K and F165A, respectively, were expressed in the DG75 EB cell line. Retroviral transduction of the corresponding cDNAs ensured analysis of a batch of many thousand transfected cells rather than clones prone for clonal artifacts. Transfected cells were selected with Puromycin and analyzed for equal surface expression of the fusion proteins by FACS (figure 13d, g). Cells expressing wt or NA mutant mIgG were taken as references (figure 13a-c).

Ligation of the mIgG YF-Grb2C-SH3 fusion protein shows the same Ca^{2+} release pattern as the NA mutant mIgG-BCR and the absence of signaling difference between wt and F165A mutant of the Grb2 C-SH3 suggest that the C-SH3 domain cannot compensate for the mutation of the ITT within the fusion protein and therefore does not seem to be involved in the Ca^{2+} signal amplification (figure 13h). However, stimulation of the mIgG YF-Grb2N-SH3 fusion protein boosts Ca^{2+} mobilization to a similar extent as wt mIgG stimulation (figure 13b, e). The fact that only the wt Grb2 N-SH3 domain but not the W36K mutant amplifies Ca^{2+} signaling when fused to the YF mIgG-BCR shows that the N-SH3 function is required to drive the enhancement of Ca^{2+} flux. To test whether all transfectants are equally capable of releasing Ca^{2+}, the endogenously expressed mIgM-BCR was stimulated as control (figure 13c, f, i).

These results imply that Grb2, when recruited to the ITT, brings along a Ca^{2+} promoting factor binding to its N-SH3 domain. As shown earlier, ITT-costimulation results in an enhanced phosphorylation of the Ca^{2+} initiation complex and therefore this Ca^{2+} promoting protein is most likely acting upstream of this complex.

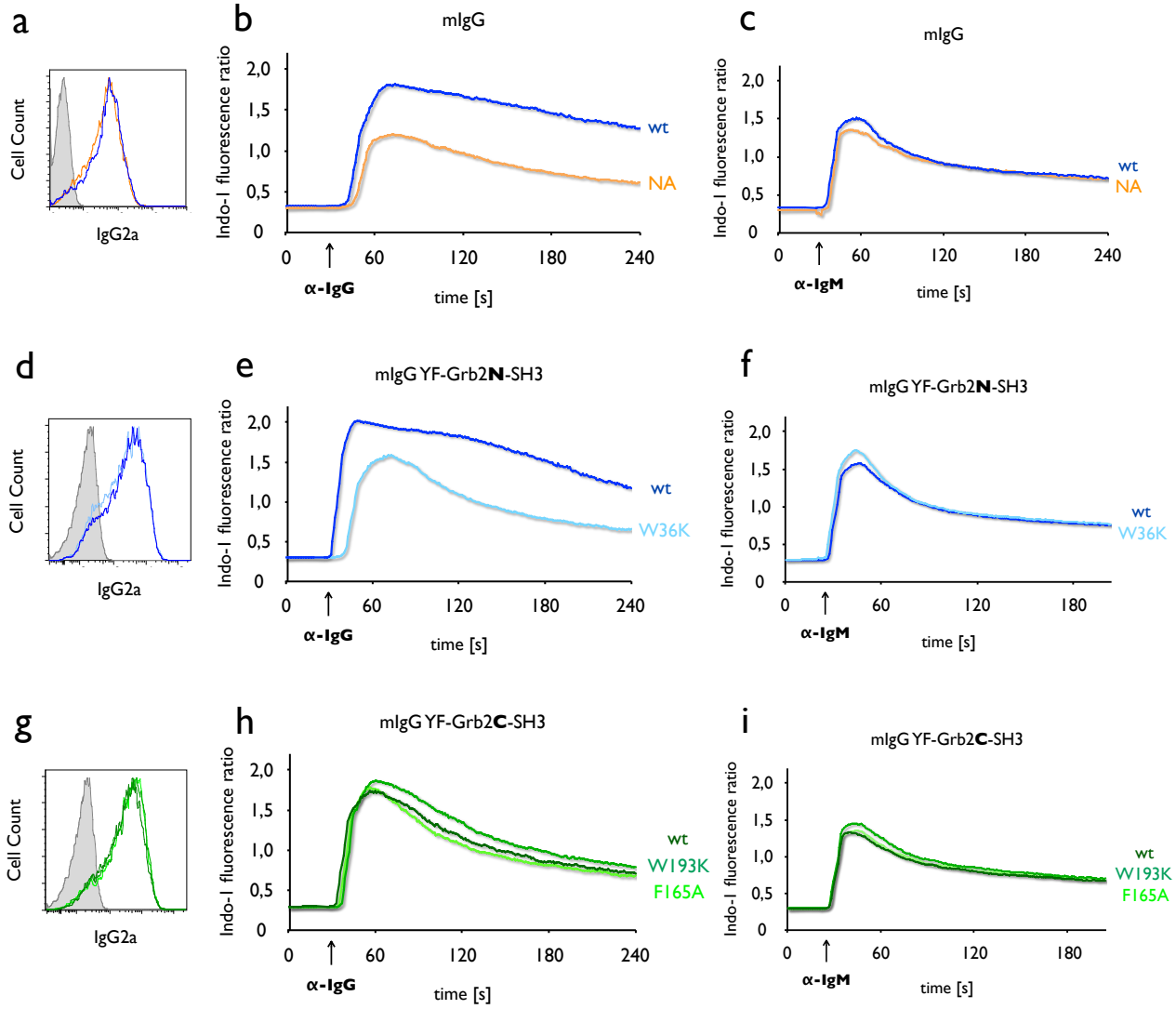

Figure 13 The N-terminal SH3 domain of Grb2 promotes mIgG-BCR-induced Ca^{2+} mobilization. DG75 EB cells were retrovirally infected using a pMSCVpuro vector for virus production containing wt or mutant γ2am cDNA (**a-c**) or cDNA encoding for wt or mutant mIgG YF-Grb2N-SH3 (**d-f**) and –Grb2C-SH3 (**g-i**) fusion proteins as indicated (see color code of figure legends). Cells were selected with Puromycin and surface expression of all constructs was analyzed by FACS using a Cy5-labeled anti-mouse IgG (**a, d, g**). Cells were loaded with Indo1-AM in order to measure intracellular Ca^{2+} mobilization by ratiometric flow cytometry before and after stimulation of the indicated receptor variant with 10 µg/ml anti-mouse IgG $F(ab)_2$ fragments (**b, e, h**) or 20 µg/ml anti-human IgM $F(ab)_2$ fragments (**c, f, i**). Data are representative of at least 5 independent experiments.

5.4.2 The Grb2 N-SH3 Domain is Sufficient to Restore BCR Costimulation in Grb2-Deficient B Cells

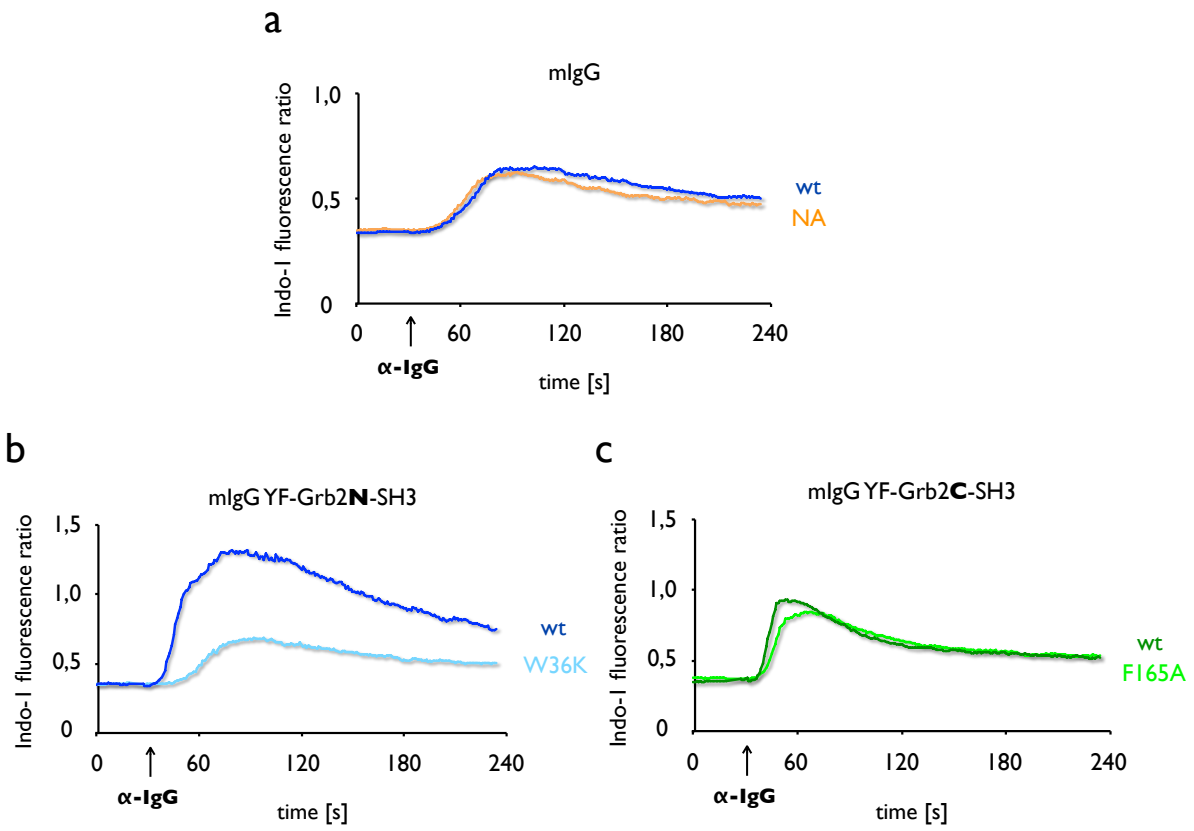

Figure 14 The N-terminal SH3 domain of Grb2 is sufficient to restore Ca^{2+} signal amplification when integrated into the BCR. DG75 $Grb2^{-/-}$ cells were retrovirally transduced to express wt or NA mutant mIgG-BCR (**a**, blue and yellow curves, respectively), wt or W36K mutant mIgG YF-Grb2N-SH3 (**b**, dark and light blue curves, respectively) or wt or F165A mutant mIgG YF-Grb2C-SH3 fusion proteins (**c**, dark and light green, respectively). **a-c** depict Ca^{2+} mobilization pattern before and after stimulation of the indicated BCRs with 10 µg/ml anti-mouse IgG $F(ab)_2$ fragments. One of three independent experiments is shown.

In the absence of Grb2 wt mIgG-BCR stimulation fails to administrate its intrinsic ITT-based BCR-costimulation as shown in primary B cells in chapter 5.2.4. Here, I used a $Grb2^{-/-}$ DG75 B cell line (kindly provided by Johannes Lutz from our group) to test whether the chimeric mIgG-Grb2SH3-BCRs can restore the co-stimulatory function in the complete absence of Grb2. For this, I retrovirally transfected Grb2-deficient DG75 cells to express wt or NA mutant mIgG2a and mIgG2a YF-Grb2N-SH3 or mIgG2a YF-Grb2C-SH3 with their respective SH3 domain inactivating mutant. Comparison of the Ca^{2+} mobilization after stimulation of wt or NA mutant

mIgG recapitulate the results obtained in primary B cells with both receptors showing very similar Ca^{2+} release patterns (figure 14a). In line with the results obtained in wt DG75 cells, fusion of the wt but not mutant Grb2 N-SH3 domain to mIgG2a YF amplified the Ca^{2+} mobilization after receptor stimulation (figure 14b). Ligation of mIgG2a YF-Grb2C-SH3 wt did not enhance the Ca^{2+} mobilization compared to the SH3 inactive F165A mutant (figure 14c).
Taken together, in the absence of Grb2 the ITT-based Ca^{2+} amplification can be reconstituted by the N-terminal SH3 domain of Grb2 fused to the mIgG YF-BCR alone. The C-SH3 domain, on the other hand, seems to be dispensable for the augmented Ca^{2+} mobilization.

5.4.3 Potential Binding Partners in Charge

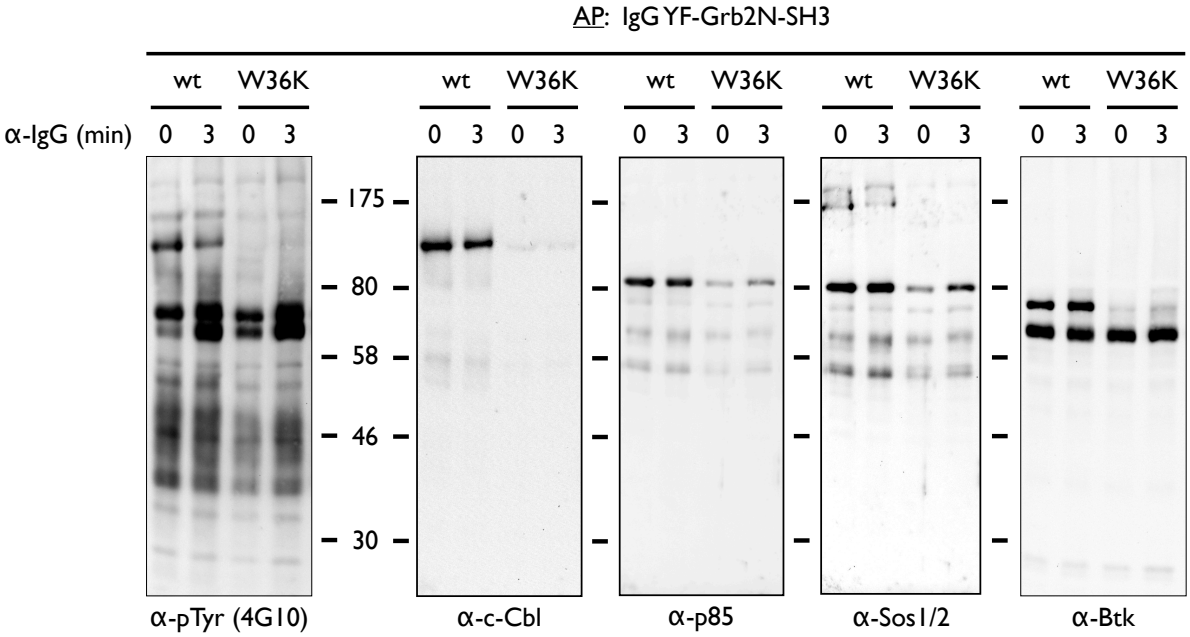

Figure 15 Affinity purification of Grb2 N-SH3 binding partners. Wild-type or W36K mutant mIgG YF-Grb2N-SH3 fusion proteins were immunoprecipitated from DG75 EB expressing the respective BCR using a biotinylated anti-mouse IgG antibody subsequently immobilized on streptavidin-sepharose beads. Cells were unstimulated (0 min) or stimulated (3 min) with the precipitating anti-IgG-biot. antibody. Co-purified proteins were analyzed with immunoblots probed for phospho-tyrosine (4G10), c-Cbl, p85, Sos1/2 and Btk as indicated below the respective blot. Data represent one example of at least four independent experiments.

In order to find the binding partner of the Grb2 N-SH3 domain mediating the Ca^{2+} signal amplification, I used biotinylated anti-IgG antibodies to stimulate and

subsequently affinity-purify mIgG-Grb2 N-SH3 together with its potential binding partners using a streptavidin matrix. The purified proteins were analyzed by western blotting probed for phospho-tyrosine and subsequently for some of the known binding partners. To distinguish N-SH3-specific binding from BCR-specific and background binding the W36K mutant was used as a control for affinity purification. The phospho-tyrosine blot (figure 15, left) shows a prominent phospho-protein band at about 120 kD only purified by wt but not by the W36K mutant. This band co-migrates with c-Cbl as demonstrated by direct immunostaining for c-Cbl (figure 15, second from left). Additionally, other known binding partners of the Grb2 N-SH3 domain like p85 and Sos1/2 were co-purified during the experiment. This validates the integrity of the N-SH3 domain within the fusion protein but also suggests that any protein with binding affinity for the N-SH3 domain will be co-purified in this experimental setup. Interestingly, Bruton's tyrosine kinase Btk is also able to bind to the N-terminal Grb2 SH3 domain (figure 15, right). Due to its function within the Ca^{2+} initiation complex during BCR signaling, Btk is a very intriguing candidate for mediating the ITT-based signal amplification. However, with this experiment none of the other binding partners can be excluded for its role in this signaling pathway. This multifaceted binding ability of Grb2 exemplifies the challenge of finding a pathway-specific binding partner for the ITT signaling pathway.

5.4.4 The SH3 Domains of Grap are Incapable of Enhancing Ca^{2+} Signaling

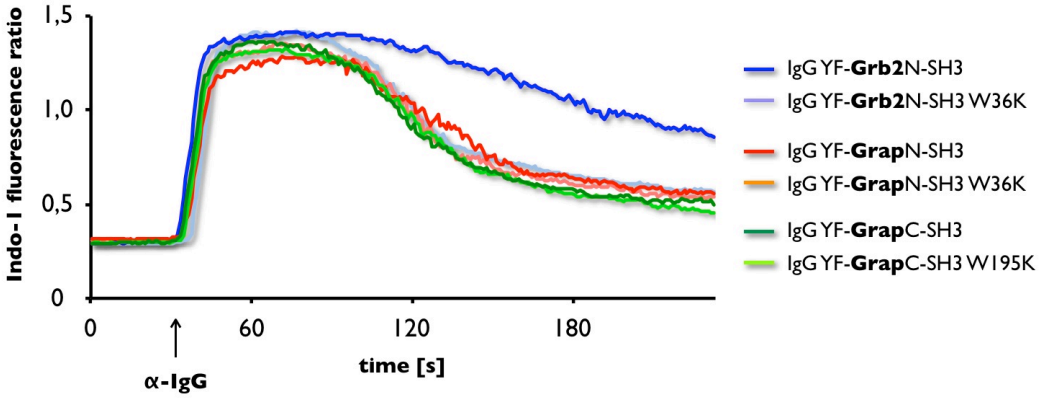

Figure 16 mIgG YF-GrapSH3 fusion proteins fail to promote Ca^{2+} signal amplification. Ca^{2+} mobilization pattern are shown for primary B cells expressing mIgG YF-Grb2N-SH3 or mIgG YF-GrapSH3 domains with their respective inactive mutant as indicated in the figure legend. An additional IRES-eGFP cassette allowed gating on infected cells during flow cytometric measurement of intracellular Ca^{2+} flux using the Ca^{2+}-sensitive dye Indo1-AM. After basal Ca^{2+} levels were measured for 30 sec, cells were stimulated with 10 µg/ml goat anti-IgG $F(ab)_2$. Data are representative of three independent experiments using splenic B cells from three at least 8 week old C57BL/6 mice.

An opportunity to narrowing down the list of potential binding partners in search of the Ca^{2+} promoting factor is a comparative analysis using SH3 domains with an overlapping set of binding partners. Due to the great similarities (58,9% identity in amino acid sequence) between Grb2 and Grap I used the Grap SH3 domains to fuse to the YF mutant mIgG-BCR, as done with the Grb2 SH3 domains and expressed them together with the respective inactive variants in LPS-stimulated primary B cells. Comparison of the Ca^{2+} flux after stimulation of the mIgG YF-Grap-/Grb2-SH3 fusion proteins shows that both the N- and C-terminal Grap SH3 domains are incapable of amplifying the BCR-induced Ca^{2+} signaling compared to the Grb2 N-SH3 domain (figure 16). This further validates the exclusive role of Grb2 in ITT-based Ca^{2+} signal amplification and showed the feasibility of a comparative binding analysis in which all overlapping binding partners of the Grap N-SH3 and Grb2 N-SH3 domains can be excluded as a Ca^{2+} promoting factor since the Grap SH3 domain is unable to boost the Ca^{2+} signal.

5.4.5 Comparative Binding Analysis between Grb2 N-SH3 and Grap N-SH3 Helps Narrowing Down Potential Relevant Binding Partners

To investigate the binding abilities of the Grap N-SH3 and Grb2 N-SH3 domains I used GST-fusion proteins for affinity purification of binding partners from DG75 cell line lysates (figure 17a). The N-SH3 domain of Grb2 binds a huge variety of phospho-proteins compared to only three obvious protein bands after purification with the Grap N-SH3 domain. As expected, the W36K mutants of the N-SH3 domains lost their ability to bind any proteins. As observed by further immunostaining for Sos1/2, Cblb and c-Cbl both Grap and Grb2 N-SH3 domains share the binding ability for these proteins (figure 17b) due to which they can be excluded as a functional binding partner in ITT Ca^{2+} signal amplification. However, Btk is only purified by wt GST-Grb2 N-SH3 making it an excellent candidate as a functionally relevant binding partner during ITT signaling.

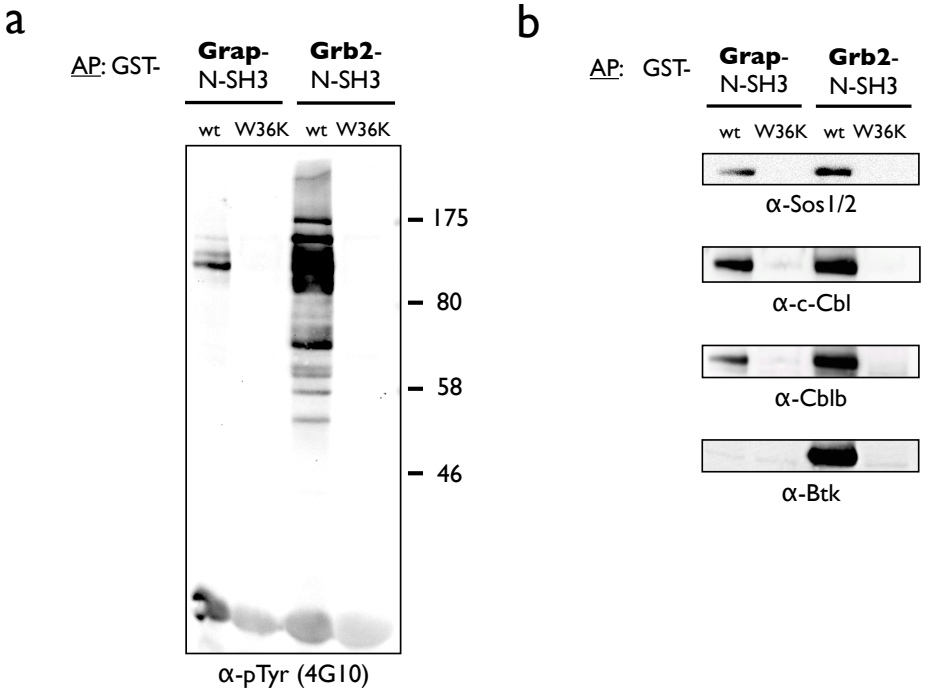

Figure 17 Comparative binding analysis of Grb2 and Grap N-SH3 domains. Immunoblot analysis of affinity-purified proteins from DG75 EB transfectants expressing wt mIgG. Cells were stimulated for 3 min with anti-IgG $F(ab)_2$ fragments and proteins were affinity purified from cleared lysates using recombinant GST-Grap or Grb2 N-SH3 fusion proteins in wild-type or mutant variant. Immunoblots were analyzed with anti-phospho tyrosine (**a**), anti-Sos1/2, anti-c-Cbl, anti-Cblb and anti-Btk antibodies (**b**). Immunoblots are representatives of three independent experiments.

5.4.6 Bruton's Tyrosine Kinase Mediates the Enhanced Ca^{2+} Signaling Capacity of the N-SH3 over the C-SH3 domain of Grb2 in ITT signaling

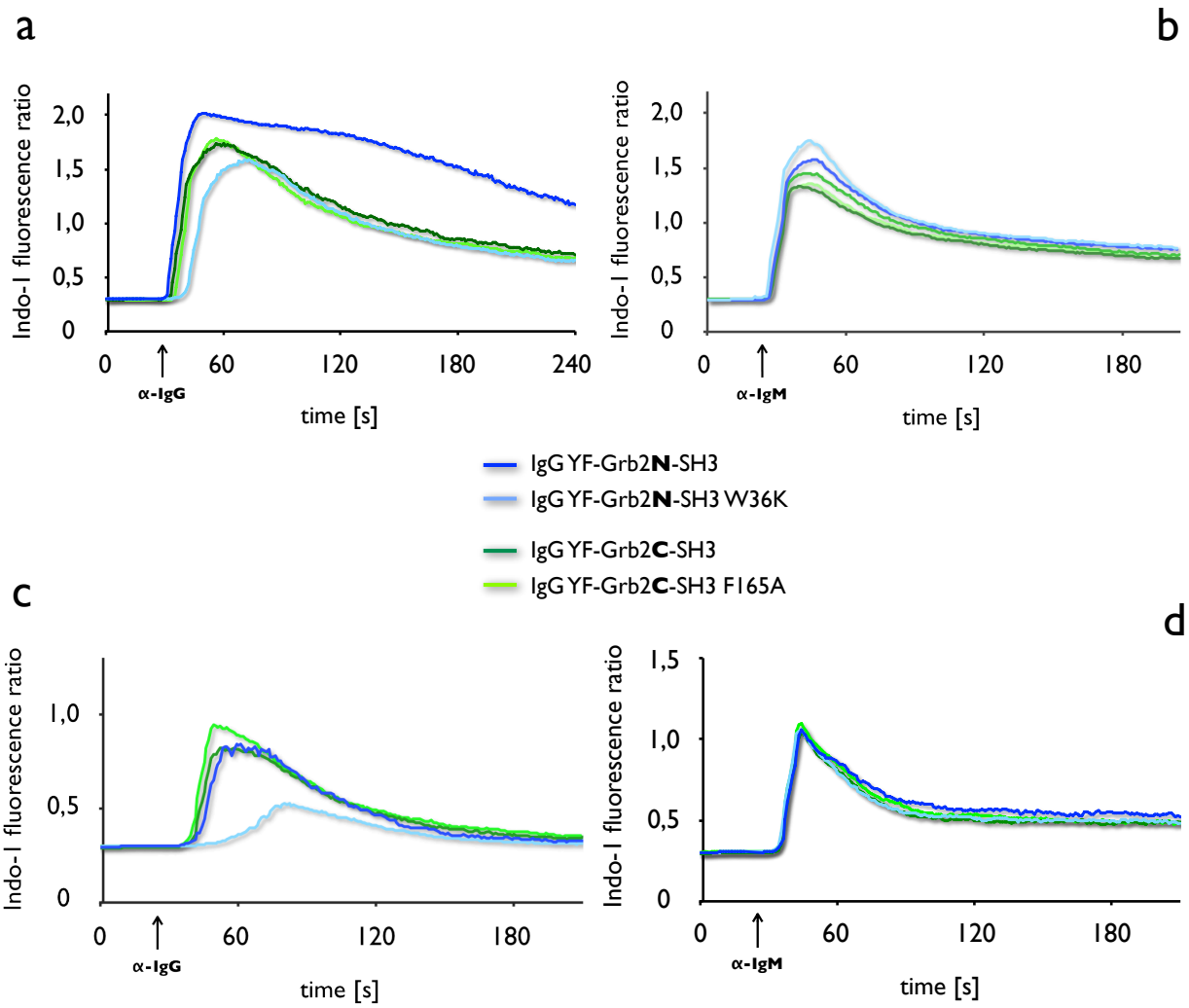

Figure 18 Btk distinguishes the signal capacity of the Grb2 N-SH3 and Grb2 C-SH3 in ITT-based BCR costimulation. (**a**) Wild-type DG75 EB expressing the indicated mIgG YF-Grb2SH3 fusion proteins were loaded with Indo1-AM and intracellular Ca^{2+} flux was analyzed by flow cytometry. Cells were stimulated with 10 µg/ml anti-IgG $F(ab)_2$ fragments after monitoring basal levels for 30 seconds. (**b**) Cells from **a** were stimulated with 20 µg/ml anti-IgM $F(ab)_2$ fragments as a control for equal Ca^{2+} mobilization capacities between the different transfectants. (**c**) DG75 EB Btk knock out (cells kindly provided by Wiebke Schulze) were retrovirally transfected to express same constructs as in **a** and analyzed by flow cytometric Ca^{2+} measurement as described in **a**. (**d**) Cells from **c** were stimulated with anti-IgM instead of anti-IgG as mentioned in **b**. Data are representative of three independent experiments.

To investigate the role of Btk in Grb2 N-SH3 mediated Ca^{2+} signal amplification I transfected DG75 EB Btk knock out cells (kindly provided by Wiebke Schulze from our group) with cDNAs encoding the mIgG YF-Grb2SH3 fusion proteins. If Btk was the missing link between Grb2 N-SH3 and the enhanced Ca^{2+} release, mIgG YF-Grb2N-SH3 ligation in Btk-deficient cells should fail to increase the Ca^{2+} mobilization. In figure 18, Ca^{2+} flux after engagement of the different mIgG YF-Grb2 SH3 fusion BCRs in wild-type DG75 EB (a, b) and Btk-deficient DG75 EB (c, d) is compared. In wt DG75 EB Ca^{2+} release is much stronger after stimulation of wt mIgG YF-Grb2N-SH3 compared to either the respective W36K mutant or both wt and mutant mIgG YF-Grb2C-SH3 (a). General signaling capacity of the different transfectants was comparable as assessed by stimulation of the endogenous mIgM-BCR (b, d).

In Btk knock out cells the difference between N- and C-SH3 BCR fusion proteins were completely abolished. However, the W36K mutant showed an even decreased signal. An explanation for this unexpected finding is difficult. Either the W36K mutant has an altogether lower canonical BCR signaling capacity as Ca^{2+} flux in wt DG75 EB cells the is also slightly lower or the W36K mutant shows the basal canonical signaling capacity of the BCR and wt N-SH3 increases the signal due to binding of an additional factor. While latter seems more likely it would implicate that the wt and F165A mIgG YF-Grb2-C-SH3 have also additional signaling capacity. Further investigation should address the lower signal of the W36K mutant mIgG YF-Grb2N-SH3.

Taken together, the earlier mentioned Ca^{2+} signaling differences between mIgG YF-Grb2N- and C-SH3 is completely lost in Btk deficient cells indicating that Btk binding to the N-SH3 domain is the factor that distinguishes the signaling potency of both domains. The findings fit very well with the enhanced phosphorylation of the Ca^{2+} initiation complex after mIgG YF-Grb2N-SH3 stimulation as Btk, when associated with SLP-65 and PLC-γ2, phosphorylates PLC-γ2 during the canonical BCR signaling pathway. Thus, Grb2 binding to the pITT would recruit more or stabilize existing factors of the Ca^{2+} initiation complex by sequestering Btk in the mIgG-BCR signalosome.

5.5 ITT-based Modulation of BCR Signaling Pathways

5.5.1 The Grb2 N-SH3 Domain Boosts BCR-induced Protein Kinase C Activity

In earlier experiments Niklas Engels showed the enhanced phosphorylation of the Ca^{2+} initiation complex including phospholipase C (PLC)-γ2 by ITT-costimulation, which successively leads to an increased production of 1,4,5-trisphosphate (IP3) and amplification of Ca^{2+} mobilization. Besides IP3, another product of PLC-γ2-mediated hydrolysis of phosphatidylinositol 4,5-bisphosphate (PIP2) is diacylglycerol (DAG), which in turn recruits protein kinase C (PKC) to the plasma membrane leading to its activation. Even though it seems obvious that increased PLC-γ2 activity results also in a stronger production of DAG besides IP3, I aspired to test if this directly translates into an enhanced activity of PKC. To this end, I transiently transfected DG75 EB expressing either wt or W36K mutant mIgG2a YF-Grb2N-SH3 with the genetically-encoded FRET-based PKC biosensor 'C kinase activity reporter' (CKAR) (Violin et al., 2003) by Amaxa nucleofection. PKC activity was subsequently measured by flow-cytometric FRET (FCET) analysis. CKAR is engineered in a way that the FRET signal decreases when its PKC substrate sequence is phosphorylated by PKC. Therefore, a decrease in FRET/CFP ratio demonstrates an increase in PKC activity. As a control of the reporter, cells were stimulated with 20 ng/ml PMA, a strong inducer of PKC activity. When stimulated with anti-IgG, but not with anti-

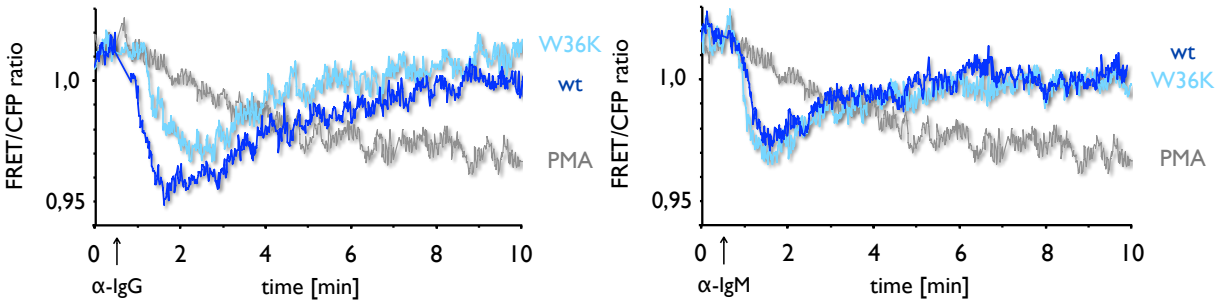

Figure 19 Grb2 N-SH3 mediated ITT-costimulation increases protein kinase C activity. DG75 cells expressing wt or W36K mutant mIgG YF-Grb2N-SH3 BCRs were transiently transfected to co-express the FRET-based biosensor CKAR that reports PKC activity by a reduction of FRET. Cells were measured by flow cytometric FRET-analysis before and after stimulation with 10 µg/ml anti-IgG (left) or 20 µg/ml anti-IgM $F(ab)_2$ antibody fragments (right). 20 ng/ml PMA was administered as a reference acting as a strong PKC activity inducer. FRET over CFP ratio was monitored for 10 minutes. Data are representative of two independent experiments.

IgM $F(ab)_2$ fragments, CKAR reported a more rapid and stronger PKC activity in cells expressing wt mIgG2a YF-Grb2N-SH3 compared to the W36K mutant as depicted in the decrease in FRET/CFP ratio in figure 19 (left). Stimulation of the endogenously expressed mIgM-BCR showed a similar activation profile in both transfectants (figure 19, right). PMA resulted also in a strong, despite slower, decrease in FRET signal validating the reporter's functionality.

In conclusion, using the FRET-based biosensor CKAR it was possible to directly measure PKC activity in living cells by flow-cytometric analysis showing that the Grb2 N-SH3-mediated increase of PLC-γ2 activity results not only in the enhanced Ca^{2+} mobilization via production of IP3 but indeed translates directly into a stronger PKC activity most likely due to the higher amount of DAG produced.

5.5.2 ITT-Costimulation Increases Phosphorylation of Vav1 and SLP-65

To assess whether ITT-based signal amplification leads to an enhancement in phosphorylation of other major BCR-downstream signaling proteins related to Grb2 adaptor functionality, wt or NA mutant mIgG2a expressing DG75 EB cells were stimulated for different time periods with anti-IgG $F(ab)_2$ antibody fragments and phosphorylation of Vav1, Akt, SLP-65 and Erk were analyzed by immunoblotting with phospho-specific antibodies. In addition to a stronger SLP-65 phosphorylation, which had been shown before by Niklas Engels, also Vav1 is phosphorylated to a much stronger extent in wt mIgG stimulated cells (figure 20).

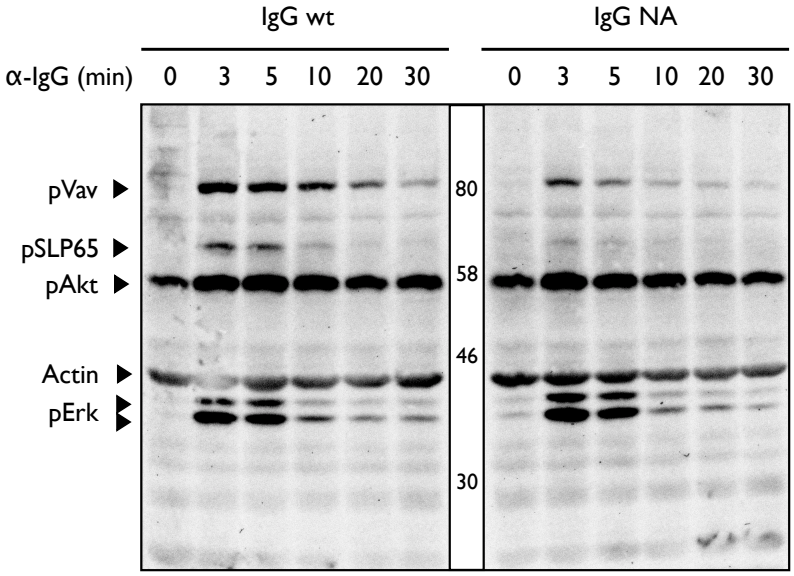

pVav	0	**1**	0,7	0,6	0,3	0,2		0	**0,3**	0,2	0,1	0,1	0,1
pSLP65	0	**1**	0,4	0,1	0,1	0		0	**0,2**	0,1	0,1	0	0
pAkt	0,1	**1**	0,6	0,4	0,3	0,4		0,3	**1**	0,7	0,7	0,6	0,5
pErk	0	**1**	0,4	0,1	0,1	0,1		0	**0,8**	0,5	0,2	0,2	0,1

Figure 20 mIgG-BCR engagement leads to increased phosphorylation of SLP-65 and Vav1. Immunoblot analysis of DG75 EB transfectants expressing either wt or NA mutant mIgG2a-BCRs. Cells were left unstimulated or simulated for the indicated time frames with 10 µg/ml anti-IgG $F(ab)_2$ fragments and cleared lysates of 1,5 $x10^6$ cells per lane were analyzed by immunoblotting subsequently with anti-pVav1, anti-pSLP-65, anti-pAkt, anti-pErk and anti-actin as loading control. Without HRPO inhibition of the secondary antibodies all primary antibodies could be made visible at the same time. Numbers in the middle represent relative molecular weight of the marker proteins. The table below depicts relative densitometry quantification of the phospho-protein bands corrected by actin loading control and normalized to the 3 min stimulation time point of wt mIgG expressing cells. The figure shows one out of five independent experiments.

PI3K induction by Grb2 related recruitment of p85 would translate into stronger recruitment and phosphorylation of Akt. Thus, Akt phosphorylation can be used as a read-out for PI3K activity (Okkenhaug and Vanhaesebroeck, 2003). Figure 20 shows that Akt is equally strong phosphorylated after wt or NA mutant mIgG stimulation in DG75 EB cells excluding the involvement of PI3K in ITT-based BCR-costimulation. Grb2 is well known and characterized in its name-giving function coupling growth factor receptors like EGFR and PDGFR to the Ras pathway via binding of the nucleotide exchange factors Sos (Lowenstein et al., 1992). Further downstream the Ras/Raf/Mek pathway leads to the activation of extracellular regulated kinase Erk causing the mitogenic effect of growth receptor activation. Also in lymphocyte signaling, Grb2 is thought to be associated with the activation of the MAPK pathway via Sos (Jang et al., 2009). However, its role downstream of the BCR is still controversial. To test whether Grb2 recruitment in the context of ITT signaling results in stronger Erk activity that could account for the proliferative effect demonstrated in 5.3, Erk activation was analyzed. To this end, both phosphorylation of Erk1/2 by western blot probed with phospho-specific anti-Erk1/2 antibodies and direct Erk activity via flow cytometric analysis of the biosensor EKAR after mIgG ligation was measured in transfected DG75 cells expressing wt or NA mutant mIgG-BCRs. Using both techniques it was shown that there is no difference in Erk phosphorylation (figure 20) and/or activity after stimulation of wt or NA mutant mIgG (figure 21)

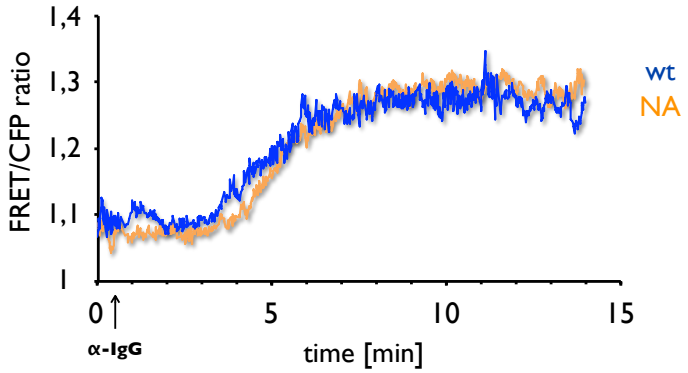

Figure 21 ITT costimulation does not enhance activity of extracellular regulated kinases Erk1/2. Flow cytometric FRET analysis of DG75 EB transfectants expressing either wt or NA mutant mIgG-BCRs and Erk kinase activity reporter (EKAR). Cells were stimulated with 10 µg/ml anti-IgG $F(ab)_2$ fragments after examining basal FRET levels for 30 seconds. The reporter monitors direct phosphorylation of a substrate peptide of Erk by an increase in FRET signal. Data are representative of at least three independent experiments.

suggesting that the burst-enhancing role of Grb2 in ITT signaling is not dependent on coupling the BCR to the Ras signaling pathway.
In conclusion, besides the amplified Ca^{2+} mobilization, which is caused by an increased phosphorylation of SLP-65 and PLC-γ2 (Engels et al., 2009), Vav1 phosphorylation is strongly induced by mIgG-BCR signaling, while Akt and Erk show an equal phosphorylation status after wt or NA mutant mIgG-BCR ligation. As Vav1 activity has been described to have a proliferative effect through activation of small GTPases of the Rho family, its increased phosphorylation might contribute to the proliferative effect demonstrated for the ITT.

5.5.2.1 SLP-65 Phosphorylation is Enhanced by Effects of Both Grb2 SH3 Domains, while Vav1 Phosphorylation is Specifically Increased by the Grb2 C-SH3 Domain

Next, I wanted assess whether both Grb2-SH3 domains contribute to the stronger Vav1 and SLP-65 phosphorylation or if the N- and C-terminal SH3 domains specifically enable phosphorylation of either one. To this end, I used the DG75 EB cells expressing mIgG YF-Grb2N/C-SH3 fusion BCRs in wt or mutant form that were introduced in chapter 5.3.1. I stimulated the DG75 EB transfectants with anti-IgG $F(ab)_2$ antibody fragments for different times and analyzed lysates via phospho-specific immunoblotting for their ability to enhance SLP-65 and/or Vav1 phosphorylation. As shown in figure 22a, SLP-65, as part of the Ca^{2+} initiation complex, is indeed stronger phosphorylated after wt mIgG YF-Grb2N-SH3 compared to the W36K mutant giving a potential explanation for the Ca^{2+} signal amplification. The increased Vav1 phosphorylation shown for wt mIgG-BCR stimulation in figure 21, however, is not repeated by the mIgG YF-Grb2N-SH3 fusion protein and, thus, not mediated by binding partners of the N-SH3 domain of Grb2.

In contrast, stimulation of wt mIgG YF-Grb2C-SH3 led to an increased phosphorylation of Vav1 compared to the F165A mutant demonstrating that Vav1 is specifically phosphorylated through effects of the Grb2 C-SH3 domain (figure 22b). Ligation of mIgG YF-Grb2C-SH3 also enhanced phosphorylation of SLP-65 and even to a stronger extent as mIgG YF-Grb2N-SH3 stimulation (compare figure 22a and c). This finding is very surprising, as one would expect stronger SLP-65 phosphorylation to correlate with an enhanced Ca^{2+} mobilization.

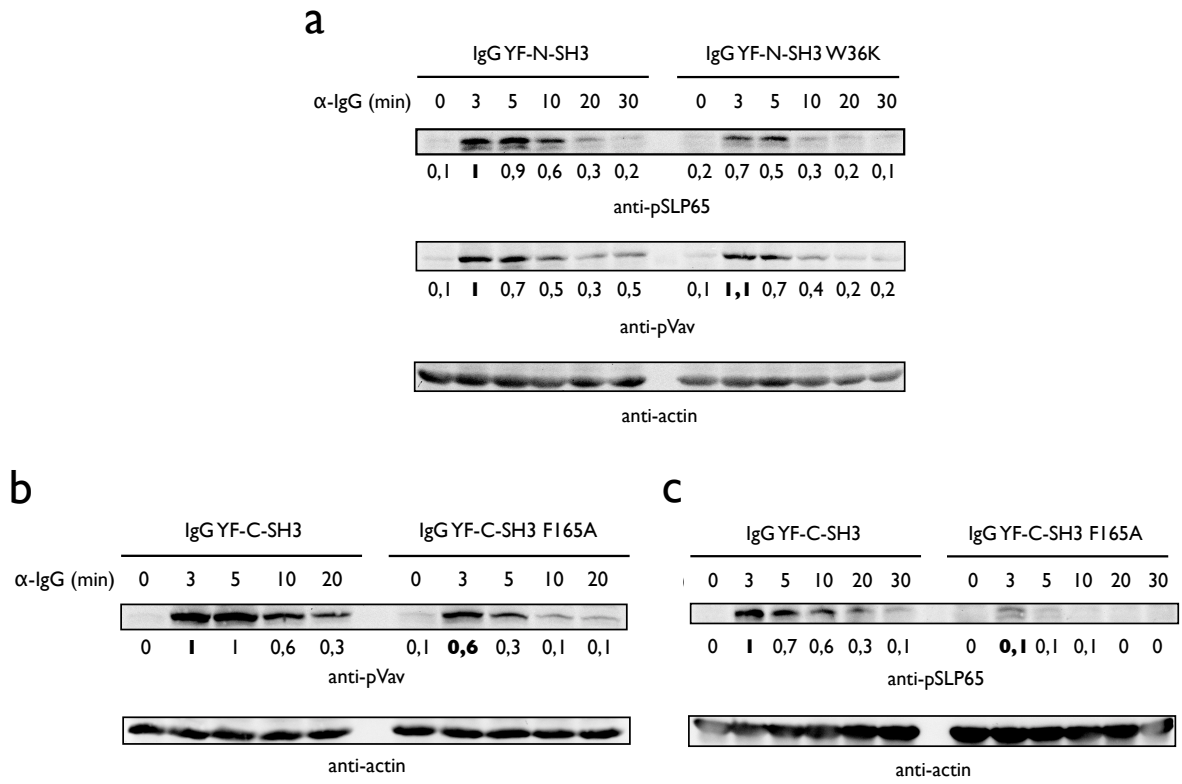

Figure 22 Both Grb2 SH3 domains contribute to the increased SLP-65 phosphorylation, but only the Grb2 C-SH3 mediates enhanced Vav1 phosphorylation. (**a**) Immunoblot analysis of DG75 EB cells expressing wt or W36K mIgG YF-Grb2N-SH3 fusion proteins stimulated with 10 µg/ml anti-IgG $F(ab)_2$ fragments for the indicated time points. Lysates were probed for phospho-Vav1, phospho-SLP-65 and actin as loading control. Data are representative of three independent experiments. (**b**) DG75EB cells expressing wt or F165A mutant mIgG YF-Grb2C-SH3 were treated as in **a** and lysates were analyzed by immunoblotting for Vav1 phosphorylation with a phospho-specific anti-Vav1 (**b**) or anti-pSLP65 antibody (**c**) on to different blots. Actin served as loading control. Numbers below blots represent densitometric measurements of pVav1 and pSLP-65 bands corrected by actin loading control and normalized to 1 at the 3 min stimulation time point of the respective wt mIgG YF-Grb2N/C-SH3. All blots are represents of three independent experiments.

In conclusion, both Grb2 SH3 domains mediate the increased phosphorylation of SLP-65 during ITT-based costimulation. Furthermore, each SH3 domain contributes to the activation of different pathways. The N-terminal SH3 domain leads to an enhanced Ca^{2+} signal by recruitment of Btk, while the C-terminal SH3 specifically amplifies Vav1 phosphorylation. If the latter is mediated by direct binding or an indirect effect through binding of another factor will be explored next.

5.5.2.2 Increased Phosphorylation of SLP-65 and Vav1 is Dependent on Direct Recruitment to the Grb2 C-SH3 Domain During ITT-costimulation

Although, SLP-65 and Vav1 are both described binding partners of the Grb2 C-SH3 domain, I wanted to determine if they also bound to the mIgG YF-Grb2C-SH3 BCRs in the cellular context explaining the stronger phosphorylation of these proteins upon mIgG YF-Grb2C-SH3 stimulation.
For this, I affinity co-purified proteins using the mIgG YF-Grb2C-SH3 fusion protein. Ramos transfectants expressing either tailless mIgG or mIgG YF-Grb2C-SH3 were left unstimulated or stimulated for 3 min with 10 μg/ml anti-IgG antibodies, lysed and the respective modified mIgG was precipitated with a biotinylated anti-IgG, subsequently immobilized on streptavidin-sepharose beads. Purified proteins were analyzed by immunoblots probed for phosphorylated proteins with the phospho-tyrosine-specific antibody 4G10. Two prominent phospho-protein bands are only observed after co-purification of mIgG YF-Grb2C-SH3 (marked with blue asterisks in figure 23 a, b). The upper phospho-band corresponds to a molecular weight of about 100 kD, which correlates roughly with the molecular weight of Vav1 (95 kD), a known binding partner of the C-SH3 domain. Indeed, the anti-Vav1 antibody recognizes bands co-migrating at the exact same position as the phospho-protein bands indicating that these bands represent phosphorylated Vav1 (figure 23a). As the SH3 domains represent constitutive binding characteristics, there was no difference in the co-purified proteins from unstimulated or stimulated cells. Therefore, in figure 23b, only stimulated cells were used for affinity purification.
The lower phospho-protein band seen in figure 23b runs at just above 60 kD. To test, whether this band might corresponds to SLP-65 the blot was directly probed with an anti-SLP-65 antibody displaying that SLP-65 is co-purified with mIgG YF-Grb2C-SH3

and it exactly co-migrates with the lower phospho-protein band in the left blot of figure 23b.

In conclusion, two phosphorylated proteins were co-purified with the mIgG YF-Grb2C-SH3 fusion protein and these proteins could be identified as SLP-65 and Vav1. Both proteins are known binding partners of the C-SH3 domain of Grb2. Interestingly, although the C-SH3 domain can also bind to Cbl proteins, no phosphorylated Cbl is co-purified as it was observed for mIgG YF-Grb2N-SH3 in figure 16 implicating that the experiment led to co-purification of pathway-specific proteins rather than any binding partners of the C-SH3.

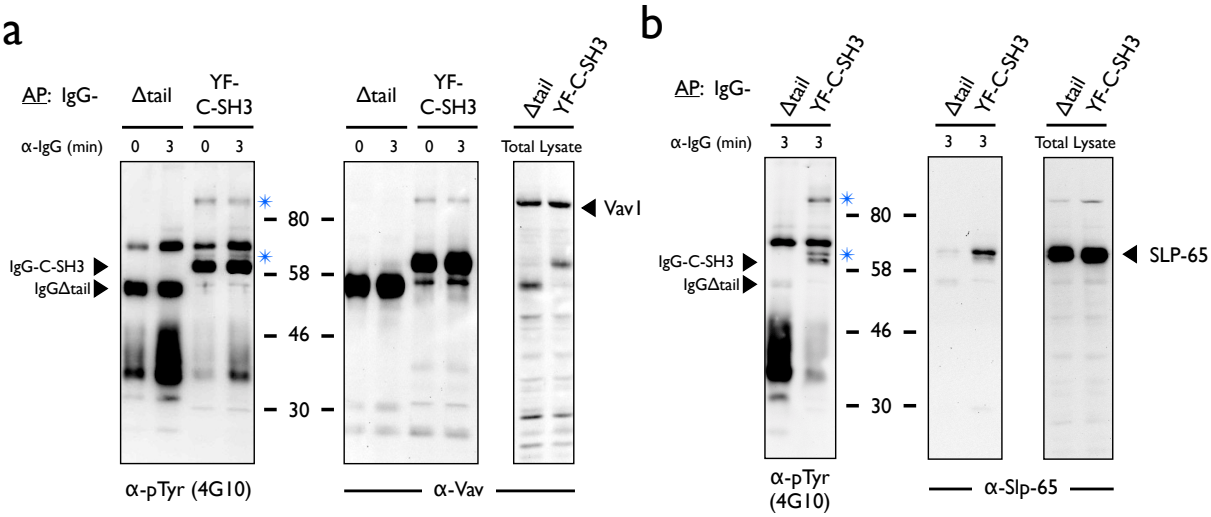

Figure 23 Affinity purification of binding partners of the Grb2 C-SH3 domain. (**a**) mIgG YF-Grb2C-SH3 or tailless mIgG were immunoprecipitated from unstimulated (0 min) or BCR stimulated (3 min) Ramos transfectants using an anti-IgG-biot. antibody and subsequent immobilization on streptavidin-sepharose beads. Purified proteins were analyzed by immunoblotting. Immunoblots were assessed with anti-phospho-tyrosine (pTyr) antibody (4G10) and subsequently with anti-Vav1 antibody. Blot on the right shows total lysates controls. (**b**) Same experiment as in **a**, but without unstimulated cells. Blots were probed for pTyr and SLP-65. Phospho-protein bands specifically purified by the mIgG YF-Grb2C-SH3 fusion protein are marked with a blue asterisks. Numbers between blots indicate relative molecular mass of marker proteins. Data are representative of three independent experiments.

These results suggest that Vav1 and SLP-65 are recruited via Grb2 C-SH3 to the mIgG-BCR and encounter greater phosphorylation. SLP-65 contains a proline-rich Grb2 consensus-binding motif only in its longer isoform. Also, the stronger phosphorylation of SLP-65 by mIgG YF-Grb2C-SH3 stimulation seems to be

restricted to the upper band corresponding to the longer SLP-65 isoform. This indicates that SLP-65's increased phosphorylation is due to direct binding to the IgG-bound C-SH3 domain. As Vav proteins are known to bind to SLP-65 during the canonical BCR pathway, the increased Vav1 phosphorylation may be explained by an indirect effect via SLP-65 binding. To investigate this possibility I made use of the finding that the commonly used W193K mutant of the C-SH3 domain lacks the classical SH3 binding ability to proline-rich motifs but is still able to bind Vav1. The Grb2-Vav1 interaction is different in that it is a SH3-SH3 domain interaction. Thus, the C-SH3 has two partially overlapping binding sites. After studying the crystal structure of both binding modalities I found the phenylalanine 165 in Grb2 to be very important for both the classical SH3 binding site and the Grb2-Vav1 interaction. As presumed, introduction of a phenylalanine 165-to-alanine mutation destroyed both binding sites in the C-SH3 domain, which was confirmed by affinity purification from DG75 EB lysates with wt, W193K and F165A GST-C-SH3 fusion proteins. Figure 24a shows that wt GST-C-SH3 fusion proteins co-purified Vav1 and Sos, as an example of the classical SH3 binding. The W193K mutant failed to purify Sos from cell lysates while Vav1 binding was preserved, even though to a slightly lesser extent. The F165A mutant abolishes protein binding to any of the two binding sites.

I next stimulated DG75 EB cells expressing wt, W193K or F165A mutant mIgG YF-Grb2C-SH3 and compared phosphorylation of Vav1 and SLP-65 by immunoblot analysis. Figure 24b exposes that Vav1 is stronger phosphorylated after both wt and W193K mutant mIgG YF-Grb2C-SH3 stimulation compared to the F165A mutant. The W193K mutant led to an even stronger phosphorylation of Vav1 than wt mIgG YF-Grb2C-SH3. SLP-65, however, was only increasingly phosphorylated by stimulation of wt mIgG YF-Grb2C-SH3. Thus, in both cases the proteins were only stronger phosphorylated when direct binding to the C-SH3 could occur. The fact, that Vav1 phosphorylation is increased in the W193K mutant compared to wt suggests that SLP-65 and Vav1 compete for binding to the C-SH3 domain. Therefore, when SLP-65 cannot bind to the W193K mutant, more Vav1 can be recruited and phosphorylated.

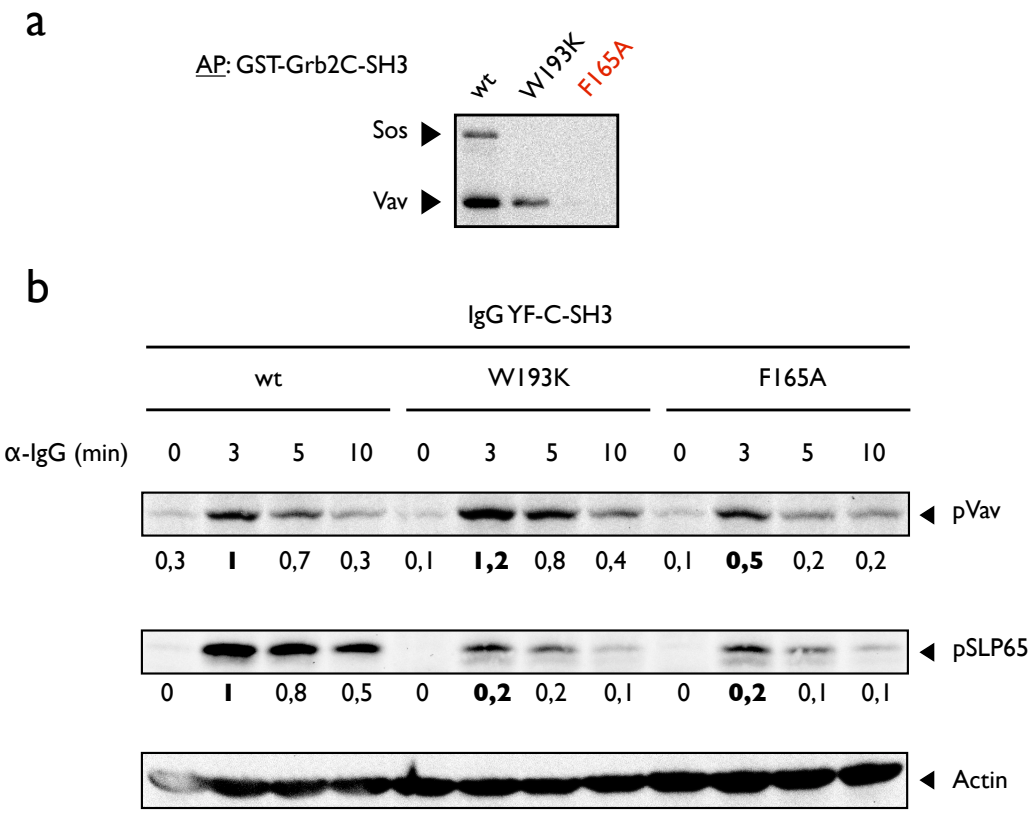

Figure 24 Phosphorylation of SLP-65 and Vav1 is increased by direct recruitment to the C-SH3 domain of Grb2 in ITT signal amplification. (**a**) Immunoblot of purified proteins from DG75 EB cell lysates with wt, W193K or F165A mutant GST-Grb2 C-SH3 fusion proteins. Blot was analyzed with anti-Vav1 and anti-Sos antibodies. (**b**) DG75EB cells expressing wt, W193K or F165A mutant mIgG YF-Grb2C-SH3 were stimulated for the indicated time frames with 10 µg/ml anti-IgG $F(ab)_2$ fragments and lysates were analyzed by immunoblotting for Vav1 phosphorylation with a phospho-specific anti-Vav1 antibody. Actin served as loading control. Numbers below blots represent densitometric quantification of pVav1 and pSLP-65 band intensities corrected by actin loading control and normalized to the intensity of the 3 min time point of wt mIgG YF-Grb2C-SH3 stimulation. Data are representative of three (**a**) and four (**d**) independent experiments.

5.6 ITT-Like Motifs as a Common Theme in Lymphocyte Costimulation

The idea of the ITT-motif causing BCR-intrinsic 'costimulation' has not only originated by the fact that this signaling entity has to be integrated into the canonical BCR pathway as shown in chapter 5.1.2, but also because it shares remarkable homology to signaling motifs in some major co-receptor in lymphocyte signaling. The most prominent example with an almost identical motif is the T cell co-receptor CD28 (ITT-like motif: DYMNM). Co-ligation of CD28 with the T cell receptor (TCR) leads to an enhancement of TCR-induced signaling and IL-2 cytokine production and is required for a productive activation of naïve T cells (Acuto and Michel, 2003). This phospho-tyrosine based motif has been shown to recruit both Grb2 and PI3K in order to fulfill its function, though it was debated to which extent Grb2 is involved in CD28 signaling (Prasad et al., 1994; Schneider et al., 1995; Acuto and Michel, 2003).
Another very similar motif lies within the cytoplasmic tail of the DNAX activating protein (Dap) 10 receptor (ITT-like motif: DYINM) expressed on NK, myeloid and T cells. Its activation has been shown to be required for inducing cytotoxicity of NK cells by the recruitment of Grb2/Vav1-complex and PI3K (Upshaw et al., 2006). There are more lymphocyte co-receptors that harbor an ITT-like motif, some of which recruit Grb2 and others recruit PI3K or both proteins. For an overview I refer to (Engels and Wienands, 2011). The rationale to analyze the above mentioned ones is that CD28 and Dap10 both include a consensus sequence for Grb2 binding and PI3K binding as true for the γ2am ITT while others lack the binding consensus for Grb2. Due to the great sequence similarities it was intriguing to investigate the interchangeability of these motifs in order find out if they also translate into functional similarities. To this end, I genetically exchanged the cytoplasmic tail of γ2am with the cytoplasmic part of CD28 containing the ITT-like motif but lacking the last 25 amino acids with the proline-rich motif (CD28Δ25). Alternatively, I exchanged the γ2am tail with the cytoplasmic tail of Dap10.
Another protein of interest was the latent membrane protein (lmp) 2a of the Epstein-Barr-Virus (EBV), which is expressed on the surface of EBV-infected B lymphocytes and manipulates BCR signaling in various ways. It resembles the BCR function with many, though constitutively phosphorylated, signaling motifs within its N-terminal cytoplasmic part comprising a phospho-tyrosine motif for Lyn recruitment, an ITAM

for Syk recruitment and additional phospho-serine residues for activation of the MAPK-pathways. However, Lmp2a administers a negative effect on BCR signaling by constantly recruiting kinases sequestering them away from the BCR. Interestingly, in its short 27 amino acid C-terminal cytoplasmic tail is an ITT-like motif with the single-letter code amino acid sequence 'PYTNV' that might contribute to lmp2a signaling in a similar manner as the cytoplasmic tails of mIgG and mIgE to the canonical BCR pathway. However, this possibility has not been investigated so far. To determine if this signaling motif may actively contribute to the BCR signaling I also exchanged the cytoplasmic part of γ2am with the C-terminal cytoplasmic tail of lmp2a (lmp2aCtail) and analyzed its signaling capacity within the BCR context in primary B cells.

All of the above mentioned chimeric BCRs were retrovirally transfected into primary B cells in the wild-type form or with the respective ITT inactive YF mutant to compare their ability to boost BCR signaling. Together with the cDNAs an IRES-eGFP cassette was introduced to distinguish transfected from non-transfected cells. Figure 25 shows the Ca^{2+} mobilization after engagement of the chimeric BCRs with anti-IgG $F(ab)_2$ fragments. mIgG2a-CD28Δ25 as well as mIgG2a-lmp2aCtail did not exhibit any differences between wt and YF form indicating that potential phosphorylation of the ITT-like motif did not have an effect on the Ca^{2+} signal (figure 25a and b, respectively) or the tyrosines were not phosphorylated in the first place. Surprisingly, stimulation of wt mIgG-Dap10 boosts Ca^{2+} mobilization in a phosphorylation dependent manner to an even higher extent as wt mIgG (figure 25c). This finding led to the intriguing question whether this strong co-stimulatory effect is also dependent on the recruitment of Grb2 or not. I therefore expressed the wt and YF IgG-Dap10-BCRs in Grb2-deficient primary B cells. The absence of Grb2 resulted in the complete elimination of the Ca^{2+} signal amplification of wt mIgG-Dap10 (figure 22d) resembling the results of wt mIgG stimulation in Grb2-deficient cells. To exclude any differences in the Ca^{2+} signaling capacity between wt and YF mIgG-Dap10 transfected wt and Grb2-deficient cells, the Ca^{2+} signal after stimulation of endogenous mIgM was compared showing no differences (figure 25e and f, respectively).

In conclusion, though similar in sequence, ITT-like motifs can be functionally different. The amino acids surrounding the ITT seem to be important for the binding

of the SH2 domains of either Grb2 or PI3K and single amino acid exchanges in the +1 position of the ITT can alter the signaling outcome. The ITT-like motif of Dap10 and the ITT motif of mIgG seem to follow the same signaling mechanism in that both recruit Grb2 after ITT phosphorylation and the presence of Grb2 is essential to boost the Ca^{2+} signal, even though signal strength varies between the motifs.

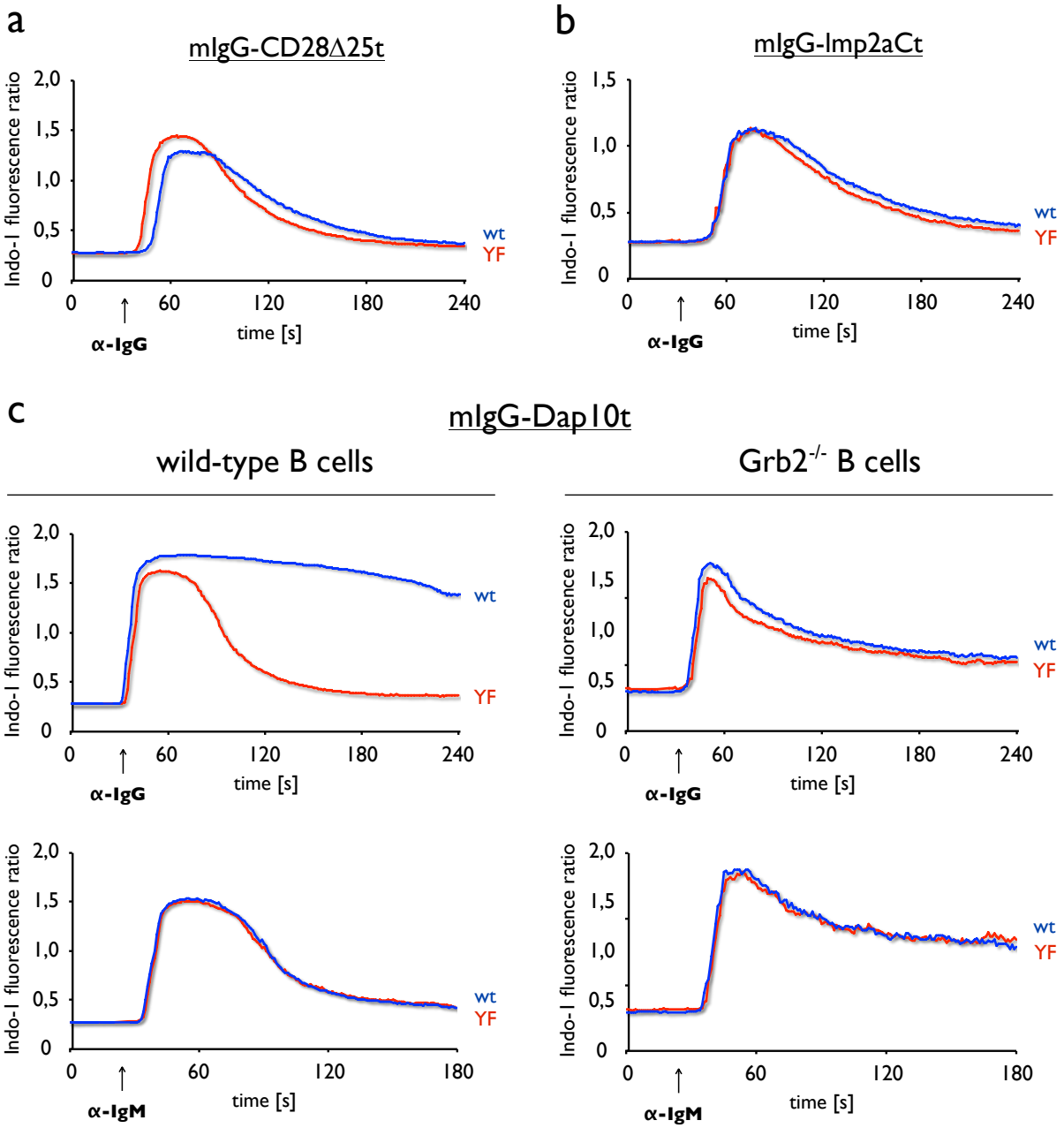

Figure 25 The ITT-like motif of Dap10 boosts Ca^{2+} mobilization in a Grb2-dependent manner in the context of the BCR. Primary B cells from wt mice were isolated, pre-stimulated with LPS for 48 hours and then retrovirally infected to express wt or YF mIgG-CD28Δ25tail (**a**), -Imp2aCt (**b**) or mIgG-Dap10tail (**c**, left side) fusion proteins along with an IRES-eGFP cassette. Cells were loaded with Indo1-AM and intracellular Ca^{2+} release was measured by flow cytometry in eGFP-positive cells before and after stimulation with 10 µg/ml anti-IgG $F(ab)_2$ or 20 µg/ml anti-IgM $F(ab)_2$ as indicated with the black arrow. Primary B cells from B cell-specific Grb2-deficient mice were treated as described above to express wt or YF mIgG-Dap10tail chimeric protein (**c**, right side). GFP positive cells were analyzed for Ca^{2+} flux by flow cytometry as described above. Data are representative of two independent experiments for wild-type and one experiment for Grb2-deficient B cells.

6 Discussion

Previous work of our group and the work presented here explore the molecular mechanisms by which the cytoplasmic tails of mIgG and mIgE administrate burst-enhancing signals that distinguish class-switched from naïve B cells. Niklas Engels showed that a conserved tyrosine residue within the cytoplasmic tails of mIgG and mIgE, entitled the immunoglobulin tail tyrosine (ITT), is phosphorylated upon BCR ligation and leads to amplified Ca^{2+} mobilization by recruitment of the cytosolic adaptor Grb2 via its SH2 domain. I could confirm the increased Ca^{2+} mobilization using primary mouse B cells and further demonstrated that these signals in fact culminate in a proliferative burst that was dependent on the integrity of the Grb2 consensus binding site of the ITT motif. I further elucidated the molecular mechanisms of this signal amplification with the main findings outlined below:

1. The signal amplification relied on the integration into the BCR signalosome suggesting that it acts in the fashion of a classical coreceptor.

2. The complete abrogation of Ca^{2+} signal amplification in Grb2-deficient B cells proved Grb2 to be indispensable for the ITT-based costimulation.

3. ITT costimulation amplified a subset of BCR signaling pathways, namely Ca^{2+} release, PKC activity and Vav1 phosphorylation, while Akt and Erk phosphorylation was not altered.

4. Increased Ca^{2+} mobilization and PKC activity was mediated by the N-terminal SH3 domain of Grb2, most likely through the interaction with Btk stabilizing the Ca^{2+} initiation complex.

5. Direct binding of the C-terminal SH3 domain of Grb2 to SLP-65 and Vav1 facilitated their enhanced phosphorylation, which was independent of initiating the increased Ca^{2+} release.

6. ITT-costimulation in fact led to a proliferative burst, which constitutes one hallmark of memory immune responses.

Primary cells are advantageous over tumor cell lines in terms of reliability and validity of the obtained data. To validate data obtained in cell culture and also extend available readouts to proliferation assays I used primary splenic mouse B cells to study ITT-based signal amplification. For this, some technical challenges had to be addressed. Resting mouse B cells only survive one or two days in culture if not stimulated with a mitogen. In addition, these cells can only be transfected upon proliferation. LPS is commonly used to encounter these restrictions giving a strong mitogenic signal. However, it was not known if this pre-activation interferes with the BCR responsiveness. As it turned out, LPS-stimulated primary B cells showed a robust Ca^{2+} flux after BCR stimulation that was reminiscent of the Ca^{2+} flux pattern observed in B cell lines. This fact enabled the analysis of Ca^{2+} flux of transfected, mIgG2a expressing primary B cells. Even though, through optimization of the infection protocol, the primary B cells were very efficiently transfected, the remaining untransfected cells still remained a problem for subsequent experiments. This issue could be addressed by coexpression of eGFP together with the γ2am cDNA that allowed distinguishing transfected from untransfected cells by flow cytometry. The establishment of this experimental setup was an important step to validate cell line results in primary B cells and moreover enabled the analysis of the proliferative response upon IgG-BCR stimulation (discussed in 6.5).

6.1 ITT Signaling Relies on Integration into the BCR Signalosome

'Outsourcing' of the ITT-containing εm tail by fusing it to the extracellular and transmembrane domains of CD8 revealed that the ITT requires to be integrated into the BCR signalosome in order to administrate its role in signal amplification. The CD8-εm construct was only phosphorylated and boosted Ca^{2+} mobilization upon cocrosslinking with the BCR. 'Supercrosslinking' of the isolated CD8-εm fusion protein resulted only in a minor and very delayed Ca^{2+} response. This is very reminiscent of the coreceptor CD28 that has been shown to require the presence of the TCR signalosome (Dennehy et al., 2007). Thus, the ITT motif in the cytoplasmic tails of mIgG and mIgE seem to function in manner of a classical coreceptor. Class-switching to these isotypes directly integrates the costimulatory unit into the BCR making it amenable to speculate that mIgG and mIgE expressing B cells are less dependent on costimulation and bystander activation than mIgM expressing B cells.

A T cell independent reactivation of mIgG expressing memory B cells was indeed shown using different enveloped viruses as antigens (Hebeis, 2004). For soluble antigens and other T-cell dependent antigens, however, T cell help still seems to be required for reactivation of class-switched B cells. The cellular response of ITT costimulation will be discussed in chapter 6.5.

6.2 Grb2 is Essential for ITT Signal Amplification

The ITT motif of mIgG2a contains putative binding sites for Grb2 and PI3K. It was therefore very intriguing to find out, which of these binding partners causes the ITT-based signal amplification of mIgG2a-BCR. I addressed this question using different approaches. First, using mutational analysis of the ITT motif disrupting either the Grb2 or p85 binding consensus site ('pYxN' and 'pYxxM') I analyzed which one is required for the enhanced Ca^{2+} signal upon BCR stimulation. Mutation of asparagine at the +2 position, but not of methionine in the +3 position of the ITT, abrogated the enhanced Ca^{2+} mobilization of wt mIgG2a, demonstrating that only the Grb2 binding motif is required for signal amplification. The same requirement was shown for the Grb2 binding motif in the coreceptors CD28 and Dap10 (Prasad et al., 1994; Upshaw et al., 2006) that both harbor very similar motifs in their cytoplasmic tails (YMNM and YINM, respectively). However, for both coreceptors additional binding of p85 for their function was described. In contrast, Niklas Engels demonstrated for the IgG2a ITT by affinity purification using biotinylated phospho-peptides resembling the ITT motif that Grb2 is the major co-purified protein of the pITT motif. The preferential binding of the Grb2-SH2 versus p85-SH2 domain may be explained by the conserved positively charged arginine that is positioned in the +1 position of γm ITTs. A peptide library screen by Kessels et al. examined that the SH2 domain of Grb2 but not p85 tolerates a positively charged amino acid in this position (Kessels et al., 2002). However, as the alanine in the +1 position of the εm-tail does not compromise the ITT's function there might be other mechanisms that facilitates preferential binding of Grb2 to the ITT.

The findings did not yet prove Grb2 to be the relevant effector for signal amplification, as I could show that the Grb2/Sem-5 family member Grap can also bind to the pYxN motif. However, the collaboration with the group of Lars Nitschke (Friedrich-Alexander-University, Erlangen) allowed me to use primary B cells from

their B cell specific Grb2$^{-/-}$ mouse (Ackermann et al., 2011) demonstrating that in the signaling differences between wt and YF mIgG2a were completely diminished in the absence of Grb2. Moreover, reintroduction of Grb2 cDNA in addition to the γ2am cDNA restored the Ca^{2+} signal amplification after stimulation of wt compared to YF mutant mIgG2a proving Grb2 to be the main 'downstream' effector of ITT costimulation.

6.3 Ca^{2+} Signal Amplification Depends on the N-terminal SH3 Domain of Grb2

A major obstacle investigating the downstream effectors of Grb2 was the fact that Grb2 has a multitude of known interaction partners with partially opposing functions. As described in the introduction, Grb2 is involved in many signaling pathways that exert positive as well as negative functions in BCR signaling (Jang et al., 2009; Neumann et al., 2009). Any modifications of Grb2 will therefore have an effect on all pathways Grb2 is involved in making it impossible to decipher the impact the modification has specifically for the ITT signaling pathway. Reconstitution of Grb2-deficient primary mouse B cells with Grb2 harboring inactivating mutations for the N- or C-SH3 domain, respectively, suggested an equal contribution of both SH3 domains to the increased Ca^{2+} mobilization (figure 13). Due to the above-mentioned challenges, I tried a different approach simplifying the ITT signaling initiation mechanism. To this end, I fused either the N- or the C-terminal SH3 domain of Grb2 to YF mutant mIgG2a. With this move, the initial recruitment of Grb2 to the ITT is skipped anchoring the SH3 domains right to the site of ITT signaling. As Grb2 is recruited to the ITT by virtue of its SH2 domain (Engels et al., 2009), the flanking SH3 domains are able to bind two additional proteins to exert the ITT's signaling function. Fusing the SH3 domains to YF mIgG2a had two major advantages for analyzing the function of Grb2 in ITT signaling. First, all effects observed were ITT pathway specific, since cytosolic Grb2 was not modified and, thus, was available to all other Grb2 signaling pathways. Second, fusing only one SH3 domain to mIgG2a at a time enabled to examine function and binding partners of each SH3 domain individually. Fortunately, the mIgG YF-Grb2N/C-SH3 fusion proteins were readily expressed on the cell surface. Stimulation of SH3 inactivated fusion proteins showed the same Ca^{2+} mobilization pattern as YF mIgG. Hence, the

canonical BCR signaling pathway was not disrupted and all changes in Ca^{2+} mobilization by stimulation of mIgG YF-Grb2N/C-SH3 could be attributed to the function of the respective SH3 domain. With this experimental setup it was clearly demonstrated that the N-SH3 but not the C-SH3 boosts Ca^{2+} flux after BCR ligation.
Another very important aspect of this experiment was, that Ca^{2+} amplification was due to recruitment of a positive effector protein by the Grb2 N-SH3 rather than sequestration of Grb2 from inhibitory signal complexes, a mechanism proposed for the non-T cell activation linker (NTAL) (Stork et al., 2004). Furthermore, integrating the N-SH3 domain right into the BCR is sufficient to amplify Ca^{2+} mobilization in the complete absence of Grb2 (figure 15).
I could show that Grb2 acts upstream of the Ca^{2+} initiation complex as SLP-65 was stronger phosphorylated by the mIgG YF-Grb2N-SH3 fusion protein, which was not caused by direct binding of the N-SH3 to SLP-65. Finding the physiological relevant binding partner of the N-SH3 was very challenging. Affinity purification of mIgG YF-Grb2N-SH3 co-purified many of the known binding partners implicating that there was no pathway specificity using the fusion protein for purification. This fact shifted my approach to address this issue to an exclusion-based process. For this, I identified overlapping binding partners between Grap N-SH3 and Grb2 N-SH3. As the Grap N-SH3 failed to induce Ca^{2+} signal amplification, I could exclude all proteins binding to the Grap N-SH3 to be responsible for the increased signaling capacity of the Grb2 N-SH3. With this approach, Sos, c-Cbl and Cblb could be excluded as relevant binding partners. Despite some contradictory studies for the Cbl proteins, none of these proteins have been reported to play a role in enhancing Ca^{2+} signaling further supporting their dispensability in ITT signal mediation. The co-purification of Btk, however, fitted well into the phenotype increasing Ca^{2+} flux. This interaction had been described using a yeast-two-hybrid screen (Papin and Subramaniam, 2004) and also by our group (unpublished results), but so far no physiological relevance has been shown. Using a Btk knock out in the DG75 B cell line (made by Wiebke Schulze from our group) I investigated the significance of this interaction in ITT signaling. The pronounced increase of Ca^{2+} release after mIgG YF-Grb2N-SH3 stimulation was abrogated in the absence of Btk with equal Ca^{2+} mobilization pattern between mIgG YF-Grb2N-SH3 and –Grb2C-SH3. This demonstrated that the difference in signaling capacity of the N-SH3 and C-SH3 in the ITT signaling pathway relied on the presence of Btk. However, the N-SH3 inactive

W36K mutant showed an even decreased Ca^{2+} mobilization implying that either the W36K mutant exhibits a decreased signaling ability through Igα/β or the N-SH3 and C-SH3 both increase Ca^{2+} mobilization slightly independently of Btk. For the N-SH3 domain it is conceivable that other players than Btk, like other Tec kinase family members or p85, may enhance Ca^{2+} flux in the absence of Btk. For the C-terminal SH3 domain it is implausible that binding of any proteins increase the Ca^{2+} release compared to the W36K mutant mIgG YF-Grb2N-SH3, because stimulation of wt and binding-deficient F165A mutant mIgG YF-Grb2C-SH3 resulted in identical Ca^{2+} mobilization.

To address this issue it would be very useful to investigate if the W36K mutant mIgG YF-Grb2N-SH3 or wt mIgG YF-Grb2N/C-SH3 Ca^{2+} release pattern constitute the basal signaling through Igα/β. After the basal Ca^{2+} release was determined one could analyze the contributions of the SH3 domains. To this end, one could use other mIgG YF-SH3 fusions with different binding abilities, for example the Grap SH3 domain fusions. Furthermore, reconstitution of wt Btk and mutant Btk lacking the Grb2 binding sequences might be very helpful to elucidate its role in ITT signaling. Despite these ambiguities, it is safe to conclude that the difference in signaling capacity between mIgG YF-Grb2N-SH3 and mIgG YF-Grb2C-SH3 relies on the presence of Btk.

It was shown for CD28 costimulation by Dennehy et al. that Itk, also a member of the Tec kinase family, and subsequent PLC-γ1 phosphorylation is dependent on an intact Grb2 binding site of the ITT-like motif 'pYMNM' (Dennehy et al., 2007). In this study the stronger Itk phosphorylation was correlated with formation of the SLP-76-Vav-Itk signalosome downstream of Vav1, that is recruited via the C-SH3 domain of Grb2. Very interestingly, one of the two Grb2 N-SH3 consensus-binding sequences of Btk (PLPP) is also found in Itk. Thus, it might be possible that Itk is not recruited by Vav1 during CD28 costimulation, but by the Grb2 N-SH3 domain similar to the Btk recruitment in the ITT signaling.

6.4 ITT-based Modulation of BCR Signaling Pathways

Horikawa et al. showed that the overall phosphorylation pattern after mIgM and mIgMG stimulation was equal. I made the same observation when immunoblotting wt and NA mIgG stimulated cell lysates with an anti-phospho-tyrosine antibody. However, by using specific phospho-protein antibodies the increased phosphorylation of SLP-65 and Vav1 could be revealed. These differences were not apparent in the total phospho-tyrosine blot.

SLP-65 and the Ca^{2+} Initiation Complex

Niklas Engels showed an increased phosphorylation of SLP-65, PLC-γ2 and a stronger production of IP3 explaining the Ca^{2+} signal amplification phenotype of ITT-based costimulation. With the chimeric mIgG YF-Grb2-SH3 fusion proteins I could demonstrate that both SH3 domains contribute to the stronger phosphorylation of SLP-65. The N-SH3 mediates this most likely through binding to Btk resulting in enhanced recruitment and/or stabilization of the Ca^{2+} initiation complex. For the C-SH3 domain, direct interaction with SLP-65 was required for its enhanced phosphorylation. Although direct interaction of the Grb2 C-SH3 with the long isoform of SLP-65 is both published (Grabbe and Wienands, 2006) and demonstrated herein for the mIgG YF-Grb2C-SH3 BCR, the increased phosphorylation of SLP-65 comes to a surprise in that one would expected it to translate into a stronger Ca^{2+} release. The phospho-SLP-65 antibody used recognizes pTyr96 in SLP-65, which resembles the docking site for Btk. It is therefore conceivable that simultaneous Btk recruitment and complex formation is the bottleneck for initiating an amplified Ca^{2+} response in this specific setup.

Vav1

The increased phosphorylation of Vav1 constitutes another similarity to Dap10 and CD28. There, the intact Grb2 binding site in the ITT-like motif was required for Vav1 phosphorylation (Upshaw et al., 2006; Dennehy et al., 2007). In parallel, wt but not NA mutant mIgG stimulation led to increased Vav1 phosphorylation in DG75 B cells. Vav proteins (Vav1, 2, 3) are associated with various activating functions in lymphocytes. They function as a guanine nucleotide exchange factor for small GTPases of the Rho-family resulting in cytoskeletal rearrangements, proliferation and Ca^{2+} mobilization (Fujikawa et al., 2003). The latter suggested that Vav1 might

contribute to the increased Ca^{2+} release after mIgG stimulation. However, this possibility was excluded by the finding that stimulation of mIgG YF-Grb2C-SH3 did not induce Ca^{2+} signal amplification. Vav1 is a known binding partner of the Grb2 C-SH3 domain and was also co-purified with the mIgG YF-Grb2C-SH3 BCR suggesting that direct binding to the C-SH3 results in its phosphorylation. It was also conceivable that Vav1 is indirectly phosphorylated through binding to SLP-65 that is recruited to the Grb2 C-SH3. This mode of action could be discounted by comparison of mutant C-SH3 domains with differential binding ability to SLP-65 and Vav1. I discovered that the commonly used W193K mutant, that is a published inactivating mutant for the Grb2 C-SH3 (Stork, 2006), has still binding capability to Vav1 while lacking affinity to SLP-65. This is explained by two different binding modes of the C-SH3 domain. Partly overlapping binding sites are responsible for either binding Vav1 via unusual SH3 domain dimerization or canonical binding to proline-rich motifs of other binding partners (Ye and Baltimore, 1994; Nishida et al., 2001). The W193K mutant abrogates canonical binding to proline-rich motifs while preserving the unusual Vav1 interaction site. Using W193K mutant mIgG YF-Grb2C-SH3 BCRs I could show that Vav1 is even stronger phosphorylated compared the wt C-SH3 containing fusion protein indicating a competitive binding modality of Vav1 and SLP-65 to the C-SH3 domain of Grb2. In the absence of SLP-65 competition, more Vav1 proteins could be recruited resulting in an increased phosphorylation. After studying the crystal structure of both binding modalities of the Grb2 C-SH3 domain (Nishida et al., 2001) I found the phenylalanine 165 in Grb2 to be very important for both the classical SH3 binding site and the Grb2-Vav1 interaction. Introduction of a phenylalanine 165-to-alanine mutation indeed destroyed both binding sites in the C-SH3 domain. As expected, stimulation of F165A mutant mIgG YF-Grb2C-SH3 did neither enhance SLP-65 nor Vav1 phosphorylation. The differential binding capabilities of W193K and F165A mutant C-SH3 constitute a great tool to functionally examine contributions of Vav1 compared to canonical binding partners. In this respect, it might be insightful to reconsider results of studies using the W193K mutant of Grb2 in lymphocytes (Vav proteins are only expressed in hematopoietic cells) in regard to Vav1 binding.

PI3K and Akt

It was shown for Dap10 and CD28 that both recruit p85 of PI3K in addition to Grb2 to administrate costimulatory functions. Also, if not directly recruited to the ITT p85 could interact with the Grb2 N-SH3 domain (Wang et al., 1995; Neumann et al., 2009). It was therefore very intriguing to find out whether the ITT costimulation increases PI3K activity. The product of PI3K activity is PIP_3 which itself leads to the recruitment and activation of Akt. Using Akt phosphorylation as a readout I found no differences after wt compared to NA mutant mIgG stimulation leading to the conclusion that PI3K activity is not altered by ITT costimulation.

Erk

Since Grb2 is in many cells associated with Sos-mediated Ras/MAPK pathway activation I analyzed phosphorylation and activity of Erk downstream of ITT signaling. Phosphorylation of Erk was equally increased after wt or NA mutant mIgG stimulation in DG75 cells. To exclude that there was a minimal effect that might be overlooked by phospho-Erk immunoblotting I used the genetically engineered FRET-based Erk kinase activity reporter EKAR (Harvey et al., 2008). This reporter enabled ratiometric analysis of Erk activity in living cells by flow cytometry. Also with this sensitive real-time measurement no difference in Erk activity was revealed after wt compared to NA mutant mIgG stimulation. The results are in line with observations by (Horikawa et al., 2007), who showed that Erk activation is not influenced by the presence of the cytoplasmic tail of mIgG1 in primary B cells. This is not surprising keeping in mind that Ras/Erk activation downstream of the BCR is mainly mediated by RasGRP instead of the Grb2/Sos complex (Oh-hora, 2003). However, the ITT also could have indirectly increased Erk activity by enhancing RasGRP recruitment through stronger PLC-γ2-mediated DAG production. Hence, RasGRP might already be fully activated by ITAM-mediated signaling or it has additional activation requirements that are not met by ITT costimulation. The enhanced DAG production by PLC-γ2 was demonstrated indirectly by Niklas Engels, who showed that IP3 levels were increased after wt compared to mutant mIgG stimulation. As IP3 and DAG emanate from the same reaction in a 1:1 stoichiometry, the DAG concentration should also rise.

Protein Kinase C

Protein kinase C is also recruited to DAG in the plasma membrane. It was therefore interesting if the increased production of DAG is translated into a stronger PKC activity. To test this, I used another genetically engineered FRET-based biosensor, called 'C kinase activity reporter' (CKAR) (Violin et al., 2003). Indeed, PKC activity was initiated more rapid and was increased after wt compared to W36K mutant mIgG YF-Grb2N-SH3 fusion proteins. Though, the biosensor has a relatively low dynamic range of about 10%, it was a reliable means to measure PKC activity in real-time in living cells by flow cytometry.

Biosensors

FRET-based biosensors have become a popular tool for studying biochemical events in live cells. They are mostly used in fluorescence microscopy as one can study the spatio-temporal activity of proteins. During this study I measured biosensors activity by flow cytometry. With this, one sets the information of the spatial distribution aside but gains a statistically reliable continuous measurement of protein activity in live cells. Although, only two biosensors were used as proof of principle, I believe they have great potential for studying biochemical events, especially in heterogeneous cell cultures, such as transfected primary cells, for which standard biochemical assays are not applicable.

In conclusion, ITT-based costimulation increased the activation of only a subset of signaling pathways downstream of the BCR leading to an enhanced Ca^{2+} mobilization, PKC activity and Vav1 phosphorylation.

6.5 ITT Boosts Proliferation in a Grb2 Dependent Manner

Several different studies using transgenic mouse models investigated the physiological role of the cytoplasmic tails of mIgG and mIgE demonstrating their fundamental role in establishing strong secondary immune responses (Achatz et al., 1997; Kaisho et al., 1997; Martin and Goodnow, 2002; Sato et al., 2007; Waisman et al., 2007). It was shown that the presence of the cytoplasmic tail of mIgG1 led to a stronger Ca^{2+} release and proliferation after BCR stimulation (Waisman et al., 2007), decreased cell loss (Horikawa et al., 2007) and subsequently to more antigen-specific

B cells and plasma cells. Thus, I was eager to explore if these signal enhancements of the ITT indeed cumulate in a cellular response that would mirror the burst-enhancing role of the cytoplasmic tails. To this end, I analyzed the proliferative response of primary B cells that were transfected with either wt or mutant mIgG2a. Using a cell proliferation marker dye that was compatible with coexpression of eGFP I could monitor proliferation of transfected cells upon BCR stimulation by flow cytometry. Even though the primary B cells had to be pre-activated with LPS for cultivation and retroviral transfection, additional stimulation of the BCR resulted in an increased proliferation. Moreover, wt mIgG stimulation induced a much stronger proliferative response than YF and NA mutant mIgG stimulation demonstrating that the burst-enhancing role can be indeed ascribed to ITT-mediated Grb2 recruitment. Vav1 has been shown to be essential for the proliferative response and blast formation downstream of the BCR (Fujikawa et al., 2003) suggesting that the Grb2 mediated Vav1 recruitment to the ITT may contribute to the proliferative effect of the ITT. In this regard, one could use the mIgG YF-Grb2SH3 fusion proteins for the proliferation assay investigating the individual contribution of increased Ca^{2+} response and Vav1 activation to the proliferative response.

The role of Grb2 in memory B cell responses was demonstrated by (Ackermann et al., 2011) 2009, who showed that Grb2 ablation in B cells diminished a robust secondary immune response. This publication further underlined the importance of Grb2 recruitment to the ITT for the reactivation of class-switched B cells.

The exact mode of action of ITT costimulation on the cellular level during an immune response is still not clear. The proliferative-burst might give class-switched B cells an advantage during the germinal center reaction leading to an increased population of class-switched versus non-class-switched B cells. In addition, class-switched memory B cells can expand more rapidly to generate a robust secondary immune response. The ITT might also additionally facilitate plasma cell differentiation. This possible role could not be addressed using our *in vitro* system with LPS stimulated transfected B cells. Still, it would be of great interest to analyze the cellular response mechanisms that the ITT administrates *in vivo*. Two studies have shown that IgM memory B cells have the tendency to re-establish a germinal center reaction, whereas IgG memory B cells favor rapid differentiation to plasma cells (Dogan et al., 2009; Pape et al., 2011). It would be of great interest to explore the influence of isotype-specific BCR signaling in this cell fate decision. In this respect, ITT signaling might alter surface expression

of cytokine or chemokine receptors that lead to targeting of the cell to different lymphoid structures. (Horikawa et al., 2007) could show that signals of the mIgG1 cytoplasmic tail failed to induce CCR7 upregulation upon BCR stimulation, which is associated to migration of B cells to the T cell zone. Further *in vivo* studies will be necessary to understand the exact cellular responses of ITT-based costimulation.

6.6 ITT-Like Motifs in Lymphocytes

Throughout the discussion I have highlighted many similarities between the ITT and similar motifs in CD28 and Dap10. The ITT-like motifs in the cytoplasmic tails of CD28 and Dap10 have been described to recruit Grb2, but also p85 (Engels and Wienands, 2011). Mutational analysis showed that for both tails the Grb2 binding site is important for Ca^{2+} mobilization and Vav1 phosphorylation (Upshaw et al., 2006; Dennehy et al., 2007). While PI3K was not required for CD28-mediated Ca^{2+} mobilization and IL-2 production (Kim et al., 1998; Dennehy et al., 2007), p85 binding to Dap10 was required to mount an optimal Ca^{2+} signal (Upshaw et al., 2006). The mode of action for the ITT-like signaling motifs seems to be very similar, though, as discussed above, p85 binding is dispensable for Ca^{2+} signal amplification in the context of the BCR. Due to the described similarities I was eager to test if the cytoplasmic tails were exchangeable. Indeed, the cytoplasmic tail of Dap10 could substitute the stimulatory function of the mIgG2a cytoplasmic tail, boosting Ca^{2+} mobilization upon mIgG-Dap10t stimulation. With the respective ITT YF mutant it was shown that this effect relied on an intact ITT. Furthermore, Grb2 was also shown to be necessary for the Ca^{2+} signal amplification.

The mIgG-CD28Δ25t and mIgG-lmp2aCt chimeras were not able to reconstitute the lack of the IgG2a ITT. For the mIgG-CD28Δ25t it would be intriguing to explore if the motif was phosphorylated at all and, if it was, other readouts such as Akt activation should be examined to test if p85 is preferentially recruited to this motif. As the lmp2aCt lacks the p85 consensus binding site and Grb2 binding has been shown to enhance Ca^{2+} mobilization, it is most likely that this motif is not phosphorylated in the first place. Both the proline residue at position -1 of the ITT as well as the bulky tryptophan at position +1 may abolish phosphorylation and/or recruitment of Grb2 to this distinct motif. However, further investigation is needed for this conclusion.

Despite the lack of function of the CD28Δ25 tail in this setup, the ITT-like motifs in CD28 and Dap10 and the ITT in mIgG and mIgE seem to share the same signaling mechanisms. Therefore, ITT-like motifs appear to represent a common theme for costimulation of ITAM-based lymphocyte signaling (Engels and Wienands, 2011) that is of fundamental importance for the effector function of the respective cell type.

7 Conclusion

With this work I could significantly contribute to the mechanistic understanding of isotype-specific signaling processes of IgG- and IgE-BCRs. The cytoplasmic tails of these isotypes comprise a signaling motif around a conserved tyrosine residue, the immunoglobulin tail tyrosine or ITT. Phosphorylation of the ITT recruits the cytosolic adaptor protein Grb2 via the consensus binding site for its SH2 domain (pYxN). The necessity of Grb2 for ITT-costimulation was demonstrated by the complete absence of Ca^{2+} signal amplification in Grb2-deficient primary B cells. Grb2 recruits additional or stabilizes existing protein complexes of the BCR signalosome. I could demonstrate that the N-terminal SH3 domain of Grb2 is necessary and sufficient to increase Ca^{2+} mobilization and PKC activity, while the C-terminal SH3

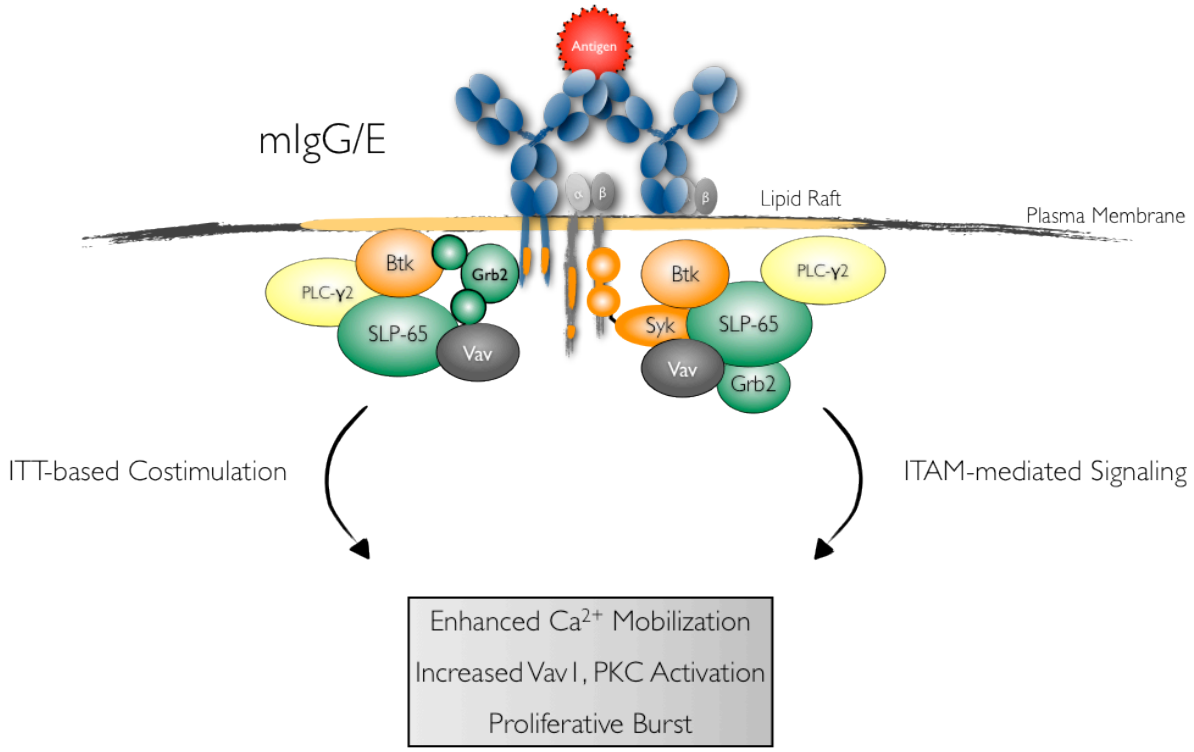

Figure 26 Model of ITT-costimulation. Ig class-switching to IgG- or IgE-BCRs integrates a costimulatory signaling motif, the ITT motif, directly into the BCR fueling ITAM-mediated signals. Upon BCR crosslinking the ITT is phosphorylated enabling binding of the SH2 domain of the cytosolic adaptor protein Grb2. The N-SH3 domain of Grb2 interacts with Btk while Vav1 and SLP-65 compete for binding to the C-SH3. Thus, Grb2 recruits additional or stabilizes pre-existing protein complexes of the BCR signalosome leading to an enhanced and sustained Ca^{2+} mobilization and increased phosphorylation of PKC and Vav1 that ultimately results in an enhanced proliferative burst of mIgG-expressing cells.

leads to an increased phosphorylation of SLP-65 and Vav1. Thus, by Ig class-switching to IgG or IgE isotypes B cells potentiate signaling through the canonical pathway by integrating the costimulatory ITT motif directly into the BCR. The ITT leads to the activation of a subset of ITAM-initiated signaling pathways culminating in a proliferative burst that is one hallmark of a robust memory immune response.

8 Abbreviations

AA	Amino acid
Amp	Ampicillin
AP	affinity purification
APS	ammonium persulphate
ATP	adenosine trisphosphate
BCR	B cell antigen receptor
BLNK	B cell linker protein
bp	base pair
BSA	bovine serum albumin
Btk	Bruton's tyrosine kinase
Cbl	Casitas B-lineage lymphoma
CD	cluster of differentiation
CFP	Cyan fluorescent protein
Citrine	Derivative of yellow fluorescent protein
CKAR	C kinase activity reporter
Cy5	Cyanine Dye 5 (far-red em.)
DAG	diacylglycerol
DMEM	Dulbecco's modified Eagle's medium
DMSO	dimethylsulfoxid
DNA	deoxyribonucleic acid
a	deoxyadenosine monophosphate (dAMP)
t	deoxythymidine monophosphate (dTMP)
g	deoxyguanosine monophosphate (dGMP)
c	deoxycytidine monophosphate (dCMP)
EB	EcoBlast (Ecotropic receptor, Blasticidin resistance in vector)
E. coli	*Escherichia coli*
ECL	enhanced chemoluminescence
EDTA	ethylenediaminetetraacetic acid
EGTA	ethylene glycol tetraacetic acid
eGFP	enhanced green fluorescent protein
EKAR	Erk kinase activity reporter
Erk	extracellular signal-regulated kinase

$F(ab')_2$	bivalent antigen-binding fragment
FACS	fluorescence activated cell sorter
Fc	fragment crystalline
FCS	fetale calf serum
FITC	fluorescein-5-isothiocyanate
FRET	Förster resonance energy transfer
Grb2	growth factor receptor-bound protein 2
GRAP	Grb2-related adaptor protein
GST	glutathione-S-transferase
HEK	human embryonic kidney
HRPO	horseradish-peroxidase
Ig	immunoglobulin
IgH	Ig heavy chain
IgL	Ig light chain
Indo-1	1H-indole-6-carboxylic acid, 2-[4-[bis[2- [(acetyloxy)methoxy]-2-o xoethyl]amino]-3-[2-[2-[bis[2-[(acetyloxy)methoxy]-2-oxoethyl]amino]-5- methylphenoxy]ethoxy]phenyl]-, (acetyloxy)methyl ester
IP	immunoprecipitation
IP_3	inositol 1,4,5-trisphosphate
IP_3R	IP_3 receptor
IRES	internal ribosome entry site
ITAM	immunoreceptor tyrosine-based activation motif
ITIM	immunoreceptor tyrosine-based inhibitory motif
ITT	immunoglobulin tail tyrosine
Kan	Kanamycin
LPS	Lipopolysaccharide
mAb	monoclonal antibody
MAPK	mitogen-activated protein kinase
mIg	membrane Ig
NFAT	nuclear factor of activated T cells
NFκB	nuclear factor for κ gene in B lymphocytes
OD	optical density
PAGE	polyacrylamide gel electrophoresis
PH	Pleckstrin-homology

PI3K	phosphatidylinositol-3´-kinase
PIP_2	phosphatidylinositol-4,5-bisphosphate
PIP_3	phosphatidylinositol-3,4,5-trisphosphate
PLC-γ	phospholipase-C-γ
PTK	Protein Tyrosine Kinase
pTyr	phospho-Tyrosine
RNA	ribonucleic acid
rpm	rounds per minute
RPMI	Roswell Park Memorial Institute
RT	reverse transcription
SDS	sodium dodecyl sulfate
SH2	Src-homology 2
SH3	Src-homology 3
SLP65	SH2-domain containing leucocyte protein of 65 kDa
Syk	spleen tyrosine kinase
tagRFP	"tag" red fluorescent protein
TCR	T cell antigen receptor
TEMED	N,N,N',N'-tetramethylethylene-diamine
Tris	Tris-(hydroxymethyl)-aminomethane
w/o	without
wt	wild-type
X-Gal	5-bromo-4-chloro-3-indolyl-beta-D-galactopyranoside

Prefixes & Units

All units are in correspondence with the **International System of Units, SI** (Système International d'Unités), established by the „General Conference on Weights and Measures" (CGPM).

Amino Acids

Amino Acid	3-Letter Code	1-Letter Code
Alanine	Ala	A
Arginine	Arg	R
Asparagine	Asn	N
Aspartic Acid	Asp	D
Cysteine	Cys	C
Glutamic Acid	Glu	E
Glutamine	Gln	Q
Glycine	Gly	G
Histidine	His	H
Isoleucine	Ile	I
Leucine	Leu	L
Lysine	Lys	K
Methionine	Met	M
Phenylalanine	Phe	F
Proline	Pro	P
Serine	Ser	S
Threonine	Thr	T
Tryptophan	Trp	W
Tyrosine	Tyr	Y
Valine	Val	V

9 Bibliography

Achatz, G., Nitschke, L., and Lamers, M.C. (1997). Effect of transmembrane and cytoplasmic domains of IgE on the IgE response. Science *276*, 409–411.

Ackermann, J.A., Radtke, D., Maurberger, A., Winkler, T.H., and Nitschke, L. (2011). Grb2 regulates B-cell maturation, B-cell memory responses and inhibits B-cell Ca(2+) signalling. Embo J *30*, 1621–1633.

Acuto, O., and Michel, F. (2003). CD28-mediated co-stimulation: a quantitative support for TCR signalling. Nat Rev Immunol *3*, 939–951.

Ahmed, R., and Gray, D. (1996). Immunological memory and protective immunity: understanding their relation. Science *272*, 54–60.

Baba, Y., Hayashi, K., Fujii, Y., Mizushima, A., Watarai, H., Wakamori, M., Numaga, T., Mori, Y., Iino, M., Hikida, M., et al. (2006). Coupling of STIM1 to store-operated Ca2+ entry through its constitutive and inducible movement in the endoplasmic reticulum. Proc Natl Acad Sci USA *103*, 16704–16709.

Batista, F.D., and Harwood, N.E. (2009). The who, how and where of antigen presentation to B cells. Nat Rev Immunol *9*, 15–27.

Ben-Bassat, H., Goldblum, N., Mitrani, S., Goldblum, T., Yoffey, J.M., Cohen, M.M., Bentwich, Z., Ramot, B., Klein, E., and Klein, G. (1977). Establishment in continuous culture of a new type of lymphocyte from a "Burkitt like" malignant lymphoma (line D.G.-75). Int. J. Cancer *19*, 27–33.

Cahalan, M.D. (2009). STIMulating store-operated Ca2+ entry. Nat Cell Biol *11*.

Campbell, M.A.M., and Sefton, B.M.B. (1992). Association between B-lymphocyte membrane immunoglobulin and multiple members of the Src family of protein tyrosine kinases. Molecular and Cellular Biology *12*, 2315–2321.

Carrasco, Y.R., and Batista, F.D. (2006). B cell recognition of membrane-bound antigen: an exquisite way of sensing ligands. Curr Opin Immunol *18*, 286–291.

Casey, P.J. (1995). Protein lipidation in cell signaling. Science *268*, 221–225.

Cheng, P.C., Dykstra, M.L., Mitchell, R.N., and Pierce, S.K. (1999). A role for lipid rafts in B cell antigen receptor signaling and antigen targeting. J Exp Med *190*, 1549–1560.

Conley, M.E., Dobbs, A.K., Quintana, A.M., Bosompem, A., Wang, Y.-D., Coustan-Smith, E., Smith, A.M., Perez, E.E., and Murray, P.J. (2012). Agammaglobulinemia and absent B lineage cells in a patient lacking the p85α subunit of PI3K. J Exp Med.

Cyster, J.G. (2010). B cell follicles and antigen encounters of the third kind. Nat Immunol *11*, 989–996.

Dennehy, K.M., Elias, F., Na, S.-Y., Fischer, K.-D., Hünig, T., and Lühder, F. (2007). Mitogenic CD28 signals require the exchange factor Vav1 to enhance TCR signaling at the SLP-76-Vav-Itk signalosome. J Immunol *178*, 1363–1371.

Dogan, I., Bertocci, B., Vilmont, V., Delbos, F., Mégret, J., Storck, S., Reynaud, C.-A., and Weill, J.-C. (2009). Multiple layers of B cell memory with different effector functions. Nat Immunol *10*, 1292–1299.

Engelke, M., Engels, N., Dittmann, K., Stork, B., and Wienands, J. (2007). Ca(2+) signaling in antigen receptor-activated B lymphocytes. Immunol Rev *218*, 235–246.

Engels, N., and Wienands, J. (2011). The signaling tool box for tyrosine-based costimulation of lymphocytes. Curr Opin Immunol *23*, 324–329.

Engels, N., König, L.M., Heemann, C., Lutz, J., Tsubata, T., Griep, S., Schrader, V., and Wienands, J. (2009). Recruitment of the cytoplasmic adaptor Grb2 to surface IgG and IgE provides antigen receptor-intrinsic costimulation to class-switched B cells. Nat Immunol *10*, 1018–1025.

Engels, N., Wollscheid, B., and Wienands, J. (2001). Association of SLP-65/BLNK with the B cell antigen receptor through a non-ITAM tyrosine of Ig-alpha. Eur J Immunol *31*, 2126–2134.

Feng, S., Chen, J.K., Yu, H., Simon, J.A., and Schreiber, S.L. (1994). Two binding orientations for peptides to the Src SH3 domain: development of a general model for SH3-ligand interactions. Science *266*, 1241–1247.

Fu, C., Turck, C.W., Kurosaki, T., and Chan, A.C. (1998). BLNK: a central linker protein in B cell activation. Immunity *9*, 93–103.

Fujikawa, K., Miletic, A.V., Alt, F.W., Faccio, R., Brown, T., Hoog, J., Fredericks, J., Nishi, S., Mildiner, S., Moores, S.L., et al. (2003). Vav1/2/3-null Mice Define an Essential Role for Vav Family Proteins in Lymphocyte Development and Activation but a Differential Requirement in MAPK Signaling in T and B Cells. J Exp Med *198*, 1595–1608.

Fusaki, N., Tomita, S., Wu, Y., Okamoto, N., Goitsuka, R., Kitamura, D., and Hozumi, N. (2000). BLNK is associated with the CD72/SHP-1/Grb2 complex in the WEHI231 cell line after membrane IgM cross-linking. Eur J Immunol *30*, 1326–1330.

Fütterer, K., Wong, J., Grucza, R.A., Chan, A.C., and Waksman, G. (1998). Structural basis for Syk tyrosine kinase ubiquity in signal transduction pathways revealed by the crystal structure of its regulatory SH2 domains bound to a dually phosphorylated ITAM peptide. J Mol Biol *281*, 523–537.

Goitsuka, R., Fujimura, Y., Mamada, H., Umeda, A., Morimura, T., Uetsuka, K., Doi, K., Tsuji, S., and Kitamura, D. (1998). BASH, a novel signaling molecule preferentially expressed in B cells of the bursa of Fabricius. J Immunol *161*, 5804–5808.

Grabbe, A., and Wienands, J. (2006). Human SLP-65 isoforms contribute differently to activation and apoptosis of B lymphocytes. Blood *108*, 3761–3768.

Gray, D. (1993). Immunological memory. Annu. Rev. Immunol. *11*, 49–77.

Harvey, C.D., Ehrhardt, A.G., Cellurale, C., Zhong, H., Yasuda, R., Davis, R.J., and Svoboda, K. (2008). A genetically encoded fluorescent sensor of ERK activity. Proc Natl Acad Sci USA *105*, 19264–19269.

Harwood, N.E., and Batista, F.D. (2010). Early events in B cell activation. Annu. Rev. Immunol. *28*, 185–210.

Hashimoto, A., Okada, H., Jiang, A., Kurosaki, M., Greenberg, S., Clark, E.A., and Kurosaki, T. (1998). Involvement of guanosine triphosphatases and phospholipase C-gamma2 in extracellular signal-regulated kinase, c-Jun NH2-terminal kinase, and p38 mitogen-activated protein kinase activation by the B cell antigen receptor. J Exp Med *188*, 1287–1295.

Hashimoto, S., Iwamatsu, A., Ishiai, M., Okawa, K., Yamadori, T., Matsushita, M., Baba, Y., Kishimoto, T., Kurosaki, T., and Tsukada, S. (1999). Identification of the SH2 domain binding protein of Bruton's tyrosine kinase as BLNK--functional significance of Btk-SH2 domain in B-cell antigen receptor-coupled calcium signaling. Blood *94*, 2357–2364.

Hebeis, B.J. (2004). Activation of Virus-specific Memory B Cells in the Absence of T Cell Help. J Exp Med *199*, 593–602.

Honjo, T., and Kataoka, T. (1978). Organization of immunoglobulin heavy chain genes and allelic deletion model. Proc Natl Acad Sci USA *75*, 2140–2144.

Honjo, T., Kinoshita, K., and Muramatsu, M. (2002). Molecular Mechanism of Class Switch Recombination: Linkage with Somatic Hypermutation. Annu. Rev. Immunol. *20*, 165–196.

Horikawa, K., Martin, S.W., Pogue, S.L., Silver, K., Peng, K., Takatsu, K., and Goodnow, C.C. (2007). Enhancement and suppression of signaling by the conserved tail of IgG memory-type B cell antigen receptors. J Exp Med *204*, 759–769.

Inoue, H., Nojima, H., and Okayama, H. (1990). High efficiency transformation of Escherichia coli with plasmids. Gene *96*, 23–28.

Isnardi, I., Lesourne, R., Bruhns, P., Fridman, W.H., Cambier, J.C., and Daeron, M. (2004). Two Distinct Tyrosine-based Motifs Enable the Inhibitory Receptor Fc RIIB to Cooperatively Recruit the Inositol Phosphatases SHIP1/2 and the Adapters Grb2/Grap. Journal of Biological Chemistry *279*, 51931–51938.

Jang, I.K., Cronshaw, D.G., Xie, L.-K., Fang, G., Zhang, J., Oh, H., Fu, Y.-X., Gu, H., and Zou, Y. (2011). Growth-factor receptor-bound protein-2 (Grb2) signaling in B cells controls lymphoid follicle organization and germinal center reaction. Proc Natl Acad Sci USA *108*, 7926–7931.

Jang, I.K., Zhang, J., and Gu, H. (2009). Grb2, a simple adapter with complex roles in lymphocyte development, function, and signaling. Immunol Rev *232*, 150–159.

Johmura, S., Oh-hora, M., Inabe, K., Nishikawa, Y., Hayashi, K., Vigorito, E., Kitamura, D., Turner, M., Shingu, K., Hikida, M., et al. (2003). Regulation of Vav localization in membrane rafts by adaptor molecules Grb2 and BLNK. Immunity *18*, 777–787.

Kaisho, T., Schwenk, F., and Rajewsky, K. (1997). The roles of gamma 1 heavy chain membrane expression and cytoplasmic tail in IgG1 responses. Science *276*, 412–415.

Kessels, H.W.H.G., Ward, A.C., and Schumacher, T.N.M. (2002). Specificity and affinity motifs for Grb2 SH2-ligand interactions. Proc Natl Acad Sci USA *99*, 8524–8529.

Kim, H.H., Tharayil, M., and Rudd, C.E. (1998). Growth factor receptor-bound protein 2 SH2/SH3 domain binding to CD28 and its role in co-signaling. J Biol Chem *273*, 296–301.

Klein, G., Giovanella, B., Westman, A., Stehlin, J.S., and Mumford, D. (1975). An EBV-genome-negative cell line established from an American Burkitt lymphoma; receptor characteristics. EBV infectibility and permanent conversion into EBV-positive sublines by in vitro infection. Intervirology *5*, 319–334.

Kurosaki, T., and Hikida, M. (2009). Tyrosine kinases and their substrates in B lymphocytes. Immunol Rev *228*, 132–148.

Kurosaki, T., Johnson, S.A., Pao, L., Sada, K., Yamamura, H., and Cambier, J.C. (1995). Role of the Syk autophosphorylation site and SH2 domains in B cell antigen receptor signaling. J Exp Med *182*, 1815–1823.

Lewitzky, M., Kardinal, C., Gehring, N.H., Schmidt, E.K., Konkol, B., Eulitz, M., Birchmeier, W., Schaeper, U., and Feller, S.M. (2001). The C-terminal SH3 domain of the adapter protein Grb2 binds with high affinity to sequences in Gab1 and SLP-76 which lack the SH3-typical P-x-x-P core motif. Oncogene *20*, 1052–1062.

Lowenstein, E.J., Daly, R.J., Batzer, A.G., Li, W., Margolis, B., Lammers, R., Ullrich, A., Skolnik, E.Y., Bar-Sagi, D., and Schlessinger, J. (1992). The SH2 and SH3 domain-containing protein GRB2 links receptor tyrosine kinases to ras signaling. Cell *70*, 431–442.

Machida, K., and Mayer, B.J. (2005). The SH2 domain: versatile signaling module and pharmaceutical target. Biochim Biophys Acta *1747*, 1–25.

Martin, S.W., and Goodnow, C.C. (2002). Burst-enhancing role of the IgG membrane tail as a molecular determinant of memory. Nat Immunol *3*, 182–188.

McHeyzer-Williams, M., Okitsu, S., Wang, N., and McHeyzer-Williams, L. (2011). Molecular programming of B cell memory. Nat Rev Immunol *12*, 24–34.

Morita, S., Kojima, T., and Kitamura, T. (2000). Plat-E: an efficient and stable system for transient packaging of retroviruses. Gene Ther. *7*, 1063–1066.

Neumann, K., Oellerich, T., Urlaub, H., and Wienands, J. (2009). The B-lymphoid Grb2 interaction code. Immunol Rev *232*, 135–149.

Nishida, M., Nagata, K., Hachimori, Y., Horiuchi, M., Ogura, K., Mandiyan, V., Schlessinger, J., and Inagaki, F. (2001). Novel recognition mode between Vav and Grb2 SH3 domains. Embo J *20*, 2995–3007.

Nitschke, L., and Tsubata, T. (2004). Molecular interactions regulate BCR signal inhibition by CD22 and CD72. Trends Immunol *25*, 543–550.

Nutt, S.L., and Tarlinton, D.M. (2011). Germinal center B and follicular helper T cells: siblings, cousins or just good friends? Nat Immunol *131*, 472–477.

Oellerich, T., Grønborg, M., Neumann, K., Hsiao, H.-H., Urlaub, H., and Wienands, J. (2009). SLP-65 phosphorylation dynamics reveals a functional basis for signal integration by receptor-proximal adaptor proteins. Mol. Cell Proteomics *8*, 1738–1750.

Oh-hora, M. (2003). Requirement for Ras Guanine Nucleotide Releasing Protein 3 in Coupling Phospholipase C- 2 to Ras in B Cell Receptor Signaling. J Exp Med *198*, 1841–1851.

Okkenhaug, K., and Vanhaesebroeck, B. (2003). PI3K in lymphocyte development, differentiation and activation. Nat Rev Immunol *3*, 317–330.

Otipoby, K.L. (2001). CD22 Regulates B Cell Receptor-mediated Signals via Two Domains That Independently Recruit Grb2 and SHP-1. Journal of Biological Chemistry *276*, 44315–44322.

Pape, K.A., Taylor, J.J., Maul, R.W., Gearhart, P.J., and Jenkins, M.K. (2011). Different B cell populations mediate early and late memory during an endogenous immune response. Science *331*, 1203–1207.

Papin, J., and Subramaniam, S. (2004). Bioinformatics and cellular signaling. Curr. Opin. Biotechnol. *15*, 78–81.

Park, C.Y., Hoover, P.J., Mullins, F.M., Bachhawat, P., Covington, E.D., Raunser, S., Walz, T., Garcia, K.C., Dolmetsch, R.E., and Lewis, R.S. (2009). STIM1 Clusters and Activates CRAC Channels via Direct Binding of a Cytosolic Domain to Orai1. Cell *136*, 876–890.

Pierce, S.K. (2002). Lipid Rafts and B-Cell Activation. Nat Rev Immunol *2*, 96–105.

Pierce, S.K., and Liu, W. (2010). The tipping points in the initiation of B cell signalling: how small changes make big differences. Nat Rev Immunol *10*, 767–777.

Prasad, K.V., Cai, Y.C., Raab, M., Duckworth, B., Cantley, L., Shoelson, S.E., and Rudd, C.E. (1994). T-cell antigen CD28 interacts with the lipid kinase phosphatidylinositol 3-kinase by a cytoplasmic Tyr(P)-Met-Xaa-Met motif. Proc Natl Acad Sci USA *91*, 2834–2838.

Reth, M. (1989). Antigen receptor tail clue. Nature *338*, 383–384.

Reth, M. (1992). Antigen receptors on B lymphocytes. Annu. Rev. Immunol. *10*, 97–121.

Reth, M., and Wienands, J. (1997). Initiation and Processing of Signals From the B Cell Antigen Receptor. Annu. Rev. Immunol. *15*, 453–479.

Reth, M., Wienands, J., and Schamel, W.W. (2000). An unsolved problem of the clonal selection theory and the model of an oligomeric B-cell antigen receptor. Immunol Rev *176*, 10–18.

Saijo, K. (2002). Protein Kinase C beta Controls Nuclear Factor kappaB Activation in B Cells Through Selective Regulation of the IkappaB Kinase alpha. Journal of Experimental Medicine *195*, 1647–1652.

Sato, M., Adachi, T., and Tsubata, T. (2007). Augmentation of signaling through BCR containing IgE but not that containing IgA due to lack of CD22-mediated signal regulation. J Immunol *178*, 2901–2907.

Schamel, W.W., and Reth, M. (2000). Monomeric and oligomeric complexes of the B cell antigen receptor. Immunity *13*, 5–14.

Scharenberg, A.M., Humphries, L.A., and Rawlings, D.J. (2007). Calcium signalling and cell-fate choice in B cells. Nat Rev Immunol *7*, 778–789.

Schneider, H., Cai, Y.C., Prasad, K.V., Shoelson, S.E., and Rudd, C.E. (1995). T cell antigen CD28 binds to the GRB-2/SOS complex, regulators of p21ras. Eur J Immunol *25*, 1044–1050.

Songyang, Z., Shoelson, S.E., McGlade, J., Olivier, P., Pawson, T., Bustelo, X.R., Barbacid, M., Sabe, H., Hanafusa, H., and Yi, T. (1994). Specific motifs recognized by the SH2 domains of Csk, 3BP2, fps/fes, GRB-2, HCP, SHC, Syk, and Vav. Molecular and Cellular Biology *14*, 2777–2785.

Sparks, A.B., Rider, J.E., Hoffman, N.G., Fowlkes, D.M., Quillam, L.A., and Kay, B.K. (1996). Distinct ligand preferences of Src homology 3 domains from Src, Yes, Abl, Cortactin, p53bp2, PLCgamma, Crk, and Grb2. Proc Natl Acad Sci USA *93*, 1540–1544.

Srinivasan, L., Sasaki, Y., Calado, D.P., Zhang, B., Paik, J.H., DePinho, R.A., Kutok, J.L., Kearney, J.F., Otipoby, K.L., and Rajewsky, K. (2009). PI3 kinase signals BCR-dependent mature B cell survival. Cell *139*, 573–586.

Stork, B. (2006). A molecular basis for differential Ca2+ signalling in B lymphocytes. Dissertation.

Stork, B., Engelke, M., Frey, J., Horejsí, V., Hamm-Baarke, A., Schraven, B., Kurosaki, T., and Wienands, J. (2004). Grb2 and the non-T cell activation linker NTAL constitute a Ca(2+)-regulating signal circuit in B lymphocytes. Immunity *21*, 681–691.

Stork, B., Neumann, K., Goldbeck, I., Alers, S., Kähne, T., Naumann, M., Engelke, M., and Wienands, J. (2007). Subcellular localization of Grb2 by the adaptor protein Dok-3 restricts the intensity of Ca2+ signaling in B cells. Embo J *26*, 1140–1149.

Tarlinton, D. (2006). B-cell memory: are subsets necessary? Nat Rev Immunol *6*, 785–790.

Treanor, B., Depoil, D., Bruckbauer, A., and Batista, F.D. (2011). Dynamic cortical actin remodeling by ERM proteins controls BCR microcluster organization and integrity. J Exp Med *208*, 1055–1068.

Treanor, B., Depoil, D., Gonzalez-Granja, A., Barral, P., Weber, M., Dushek, O., Bruckbauer, A., and Batista, F.D. (2010). The Membrane Skeleton Controls Diffusion Dynamics and Signaling through the B Cell Receptor. Immunity *32*, 187–199.

Upshaw, J.L., Arneson, L.N., Schoon, R.A., Dick, C.J., Billadeau, D.D., and Leibson, P.J. (2006). NKG2D-mediated signaling requires a DAP10-bound Grb2-Vav1 intermediate and phosphatidylinositol-3-kinase in human natural killer cells. Nat Immunol *7*, 524–532.

Venkitaraman, A.R., Williams, G.T., Dariavach, P., and Neuberger, M.S. (1991). The B-cell antigen receptor of the five immunoglobulin classes. Nature *352*, 777–781.

Victora, G.D., and Nussenzweig, M.C. (2011). Germinal Centers. Annu. Rev. Immunol.

Victora, G.D., Schwickert, T.A., Fooksman, D.R., Kamphorst, A.O., Meyer-Hermann, M., Dustin, M.L., and Nussenzweig, M.C. (2010). Germinal center dynamics revealed by multiphoton microscopy with a photoactivatable fluorescent reporter. Cell *143*, 592–605.

Violin, J.D., Zhang, J., Tsien, R.Y., and Newton, A.C. (2003). A genetically encoded fluorescent reporter reveals oscillatory phosphorylation by protein kinase C. J Cell Biol *161*, 899–909.

Waisman, A., Kraus, M., Seagal, J., Ghosh, S., Melamed, D., Song, J., Sasaki, Y., Classen, S., Lutz, C., Brombacher, F., et al. (2007). IgG1 B cell receptor signaling is inhibited by CD22 and promotes the development of B cells whose survival is less dependent on Ig /. J Exp Med *204*, 747–758.

Wakabayashi, C., Adachi, T., Tsubata, T., 4 (2002). A distinct signaling pathway used by the IgG-containing B cell antigen receptor. Science *298*, 2392–2395.

Wang, J., Auger, K.R., Jarvis, L., Shi, Y., and Roberts, T.M. (1995). Direct association of Grb2 with the p85 subunit of phosphatidylinositol 3-kinase. J Biol Chem *270*, 12774–12780.

Wienands, J., Schweikert, J., Wollscheid, B., Jumaa, H., Nielsen, P.J., and Reth, M. (1998). SLP-65: a new signaling component in B lymphocytes which requires expression of the antigen receptor for phosphorylation. J Exp Med *188*, 791–795.

Wienands, J.J., Freuler, F.F., and Baumann, G.G. (1995). Tyrosine-phosphorylated forms of Ig beta, CD22, TCR zeta and HOSS are major ligands for tandem SH2 domains of Syk. International Immunology *7*, 1701–1708.

Yamanashi, Y.Y., Kakiuchi, T.T., Toyoshima, K.K., 5 (1991). Association of B cell antigen receptor with protein tyrosine kinase Lyn. Science *251*, 192–194.

Ye, Z.S., and Baltimore, D. (1994). Binding of Vav to Grb2 through dimerization of Src homology 3 domains. Proc Natl Acad Sci USA *91*, 12629–12633.

Zhang, S.L., Yu, Y., Roos, J., Kozak, J.A., Deerinck, T.J., Ellisman, M.H., Stauderman, K.A., and Cahalan, M.D. (2005). STIM1 is a Ca2+ sensor that activates CRAC channels and migrates from the Ca2+ store to the plasma membrane. Nature *437*, 902–905.